Supporting Information

Nonribosomal lipopeptides protect *Pseudomonas nunensis* 4A2e from amoebal and nematodal predation

Sebastian Pflanze,[a] Ruchira Mukherji,[a] Anan Ibrahim,[a] Markus Günther,[a] Sebastian Götze,[a] Somak Chowdhury,[a] Lisa Reimer,[a] Lars Regestein[b] and Pierre Stallforth[a,c]

a) Department of Paleobiotechnology, Leibniz Institute for Natural Product Research and Infection Biology – Leibniz-HKI, Beutenbergstrasse 11a, 07745 Jena, Germany

b) Bio Pilot Plant, Leibniz Institute for Natural Product Research and Infection Biology – Leibniz-HKI, Beutenbergstrasse 11a, 07745 Jena, Germany

c) Faculty of Chemistry and Earth Sciences, Friedrich Schiller University (FSU), Jena, Germany

Contents

General methods 1
Isolation of *Pseudomonas nunensis* 4A2e, *Polysphondylium pallidum* RM1, and *Oscheius myriophilus* SP1 4
Genomic analysis of *Pseudomonas nunensis* 4A2e 5
Phylogenetic analysis 10
Metabolic analysis of wild type 4A2e and mutant strains 14
Regulation of nonribosomal peptide biosynthesis 15
Plaque assays with WT 4A2e and gene deletion mutants 17
Growth inhibition assays 20
Bacteria–nematode co-cultivation assay 22
Isolation of nonribosomal lipopeptides 22
Sequence analysis of nonribosomal peptides 26
Synthesis of protected 4-chloro-L-threonine 29
Marfey's analysis of nonribosomal peptides 31
Stable isotope labelling of nunapeptin C 34
Determination of the ring size of nunapeptins 36
Determination of the absolute configuration of the 3-hydroxytetradecanoic acid residue in keanumycin D 37
LCMS analysis of hydrolysed nunapeptin C 40
HCN production in *Pseudomonas nunensis* 4A2e 41
References 41
NMR Spectra 43

General methods

Reagents and materials

Chemical reagents and materials were purchased from Acros Organics, Alfa Aesar, CDN isotopes, Merck, TCI, and were used without further purification. Organic solvents were supplied by VWR and Th. Geyer as HPLC or LCMS grade. Anhydrous solvents were purchased from Acros Organics. Nematode counting dishes were supplied by the laboratory of nematology of Wageningen University & Research, Netherlands.

Table S1 List of Media

Medium	Composition (L^{-1})
Phosphate-buffered saline (PBS)	8.0 g NaCl, 200 mg KCl, 1.78 g $Na_2HPO_4 \cdot 2H_2O$, 240 mg KH_2PO_4, adjusted to pH 7.4 with NaOH.
R2A agar	500 mg yeast extract, 500 mg proteose peptone, 500 mg casamino acids, 500 mg glucose, 500 mg soluble starch, 300 mg sodium pyruvate, 300 mg K_2HPO_4, 50 mg $MgSO_4 \cdot 7H_2O$, 15 g agar, adjusted to pH 7.2 with NaOH.
Hay agar	1.5 g KH_2PO_4, 620 mg $Na_2HPO_4 \cdot 2H_2O$, 15 g agar, fill to 1 L with hay infusion (10 g hay/L, filtered through cheese cloth).
Starving agar	2.0 g K_2HPO_4, 300 mg $Na_2HPO_4 \cdot 2H_2O$, 20 g agar.
NGM	3.0 g NaCl, 17 g agar, 2.5 g tryptone/peptone ex casein, adjusted to 975 mL. After autoclave sterilization, cool to 55 °C and add 1 mL of a 1M $CaCl_2$ solution, 1 mL of a 1M $MgSO_4$ solution, 1 mL of 5 mg/mL cholesterol solution in EtOH, and 25 mL of 1M KPO_4 buffer (108.3 g KH_2PO_4, 35.6 g K_2HPO_4, filled to 1 L and adjusted pH to 6.0 with HCl).
K-medium	3.1 g NaCl, 2.4 g KCl.
S-buffer	5.85 g NaCl, 1.12 g K_2HPO_4, 5.93 g KH_2PO_4.
Modified Davis medium	18.4 g glycerol, 5.0 g $(NH_4)_2SO_4$, 2.6 g K_2HPO_4, 3.25 g trisodium citrate dihydrate, 200 mg $MgSO_4 \cdot 7H_2O$, 1 mL of a 0.1 M $FeCl_3$ solution in 1% HCl, 580 mg NaCl.
SM/5 broth	2.0 g glucose, 2.0 g tryptone/peptone ex casein, 200 mg yeast extract, 200 mg $MgSO_4 \cdot 7H_2O$, 1.9 g KH_2PO_4, 1.0 g K_2HPO_4.
SM/5 agar	SM/5 broth supplemented with 15 g agar.
LB	Lysogeny broth-Miller (Carl Roth).
HL5	HL5 medium including glucose (Formedium).
PYG	20.0 g proteose peptone, 18.0 g glucose, 2.0 g yeast extract, 1.0 g trisodium citrate dihydrate, 980 mg $MgSO_4 \cdot 7H_2O$, 355 mg $Na_2HPO_4 \cdot 7H_2O$, 340 mg KH_2PO_4, 20 mg $Fe(NH_4)_2(SO_4)_2 \cdot 6H_2O$, adjusted to pH 6.5 with HCl.
Sörensen's buffer	2.0 g KH_2PO_4, 550 mg $Na_2HPO_4 \cdot 2H_2O$, adjusted to pH 6.0 with HCl.
Co-cultivation agar	18.4 g glycerol, 5.0 g $(NH_4)_2SO_4$, 2.6 g K_2HPO_4, 3.25 g trisodium citrate dihydrate, 200 mg $MgSO_4 \cdot 7H_2O$, 1 mL of a 0.1 M $FeCl_3$ solution in 1% HCl, 580 mg NaCl, 2.5 g tryptone/peptone ex casein, 15 g agar, filled to 975 mL and adjusted to pH 6.5 with HCl. After autoclave sterilization, cool to 55 °C and add 1 mL of a 1M $CaCl_2$ solution, and 1 mL of 5 mg/mL cholesterol solution in EtOH.
Stable isotope labelling medium	1.84 g glycerol, 1.0 g $(NH_4)_2SO_4$, 2.6 g K_2HPO_4, 625 mg trisodium citrate dihydrate, 200 mg $MgSO_4 \cdot 7H_2O$, 1 mL of a 0.1 M $FeCl_3$ solution in 1% HCl, 90 mg L-alanine-2-d_1, 117 mg L-valine, 131 mg L-isoleucine.
Labelling control medium	1.84 g glycerol, 1.0 g $(NH_4)_2SO_4$, 2.6 g K_2HPO_4, 625 mg trisodium citrate dihydrate, 200 mg $MgSO_4 \cdot 7H_2O$, 1 mL of a 0.1 M $FeCl_3$ solution in 1% HCl, 89 mg L-alanine, 117 mg L-valine, 131 mg L-isoleucine.

Maintenance of social amoebae

Social amoebae (*Polysphondylium pallidum* RM1, *Polysphondylium pallidum* PN500, *Dictyostelium discoideum* AX2, *Dictyostelium purpureum* QSpu1, and *Dictyostelium caveatum* WS695) were maintained at 22 °C on SM/5 agar, on lawns of *Klebsiella aerogenes*. Cryogenic stocks were prepared by freezing amoebal spores in Sörensen's buffer at –80 °C.

Maintenance of the bacteriovorus nematode *Oscheius myriophilus* SP1

The nematode *Oscheious myriophilus* SP1 was routinely maintained at 22 °C on NGM agar, on lawns of *Pseudomonas nunensis* 4A2e Δ*nup*Δ*kea*Δ*bra*. Every 10 to 14 days, nematodes were gently washed off the plate with sterile K-medium and transferred to a new NGM plate onto a bacterial lawn. Cryogenic stocks of *Oscheius myriophilus* were prepared by freezing early developmental stages of the nematode in S-buffer containing 15% (w/v) glycerol and 1 mM $CaCl_2$ in a small styrofoam box and were kept at –80 °C.[1,2]

Gene deletion *via* homologous recombination

Markerless, in-frame gene deletion mutants of *Pseudomonas nunensis* 4A2e were generated by a gentamicin-resistance selection and a subsequent sucrose counter-selection approach.[3] The plasmid pEXG2 was linearised by restriction digestion with HindIII and EcoRI. Chromosomal regions flanking the target sequence ("left arm" (LA) and "right arm" (RA)) were amplified from genomic DNA of 4A2e with Q5 HF DNA polymerase (NEB), introducing additional overhangs of 18 – 20 bps. The linearised vector, LA and RA fragments were purified using the Monarch DNA Gel Extraction Kit (NEB).

The suicide vector was ligated by Gibson Assembly (NEB) and transformed directly into chemically competent *Escherichia coli* DH5α. Transformants were selected for on LB agar containing gentamicin at 37 °C and later confirmed by colony PCR (DreamTaq DNA polymerase, Thermo Scientific) with the primer pair pEXG2_seq_fwd/pEXG2_seq_rev. Plasmid DNA was isolated using the Monarch Plasmid Miniprep Kit (NEB) and subsequently transformed into *E. coli* S17-1λpir. Transformants were selected for on LB agar containing gentamicin at 37 °C. Then, the respective plasmids were introduced into 4A2e by conjugation. Overnight cultures of the donor (LB containing gentamicin) and recipient (LB) strain were used to inoculate new cultures (3 mL), which were grown (37 °C for *E. coli*, 28 °C for 4A2e) to an OD_{600} of 0.4–0.6. Cultures were mixed in ratios of 1:3 to 1:9 (recipient/donor) and washed by repeated centrifugation (6000 x *g*, 2 min) and resuspension in fresh LB. Cells were resuspended in LB (100 µL) and spotted onto LB agar, which was incubated at 28 °C overnight. Then, spots were resuspended in LB (450 µL) and plated on LB agar containing gentamicin and ampicillin to select for 4A2e transformants, which had integrated the pEXG2 vector into their chromosome. A single colony was resuspended in LB (450 µL) and incubated at 750 rpm at 28 °C for 4 h. The suspension was plated on LB agar containing 10% sucrose (w/v) and plates were incubated at 28 °C. Colonies were screened via colony PCR for the loss of the target sequence.

Table S2 List of Primers

Oligonucleotide	Sequence	Notes
27f	AGAGTTTGATCCTGGCTCAG	Amplify 16S rDNA
1492r	GGTTACCTTGTTACGACTT	Amplify 16S rDNA
18SSU Primer A	CCGAATTCGTCGACAACCTGGTTGATCCTGCCAGT	Amplify 18S rDNA in social amoebae[4]
18SSU Primer B	CCCGGGATCCAAGCTTGATCCTTCTGCAGGTTCACCTAC	Amplify 18S rDNA in social amoebae[4]
SSU18A	AAAGATTAAGCCATGCATG	Amplify 18S rDNA in rhabditid nematodes[5]
SSU26R	CATTCTTGGCAAATGCTTTCG	Amplify 18S rDNA in rhabditid nematodes[5]
nupA_LA_fwd	GGAAGCATAAATGTAAAGCACAAGGTCGGCTCGTCCAC	Amplify the region 5‘ to target sequence in *nupA*
nupA_LA_rev	TCAACAACTGGGAGTCAGTACAGGAATCATCG	Amplify the region 5‘ to target sequence in *nupA*
nupA_RA_fwd	TACTGACTCCCAGTTGTTGATCTTCGTAAACCACCG	Amplify the region 3‘ to target sequence in *nupA*
nupA_RA_rev	GGAAATTAATTAAGGTACCGCGCATCGACGCCTTGGCA	Amplify the region 3‘ to target sequence in *nupA*
keaA_LA_fwd	GGAAGCATAAATGTAAAGCAGCGCAGTTCGCCAGCGGC	Amplify the region 5‘ to target sequence in *keaA*
keaA _LA_rev	AGGTGCTGCGACTCAGCACCTGACCGCTGTCATCG	Amplify the region 5‘ to target sequence in *keaA*
keaA _RA_fwd	TCAGGTGCTGAGTCGCAGCACCTTGCCG	Amplify the region 3‘ to target sequence in *keaA*
keaA _RA_rev	GGAAATTAATTAAGGTACCGTGCGGTCAGATTGGCGTC	Amplify the region 3‘ to target sequence in *keaA*
braB_LA_fwd	GGAAGCATAAATGTAAAGCACGTCTCGGTGAACTGACG	Amplify the region 5‘ to target sequence in *braB*
braB _LA_rev	TGCCACCGTGCAGGGTTTGATTGTCGAAG	Amplify the region 5‘ to target sequence in *braB*
braB _RA_fwd	TCAAACCCTGCACGGTGGCACTTCCACC	Amplify the region 3‘ to target sequence in *braB*
braB _RA_rev	GGAAATTAATTAAGGTACCGGCGGTAGGCCGAACGGTG	Amplify the region 3‘ to target sequence in *braB*
nupR1_LA_fwd	GGAAGCATAAATGTAAAGCAAAATACGCCGTATGACTGAGG	Amplify the region 5‘ to *nupR1*
nupR1 _LA_rev	ACAGTAGAAGGATGGGAGGGCTCGGATAATG	Amplify the region 5‘ to

		nupR1
nupR1 _RA_fwd	CCCTCCCATCCTTCTACTGTACTGGTCAGTTAATCTTCCG	Amplify the region 3‘ to *nupR1*
nupR1 _RA_rev	GGAAATTAATTAAGGTACCGAGCCGCCTCGGCTTTTGG	Amplify the region 3‘ to *nupR1*
nupR2_LA_fwd	GGAAGCATAAATGTAAAGCACCAACAATCCTAGAGCAAATACTC	Amplify the region 5‘ to *nupR2*
nupR2_LA_rev	GGAAGTGGGGCGGCTCTCCATGTCATGATTTC	Amplify the region 5‘ to *nupR2*
nupR2_RA_fwd	TGGAGAGCCGCCCCACTTCCACTCTTTTC	Amplify the region 3‘ to *nupR2*
nupR2 _RA_rev	GGAAATTAATTAAGGTACCGTCACGCTGTCCATCGAAC	Amplify the region 3‘ to *nupR2*
pcoI_LA_fwd	GGAAGCATAAATGTAAAGCACAGTCACCACCCATGAATAATC	Amplify the region 5‘ to *pcoI*
pcoI_LA_rev	CTCTATGATGGGTCTGACGTTCTTGGTTG	Amplify the region 5‘ to *pcoI*
pcoI_RA_fwd	ACGTCAGACCCATCATAGAGCCATCCCACCC	Amplify the region 3‘ to *pcoI*
pcoI_RA_rev	GGAAATTAATTAAGGTACCGCAGGCGATCGGCAAAGCG	Amplify the region 3‘ to *pcoI*
nunF_LA_fwd	GGAAGCATAAATGTAAAGCAATTTGTCCTACAACTTACAAATGATGG	Amplify the region 5‘ to *nunF*
nunF_LA_rev	CGGGGCATTACGCGTTGGTGAGCTGATAG	Amplify the region 5‘ to *nunF*
nunF_RA_fwd	CACCAACGCGTAATGCCCCGAACCCTTCTG	Amplify the region 3‘ to *nunF*
nunF_RA_rev	GGAAATTAATTAAGGTACCGACCTTCGACGGTGGTCCG	Amplify the region 3‘ to *nunF*
pEXG2_ctrl_fwd	CATAATATCTCATTTCACTAAATAATAGTGAACGGCAGGTAAGC	Confirm pEXG2 insert
pEXG2_ctrl_rev	CATTCTGCTAACCAGTAAGGCAACCCCG	Confirm pEXG2 insert
nupA_ctrl_LA_fwd	AGGCCAAGTGATGAAGGCTG	Confirm deletion in *nupA*
nupA_ctrl_LA_rev	GTATGTGCTTGAGCAGGGGT	Confirm deletion in *nupA*
nupA_ctrl_RA_fwd	TGCAACGACACCAATCCGTA	Confirm deletion in *nupA*
nupA_ctrl_RA_rev	CCGTTTTCATCTGGCCAAGC	Confirm deletion in *nupA*
keaA _ctrl_LA_fwd	CCGGAACGTTTCTACTGGCT	Confirm deletion in *keaA*
keaA _ctrl_LA_rev	AACAGCTCGGCTTCTTCCTC	Confirm deletion in *keaA*
keaA _ctrl_RA_fwd	TCTGTCGATGCTGGAAACGG	Confirm deletion in *keaA*
keaA _ctrl_RA_rev	AACCGATCACCACTTCGTCC	Confirm deletion in *keaA*
braB_ctrl_LA_fwd	CGTTGATGGCTGGTCGTTTG	Confirm deletion in *braB*
braB_ctrl_LA_rev	GGGTGCATCATCGAGTGGTA	Confirm deletion in *braB*
braB _ctrl_RA_fwd	TGCAACAGCGTTTCATGAGC	Confirm deletion in *braB*
braB _ctrl_RA_rev	TATTGAGGAACAGCCCCAGC	Confirm deletion in *braB*
nupR1_ctrl_LA_fwd	TCGGCAGAAAGCGACTACAT	Confirm *nupR1* deletion
nupR1 _ctrl_LA_rev	CGGGCGGATGGTCAATAGAA	Confirm *nupR1* deletion
nupR1_ctrl_RA_fwd	CACAGCCCCTCAGATTCTCT	Confirm *nupR1* deletion
nupR1 _ctrl_RA_rev	CTTGCCCGAGAACTCTGTCC	Confirm *nupR1* deletion
nupR2_ctrl_LA_fwd	ACAACTGGCAAAAACCAGAC	Confirm *nupR2* deletion
nupR2_ctrl_LA_rev	AACGTTGCTGAGTCTATTGGTG	Confirm *nupR2* deletion
nupR2_ctrl_RA_fwd	GTATTCAACAAGAACACTCCAGC	Confirm *nupR2* deletion
nupR2_ctrl_RA_rev	ACGATCTCGATGCAATCAACCAA	Confirm *nupR2* deletion
pcoI_ctrl_LA_fwd	ACAGCGACATGAATGGCACA	Confirm *pcoI* deletion
pcoI_ctrl_LA_rev	ACGTGCGGGAACAATCTTTG	Confirm *pcoI* deletion
pcoI_ctrl_RA_fwd	ATTAATGCGCCACACCGATT	Confirm *pcoI* deletion
pcoI_ctrl_RA_rev	GAGTGGAAGTGGGGTTAGACG	Confirm *pcoI* deletion
nunF_ctrl_LA_fwd	GGTTTGTGGCGGGTGAAGT	Confirm *nunF* deletion
nunF_ctrl_LA_rev	TTAACGAACAACCGCCGAGA	Confirm *nunF* deletion
nunF_ctrl_RA_fwd	AATGTTTCTCACGGCACGGA	Confirm *nunF* deletion
nunF_ctrl_RA_rev	GGCGGACTTGAGCAGGTATT	Confirm *nunF* deletion

Liquid chromatography – mass spectrometry (LCMS)

LCMS data were acquired using a Shimadzu Nexera X3 UHPLC connected to a Shimadzu single quadrupole mass spectrometer (LCMS-2020). Data were analysed using Shimadzu LabSolutions software. The UHPLC was equipped with a Phenomenex Kinetex C18 (50 x 2.1 mm, 1.7 µm, 100 Å) and the column oven set to 40 °C. The scan range of MS was set to *m/z* 150 to 2000, a scan speed of 7500 u/s and an event time of 300 ms. The interface temperature was set to 350 °C, the desolvation line temperature to 250 °C and the heat block temperature to 400 °C. The nebulising gas flow was set to 1.5 L/min and dry gas flow to 15 L/min. The following method was used: flow rate of 0.7 mL/min; 0 – 0.5 min: 10% MeCN in water containing 0.1%

formic acid; 0.5 – 8.5 min: linear gradient from 10% to 100% MeCN in water containing 0.1% formic acid; 8.5 – 11.5 min: 100% MeCN containing 0.1% formic acid.

High-resolution mass spectrometry (HRMS/HRMS^2)

High-resolution mass (HRMS) and high-resolution tandem mass (HRMS^2) spectrometry data were acquired using a Thermo Scientific Accela UHPLC connected to a Thermo Scientific QExactive Orbitrap mass spectrometer. Data were analysed using Thermo Scientific Xcalibur software. The UHPLC was equipped with a Thermo Scientific Accucore C18 (100 x 2.1 mm, 2.6 µm, 80 Å). For HRMS^2 experiments, the higher-energy collisional dissociation (hcd) was set to 10%, 15%, or 25%.

Nuclear magnetic resonance spectroscopy (NMR)

NMR spectra were recorded on Bruker Avance II 300, Avance III 500, and Avance III 600 (equipped with a Bruker CryoProbe) machines. Deuterated NMR solvents were supplied by VWR (Darmstadt, Germany) and Deutero (Kastellaun, Germany). Chemical shifts δ are reported in parts per million (ppm) and coupling constants (*J*) in Hz. Residual solvent signals were used as internal standards: $CDCl_3$: δ = 7.26 (^{1}H), 77.16 (^{13}C); CD_3OD: δ = 3.31 (^{1}H), 49.00 (^{13}C); DMSO-d_6: δ = 2.50 (^{1}H), 39.52 (^{13}C). Spectra were analysed using the Bruker TopSpin 3.2 software.

Optical rotation

Optical rotation was measured on a Krüss P3000 polarimeter in a 100 mm cuvette at 22 °C.

Isolation of *Pseudomonas nunensis* 4A2e, *Polysphondylium pallidum* RM1, and *Oscheius myriophilus* SP1

All environmental samples were obtained from an isolated area (50.962 N 11.592 E) in a mixed forest in a nature reserve near Jena, Germany. We removed the upper layer of leaves and collected the top layer of decaying vegetative material and forest soil.

Pseudomonas nunensis 4A2e was isolated by resuspending vegetative forest material in PBS and serial diluting the supernatant. The suspension was plated on R2A agar and incubated at 22 °C until bacterial colonies emerged. Colonies were picked and re-streaked on R2A to obtain isolated colonies. Cryogenic stocks were prepared by freezing the bacterial suspension in glycerol-containing water (final glycerol concentration of 20% (w/v)) at –80 °C.

The social amoeba *Polysphondylium pallidum* RM1 was isolated using the straw method described by Queller and Strassmann.[6] In short, a suspension of the upper soil layer in Sörensen's buffer was plated out on hay agar and subsequently covered with a suspension of *Klebsiella aerogenes* in SM/5 broth. A few pieces of activated charcoal were sprinkled on the agar and the plates left open in the laminar flow until all liquid was absorbed. Plates were incubated at 22 °C until the emergence of fruiting bodies. Potential contaminants were removed by resuspending fruiting bodies in a suspension of *K. aerogenes* and pipetting a single strip of the cell suspension onto starving agar. Clonal isolates were obtained from clean looking fruiting bodies by a serial dilution of the respective spores in Sörensen's buffer, followed by the addition of *K. aerogenes* suspension and plating on SM/5 agar. Single colonies were picked with a sterile inoculation loop and transferred to a new SM/5 plate onto a bacterial lawn. The identity of the amoeba was determined by amplification of the 18S rDNA sequence using the primer pair 18SSU Primer A/18SSU Primer B, described by Medlin *et al.*[4] Cryogenic stocks were prepared as described above.

The nematode *Oscheius myriophilus* was isolated using the agar culture plate method described by Barrière and Félix.[7] In short, decaying vegetative material was arranged around a lawn of *Pseudomonas nunensis* 4A2e Δ*nup*Δ*kea*Δ*bra* on NGM agar. The vegetative material was moistened with K-medium and plates were incubated at 22 °C overnight. When worms were spotted in the bacterial lawn, a sterile scalpel was used to cut out the respective piece of agar which was then transferred to a single, new plate of Δ*nup*Δ*kea*Δ*bra*. Thereby, several animals were pooled and incubated for several days at 22 °C. After the emergence of new worms, the plate was flooded with K-medium and animals resuspended. Single adult animals, carrying embryos, were transferred to new Δ*nup*Δ*kea*Δ*bra* plates respectively, thereby establishing a single progenitor breed. The identity of the strain was determined by amplification of the 18S rDNA sequence using the primer pairs SSU18A/SSU26R, described by Floyd *et al*.[5] Cryogenic stocks of *Oscheius myriophilus* were prepared as described above using a styrofoam box.

Genomic analysis of *Pseudomonas nunensis* 4A2e

Genomic DNA suitable for Illumina sequencing was extracted from an overnight culture of *Pseudomonas nunensis* 4A2e using a Blood & Cell Culture DNA Kit (Qiagen) and sent to Qiagen CLC Genomics for Next Generation Illumina sequencing and contig assembly (299 contigs; N50 167,693 bp). The assembled genome was analysed using antiSMASH version 5.1.0 for any potential BGCs. Out of the 11 candidate BGCs recovered, one BGC found on contig_05 (Figure S1) showed high similarities with syringomycin and nunapeptin/nunamycin containing BGCs according to the KnownClusterBlast search (Figure S2).

Figure S1 AntiSMASH output illustration for contig_05. NRPS genes for brabantamide (335 kb – 343 kb), keanumycin (347 kb – 375 kb), and nunapeptin (386 kb – 459 kb) biosynthesis can be identified on the contig.

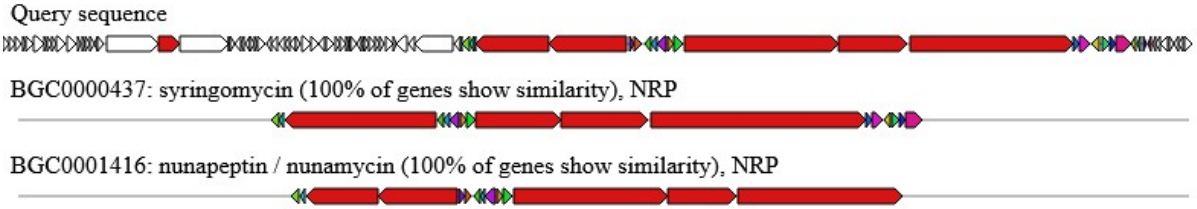

Figure S2 KnownClusterBlast analysis of contig_05 with antiSMASH version 5.1.0. High similarities with biosynthetic gene clusters for syringomycin and nunapeptin/nunamycin biosynthesis are illustrated.

Closer inspection of the domain annotation of the respective NRPS clusters predicted 22 modules for the nunapeptins, with one starter condensation (C) domain (module 1), two $^{L}C_{L}$ domains (modules 20 and 21), and 19 dual E/C domains (Figure S3). For the keanumycin NRPS genes, a starter C domain (module 1), six $^{L}C_{L}$ domains (modules 2, 4, 7, 9, and two C domains in module 6), and three dual E/C domains (modules 3, 5, and 8) were predicted (Figure S4).

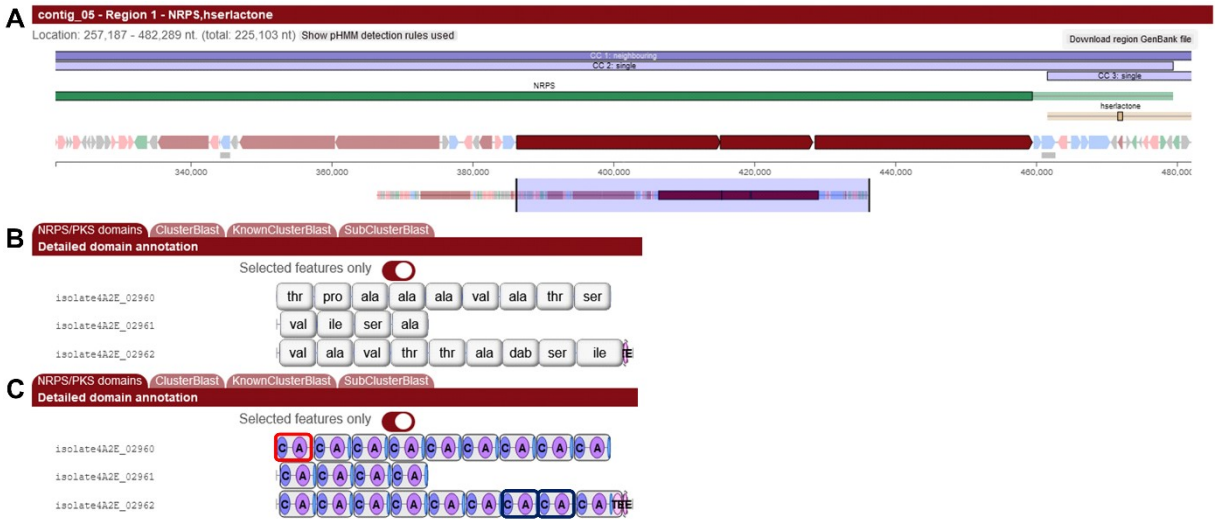

Figure S3 Predicted NRPS domain annotation for the nunapeptin NRPS genes (*nupA*, *nupB*, *nupC*). A) Location of the BGC within the amoebicidal genomic island. B) Software prediction of the amino acid sequence. C) C domain prediction: one starter C domain (red), two $^{L}C_{L}$ domains (blue), and 19 dual E/C domains (grey).

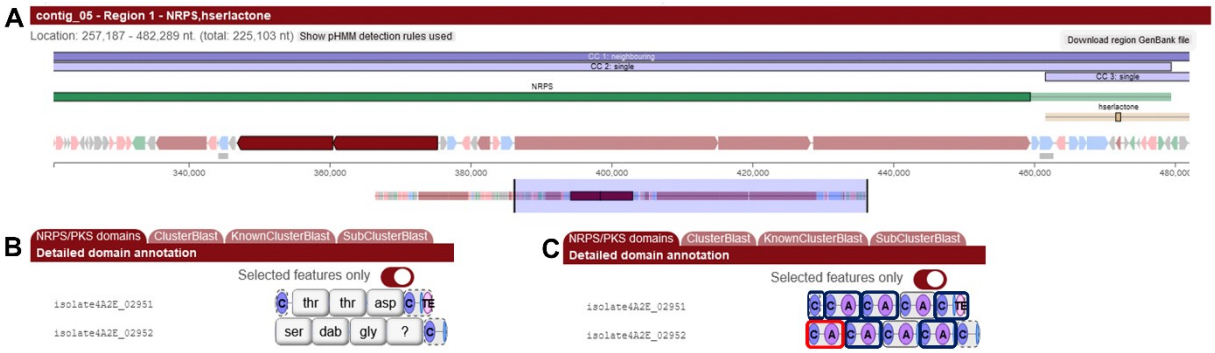

Figure S4 Predicted NRPS domain annotation for the keanumycin NRPS genes (*keaA*, *keaB*). A) Location of the BGC within the amoebicidal genomic island. B) Software prediction of the amino acid sequence. C) C domain prediction: one starter C domain (red), six $^{L}C_{L}$ domains (blue), and three dual E/C domains (grey).

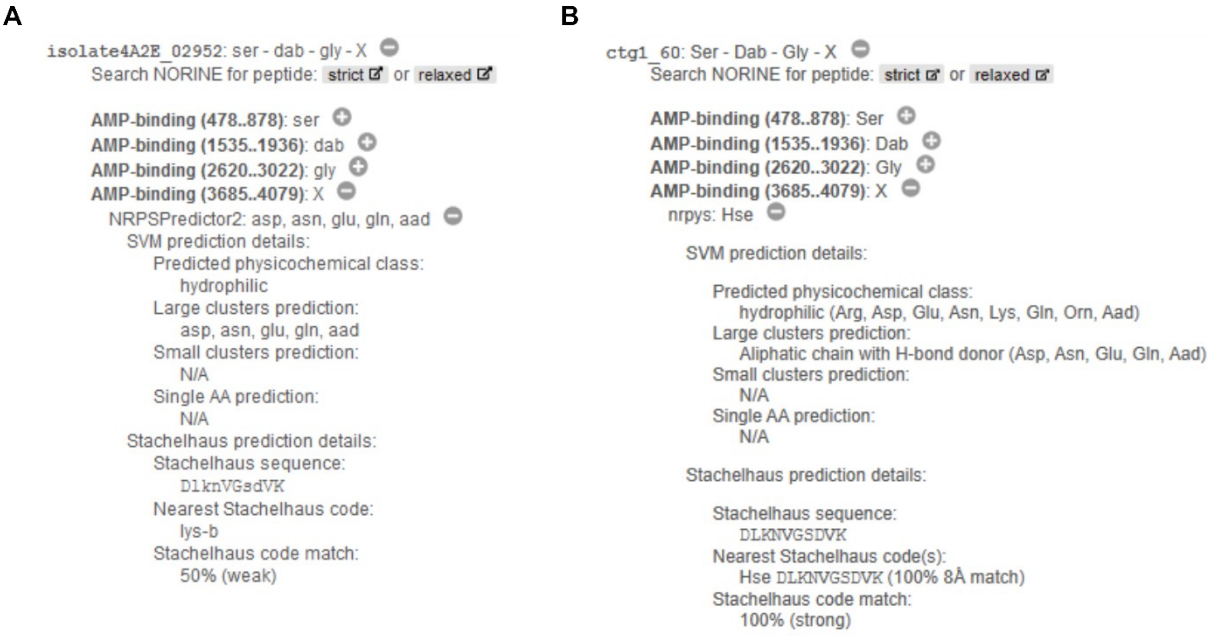

Figure S5 Amino acid specificity prediction for module 4 of KeaA. *In silico* analysis of amino acid substrate specificity for module 4 does not predict an unambiguous substrate candidate ("X") in antiSMASH version 5.1.0 and version 7.0.0.[8,9] A) The predicted Stachelhaus seqence (DLKNVGSDVK) shows little confidence ("50% (weak)") for an amino acid match in antiSMASH version 5.1.0. B) The same Stachelhaus sequence matches with homoserine (Hse) as putative amino acid substrate strongly ("100% (strong)") in version 7.0.0. The predicted substrate preference for Hse was later supported experimentally by Marfey's analysis.

Further analysis of genes adjacent to the NRPS genes of brabantamide, keanumycin and nunapeptin revealed the presence of three bacterial regulatory proteins (NupR1, NupR2, NunF) belonging to the LuxR family and an autoinducer synthase (PcoI) (Figure S6; tables S3 and S4). Closer inspection showed that NupR1 contains both a LuxR-type DNA-binding HTH domain and an autoinducer binding domain, while NupR2 and NunF only contain a LuxR-type DNA-binding HTH domain (LuxR solos) (Figure S7).

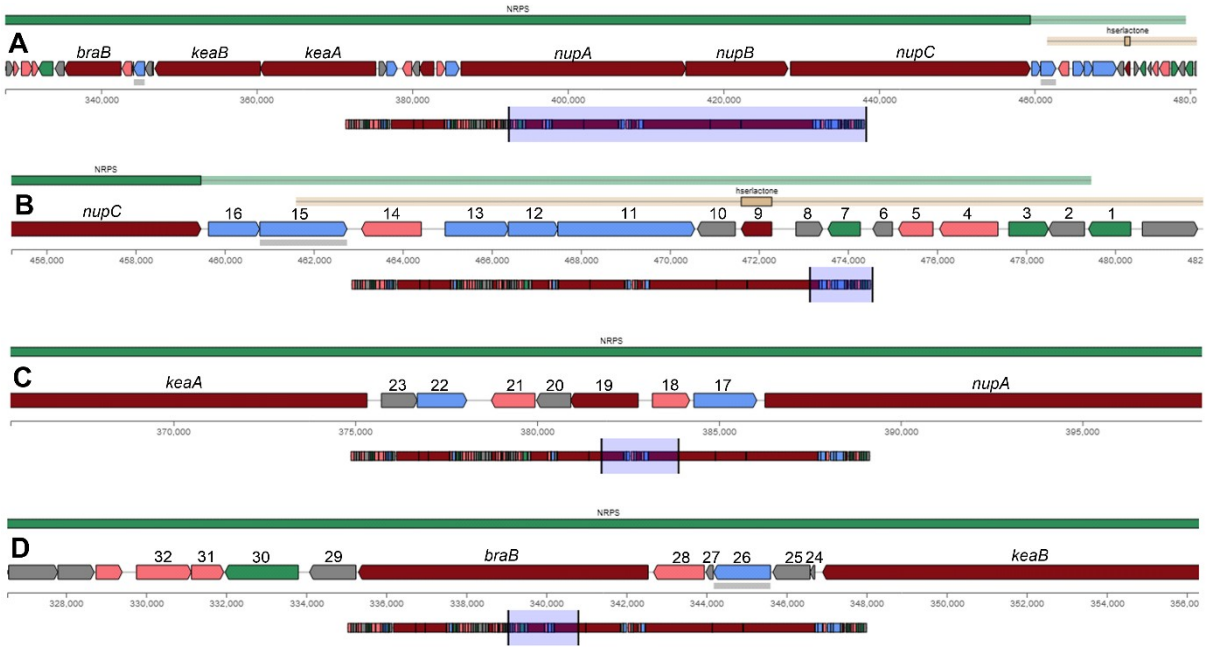

Figure S6 Detailed analysis of genes in proximity to NRPS BGCs. A) Overview. B) Genes downstream the *nup* BGC. C) Genes flanked by *keaA* and *nupA*. D) Genes downstream the *kea* BGC.

Table S3 Protein BLAST analysis of genes flanking the NRPS genes.

ORF number	prediction	E value	NCBI accession number of closest match
1	LysR family transcriptional regulator	0.0	WP_054050478.1
2	putative hydro-lyase	7 E-173	WP_054614555.1
3	AraC family transcriptional regulator	0.0	WP_054614554.1
4	sugar ABC transporter substrate-binding protein	0.0	WP_163910367.1
5	L-iditol 2-dehydrogenase	0.0	WP_054614552.1
6	hypothetical protein FX983_03450	7 E-104	KAF2395464.1
7	autoinducer binding domain-containing protein	5 E-178	WP_082356697.1
8	hypothetical protein	2 E-137	WP_054614551.1
9	hypothetical protein	2 E-154	WP_054614550.1
10	helix-turn-helix transcriptional regulator	0.0	WP_163910370.1
11	efflux RND transporter permease subunit	0.0	WP_163910371.1
12	nickel and cobalt resistance protein CnrB	0.0	KAF2395470.1
13	antibiotic efflux pump outer membrane protein ArpC	0.0	KAF2395471.1
14	diaminobutyrate—2-oxoglutarate transaminase family protein	0.0	WP_163910373.1
15	MacB family efflux pump subunit	0.0	WP_054050453.1
16	macrolide transporter subunit MacA	0.0	WP_163910374.1
17	cyclic peptide export ABC transporter	0.0	WP_163914726.1
18	TauD/TfdA family dioxygenase	0.0	WP_239512095.1
19	amino acid adenylation domain-containing protein	0.0	WP_163914722.1
20	chlorinating enzyme	0.0	WP_054049640.1
21	alpha/beta hydrolase	0.0	WP_054049642.1
22	MFS transporter	0.0	WP_054049644.1
23	hypothetical protein	0.0	AHL29303.1
24	-	-	-
25	hypothetical protein FX983_06522	0.0	KAF2392037.1
26	AdeC/AdeK/OprM family multidrug efflux complex outer membrane factor	0.0	WP_163914705.1
27	hypothetical protein	6 E-37	WP_054049663.1
28	glycosyltransferase	0.0	WP_054049657.1
29	FAD-dependent monooxygenase	0.0	WP_054049661.1
30	ATP-binding protein	0.0	WP_163914699.1
31	NADPH-dependent oxidoreductase	6 E-177	WP_163914696.1

32	LLM class flavin-dependent oxidoreductase	0.0	WP_163914694.1

Table S4 InterProScan results for analysis of genes flanking the NRPS genes. Results for Pfam database matches are listed.

ORF number	name	accession
1	LysR substrate binding domain	PF03466
	bacterial regulatory helix-turn-helix protein, lysR family	PF00126
2	D-glutamate cyclase	PF07286
3	helix-turn-helix domain	PF12833
	AraC-like ligand binding domain	PF02311
4	bacterial extracellular solute-binding protein	PF01547
5	enoyl-(Acyl carrier protein) reductase	PF13561
6	-	-
7	bacterial regulatory proteins, luxR family	PF00196
	autoinducer binding domain	PF03472
8	-	-
9	autoinducer synthase	PF00765
10	bacterial regulatory proteins, luxR family	PF00196
11	AcrB/AcrD/AcrF family	PF00873
12	barrel-sandwich domain of CusB or HlyD membrane-fusion	PF16576
13	outer membrane efflux protein	PF02321
14	aminotransferase class-III	PF00202
15	MacB-like periplasmic core domain	PF12704
	ABC transporter	PF00005
	FtsX-like permease family	PF02687
16	barrel-sandwich domain of CusB or HlyD membrane-fusion	PF16576
17	ABC transporter transmembrane region	PF00664
	ABC transporter	PF00005
18	taurine catabolism dioxygenase TauD, TfdA family	PF02668
19	AMP-binding enzyme C-terminal domain	PF13193
	AMP-binding enzyme	PF00501
	phosphopantetheine attachment site	PF00550
20	phytanoyl-CoA dioxygenase (PhyH)	PF05721
21	-	-
22	major Facilitator Superfamily	PF07690
23	cupin-like domain	PF13621
24	-	-
25	bacterial regulatory proteins, luxR family	PF00196
26	outer membrane efflux protein	PF02321
27	-	-
28	UDP-glucoronosyl and UDP-glucosyl transferase	PF00201
	glycosyltransferase family 28 N-terminal domain	PF03033
29	FAD binding domain	PF01494
30	DAHL domain	PF19443
	histidine kinase-, DNA gyrase B-, and HSP90-like ATPase	PF02518
31	nitroreductase family	PF00881
32	luciferase-like monooxygenase	PF00296

Table S5 Amino acid sequences of LuxR-type bacterial regulatory proteins (NupR1, NupR2, NunF) and the autoinducer synthase PcoI.

name	amino acid sequence
NupR1	MPKLSSSQSIFDLIQELENNIPGLNKKEYVEILEWIFGKLEVSKFAYVHMDASPFESSDIAIHSNYPAEWVETYRKNALYKSDPV MANSAITSNPFFWNEIPVESNTEIFEQSQEYGIQQGFSIPLHEPGRAFGSIHLTSEDNDPDFVRIVRENMFIIKTISIIAHQYRPIE TSTESALKLTPREHEFLHWLALGKNYKEIGLIMSITERTVKFHAKQMTEKLDCINVKQAMIKALYLNLI
PcoI	MKQFHSEFEFSGVYTSVGSYSTIPPTILEQILSIRKVAFIDRKKWDIESYQGSDYESDEYDDTDAIYIYSHQRDRVTGCVRLRPSS KPTLISGALSFMLTTDKTRPNTKHCWEATRFALAANDNCMGELNKSNIDFRTAAIFLSMIKFAFKQNVHTYEVVVDAMMEKI LKRSGWTVNRRNIAQGTKGEKVIYGTLPCTTSVFEEVFNKNTPARTTLYDEVLSDSLMAC
NupR2	MNLQRLFPHVGKVIASTGSRHFPRMLHDLIVTEVPVDATHITEQWIDDRDISELSTSSIGCVGLNNTCIDAIMDTHTVKKPYLL

	ADDIFFEDAKYQKLPDFSCCLLAQDQSDKVPPKAGAQLHLTSRKNGRRYVLSVYRSHLSQGFSPQECAFLKDFSCLLLPMVEE HVAALLPSAPSRPDAHIALDEPEHGGMETLRQRFADRLLESGLTLSSRETEVCVGLLAGHTAPELAEQFDLRVNTVESYLKRAA IKMGIGGRRSLIRWMHSVDAQSATPALRNAV
NunF	MKRNGGNLTWGQGYFRPGGRKPGQPAILVCRLMNRISSVRNIENPHIYFELGKLISSVGHEHFVANMHQLIGTSVSISLVELS EWTTDDNQGSVIDIQSLGNAGLPEELSSPSSLPCSITPRQRDEHPLLQRILEVDDSILIHMNAPMMDAKGYQLTNATHQCNL VSGKGNRRCVITLHRPLADRDFSLSELSFLKNLSETLLPLVERHARISRQVSVRKTGSPMARPVVAFEQTPLQRDFNERLTLCDV ALSAREKEVCLGLLTGGTVPEMAEKLCVKNSSVETYLKRAAAKLGVSGRHGLAKWMIGA

NupR1

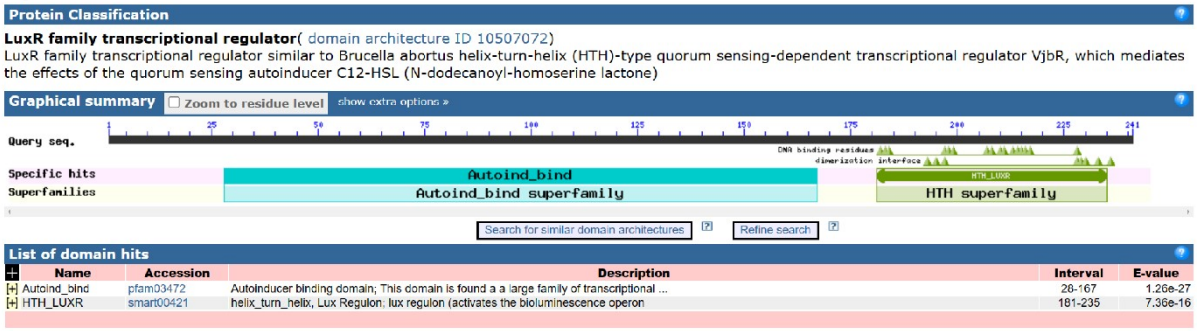

PcoI

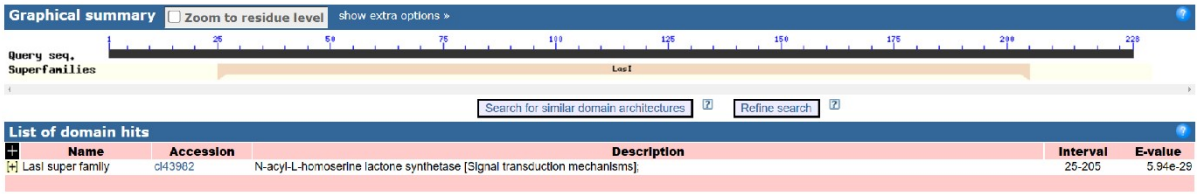

NupR2

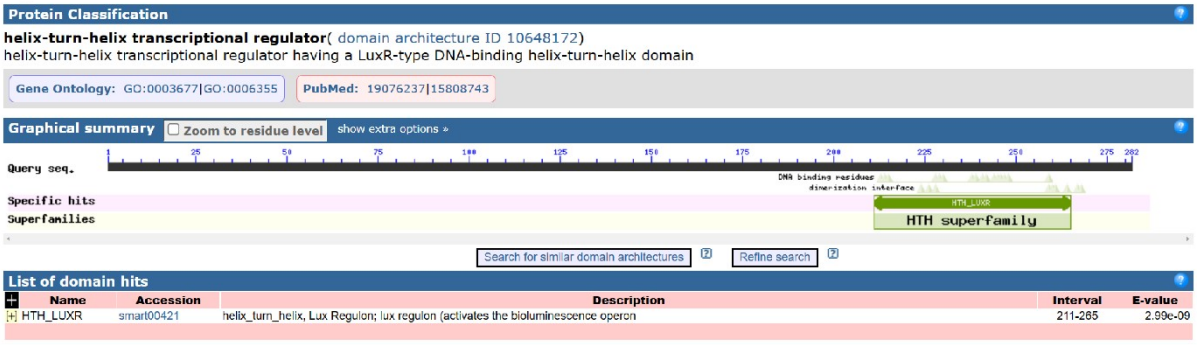

NunF

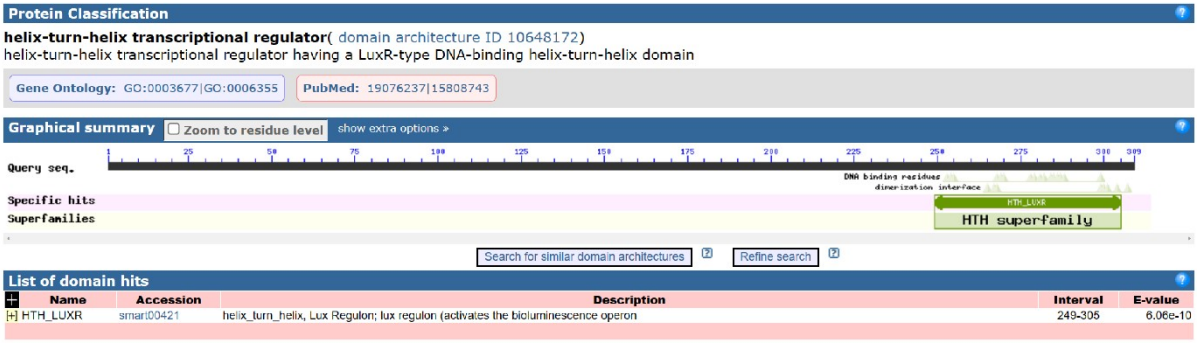

Figure S7 Conserved Domain Database/SPARCLE analysis of the autoinducer synthase PcoI and LuxR-type regulatory proteins NupR1, NupR2, and NunF against the CD database version 3.20.[10]

Phylogenetic analysis

To confirm the identity of the *Pseudomonas* species from which the BGC is recovered, an approximate maximum likelihood phylogenetic tree was constructed. All code used to generate the following genomic based analysis and supplementary tables can be found on (https://github.com/Darcy220606/NRPS-Pnunensis4A2e). A total of 1,432 'reference' and 'complete' genomes were downloaded from the assembly database[11] from NCBI on the 16th of April 2023 using entrez-direct version 15.6 (Supplementary table 1a).[12] This does not consider genomes in scaffolds or contig formats. *Aestuariirhabdus haliotis* (GCF_023509475.1) was used as the outgroup for the phylogenetic tree. The *de novo* phylogenetic tree was constructed using gtotree version 1.7.07.[13] All distant clades with closely related genomes were collapsed, when possible, for label legibility (Figure S8A). The unknown *Pseudomonas* genome was found to cluster with *Pseudomonas* sp. B21-053 (GCF_026016365.1) and *Pseudomonas nunensis* In5 (GCF_024296925.1). As the tree is based on the alignment of the amino acid sequences of all representative Gammaproteobacteria 203 core genes - which might create an alignment bias - we further investigated the cluster based on the nucleotide identities. The tree was pruned to only include the genomes occupying the parent clade of the unknown *Pseudomonas* sp. genome. This included 19 genomes (Supplementary table 1b). With these genomes a phylogenetic distance tree based on the average nucleotide identities (ANI) was constructed (Figure S6B). This was done using fastANI version 1.33[14] (Supplementary table 2), whilst excluding any contigs below 3,000 bp within the genomes. This analysis further confirms that the 4A2e genome shares >95% ANI with *Pseudomonas nunensis* In5 (GCF_024296925) and *Pseudomonas* sp. B21-053 (GCF_026016365) making it more likely to be a new strain of *Pseudomonas nunensis* which we term here as *Pseudomonas nunensis* 4A2e.

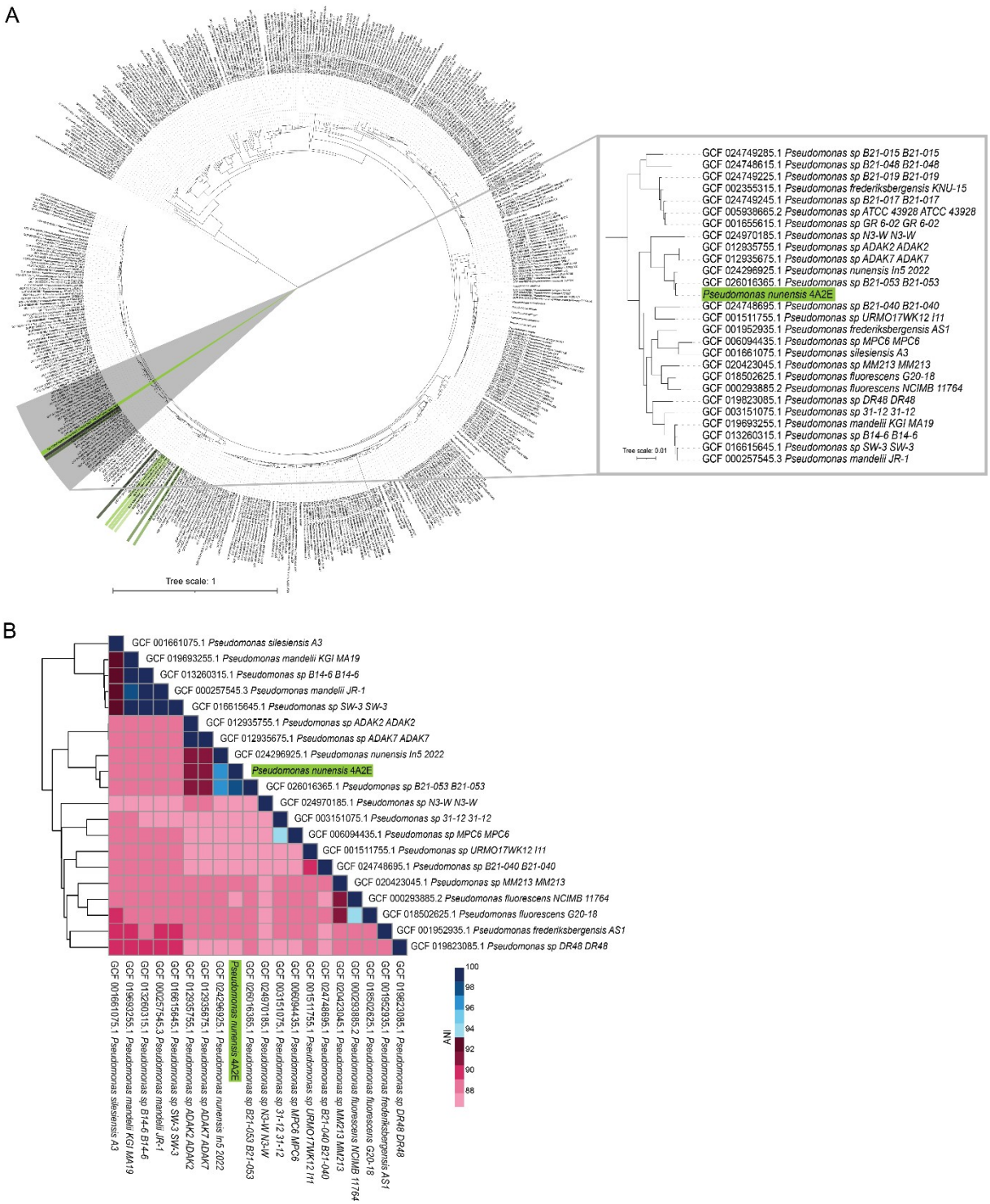

Figure S8 Alignment of *Pseudomonas nunensis* 4A2e with other closely related reference genomes. A) An approximate maximum likelihood phylogenetic tree illustrating the clustering of the *Pseudomonas nunensis* 4A2e with *Pseudomonas* sp. B21-053 (GCF_026016365.1) and *Pseudomonas nunensis* In5 (GCF_024296925.1) reference genomes in one clade based on the amino acid alignment of all representative Gammaproteobacteria core genes. Some genomes are highlighted to indicate their relationship to the BGC of interest as indicated in Figure S9. B) A heatmap illustrating the average nucleotide identities value across all genomes found in the parent clade within which the *Pseudomonas nunensis* 4A2e genome was found.

To screen for similar NRPSs with complementary topologies to that found in *Pseudomonas nunensis* 4A2e in the reference database, tblastn from *Blast+ version 2.12.0+* was carried out using the gene *tycC_4* (*keaB*) as a query. The number of maximum sequences to be recovered was set at 100 and the E value to 0.05. The nucleotide database was downloaded on April 9 2023. Multi subject high-scoring segment pairs (HSPs) were limited to one HSP hit with the longest alignment lengths. A total of 24 genomes shared more than 75% amino acid similarity and more than 95% coverage with the *tycC_4* found in

Pseudomonas nunensis 4A2e (Supplementary table 3). Their genomes were downloaded and annotated using Prokka version 1.14.6.[15] The QS1027 corresponding to accession number MW331495 was replaced by the complete contig just uploaded to the NCBI under accession number (OR047437). The genbank files were sliced to include only 20 CDSs downstream and upstream of the *tycC_4* gene. Some genomes were removed from further downstream analysis due to a missing *tycC_4* gene annotated, a completely different gene topology with no significant linkage to the gene topology of the query BGC or a truncated sequence fragment of a genome already represented. This was used as input to clinker version 0.0.27[16] to generate a gene topology across the NRPS (Figure S9).

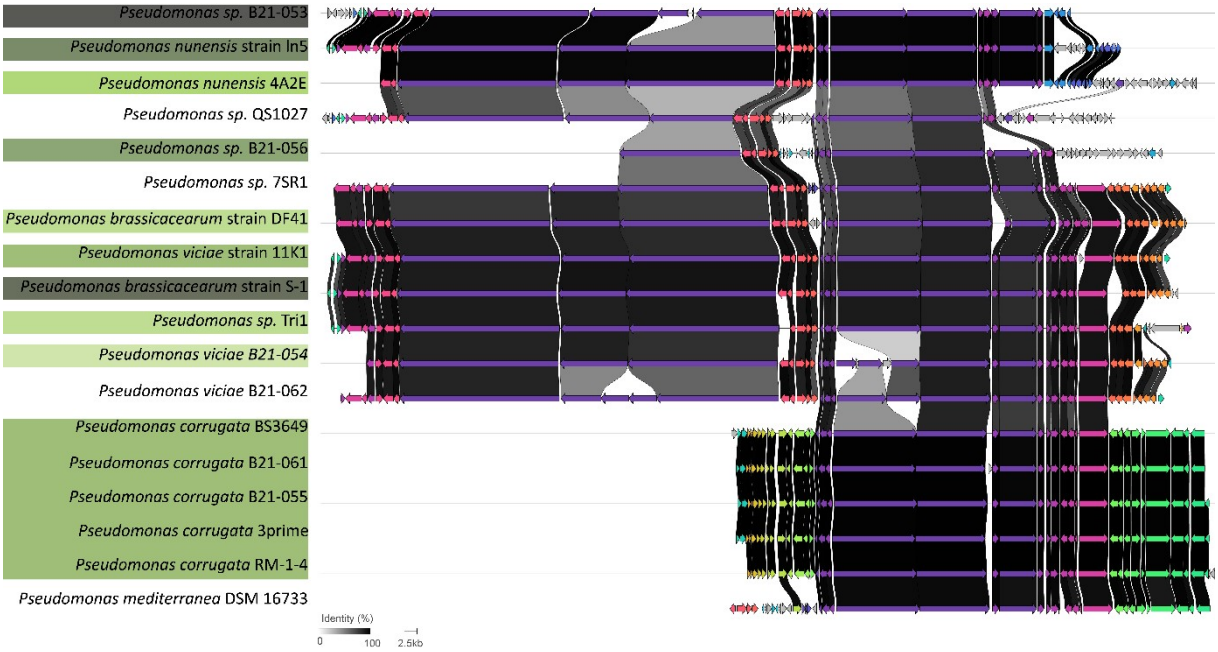

Figure S9 Gene synteny across the NRPS genomic island based on the presence of *tycC_4* (*keaB*) gene using clinker. Approximately 20 CDS are illustrated downstream and upstream of the gene. Any genes without a gene ID were annotated as hypothetical protein with no gene ID. Similar to the genome level alignments (Figure S8), *Pseudomonas nunensis* strain In5 contains an identical NRPS topology. The genomes used in this analysis were highlighted (if they correspond to the representative complete and reference genome) in the full Pseudomonas tree (Figure S8) for ease of traceability.

From the 17 bacterial genomes linked to 4A2e, *Pseudomonas nunensis* In5, *Pseudomonas* sp. QS1027 and *Pseudomonas brassicacearum* DF41 have been the source of cyclic lipopeptides similar to those described in this work, and which were at least analysed with MS^2 (Figure S10A).[17–20] Therefore, we chose these genomes for a closer comparison of their genomic architecture (Figure S10B). Although specificity differs for some modules in the NRPSs, thereby resulting in the diversity of known lipopeptides, the overall gene topology appears quite conserved across these pseudomonads. Putative regulatory (NupR1, PcoI, NupR2 in 4A2e and In5) and transporter genes are located downstream the peptin BGC. The intergenic region between the peptin and mycin BGC shows an array of a transporter, dioxygenase (KeaF) and three genes involved in the biosynthesis and incorporation of 4-Cl-Thr in the mycin biosynthesis (KeaC–KeaE), while another transcriptional regulator (NunF in 4A2e and In5) and transporter are located downstream of the mycin BGC.

A

peptin family

strain	lipid	AA1	AA2	AA3	AA4	AA5	AA6	AA7	AA8	AA9	AA10	AA11	AA12	AA13	AA14	AA15	AA16	AA17	AA18	AA19	AA20	AA21	AA22
QS1027	C_{18}OH	Dhb	Pro	Ile	Val	Ala	Ala	Ala	Val	Ser	Ala	Val	Ala	Leu	Dhb	Thr	Ala	Dab	Ser	Phe			
4A2e	C_8	Dhb	Pro	Ala	Ala	Ala	Val	Ala	Dhb	Ser	Val	Ile	Dha	Ala	Val	Ala	Val	Dhb	Thr	Ala	Dab	Ser	Ile
In5	C_{12}OH	Dhb	Pro	Ala	Ala	Ala	Val	Ala	Dhb	Ser	Val	Ile	Dha	Ala	Val	Ala	Val	Dhb	Thr	Ala	Dab	Ser	Ile
DF41	C_{10}OH	Dhb	Pro	Ala	Ile	Ala	Val	Val	Dhb	Thr	Val	Ile	Dha	Ala	Ala	Ala	Val	Dhb	Dhb	Ala	Dab	Ser	Val

mycin family

strain	lipid	AA1	AA2	AA3	AA4	AA5	AA6	AA7	AA8	AA9
QS1027	C_{16}OH	Ser	Dab	Gly	Hse	Dab	Thr	Dhb	3-OH-Asp	4-Cl-Thr
4A2e	C_{14}OH	Ser	Dab	Gly	Hse	Dab	Thr	Dhb	3-OH-Asp	4-Cl-Thr
In5	C_{14}OH	Ser	Dab	Gly	Hse	Dab	Thr	Thr	3-OH-Asp	4-Cl-Thr

B

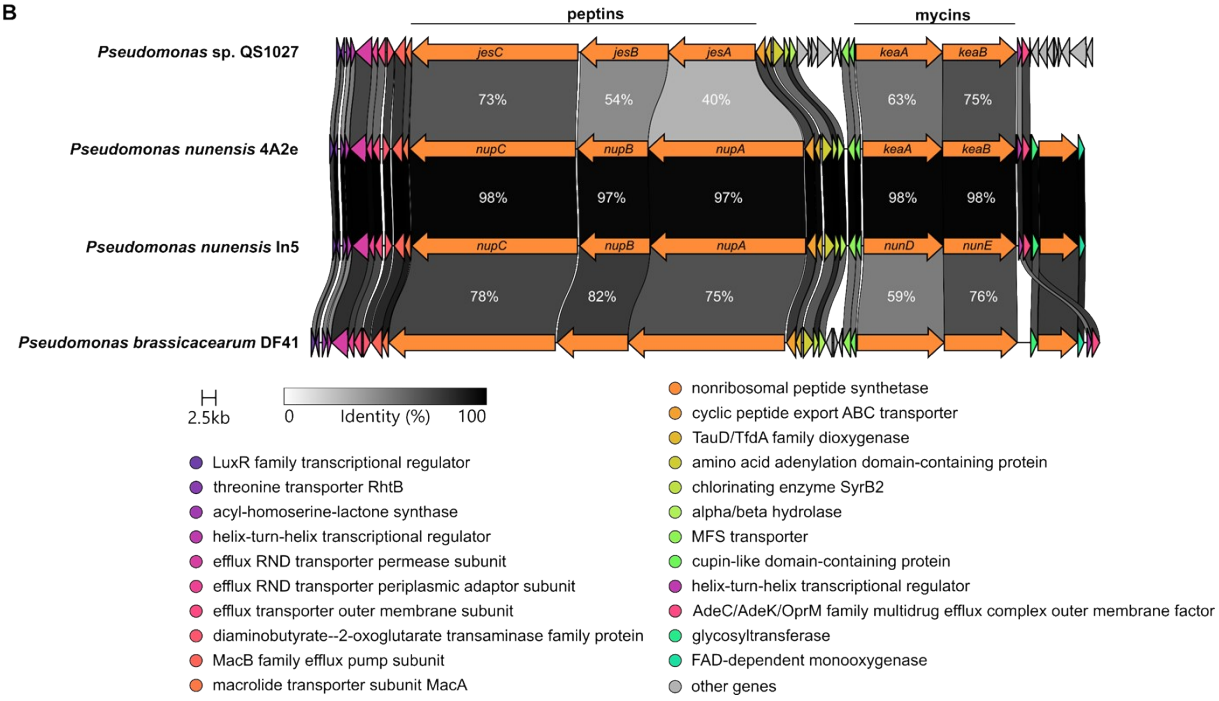

Figure S10 Comparison of NRPS genomic islands across pseudomonads with MS^2-analysed cyclic lipopeptides similar to keanumycin D and nunapeptins C. A) Amino acid sequences of jessenipeptin and keanumycin B from *Pseudomonas* sp. QS1027, nunapeptin and nunamycin from *Pseudomonas nunensis* In5, and sclerosin (peptin-like) from *Pseudomonas brassicacearum* DF41 (no characterised mycin-like lipopeptide). Lipid: C_x: x indicates the number of carbon atoms in the acyl chain; OH: indicates beta-hydroxylation of the acyl chain. Green shading indicates amino acids involved in lactone formation. B) Gene synteny across the NRPS island and blastp analysis of the respective proteins from 4A2e.

Metabolic analysis of wild type 4A2e and mutant strains

In order to link the production of natural products with the respective BGCs, we cultivated the wild type and NRPS gene deletion mutants in SM/5 broth or modified Davis medium (10 mL in 250 mL Erlenmeyer flasks) on a gyratory shaker (22 °C, 180 rpm) for 2 days. Culture aliquots (500 µL) were mixed with an equal amount of MeOH and centrifuged (21,000 x *g*, 5 min). The resulting supernatant was filtered (PTFE, 0.22 µm) and subjected to LCMS analysis using the standard method (see: "Liquid chromatography – mass spectrometry (LCMS)"). A comparison of total ion chromatograms revealed, that the main peaks correlated with an intact *kea* BGC appear around 4.4–4.6 min, whilst peaks of putative brabantamide (*bra* BGC; 5.9–6.0 min) and peptin (*nup* BGC; 7.7–8.2 min) congeners appear later.

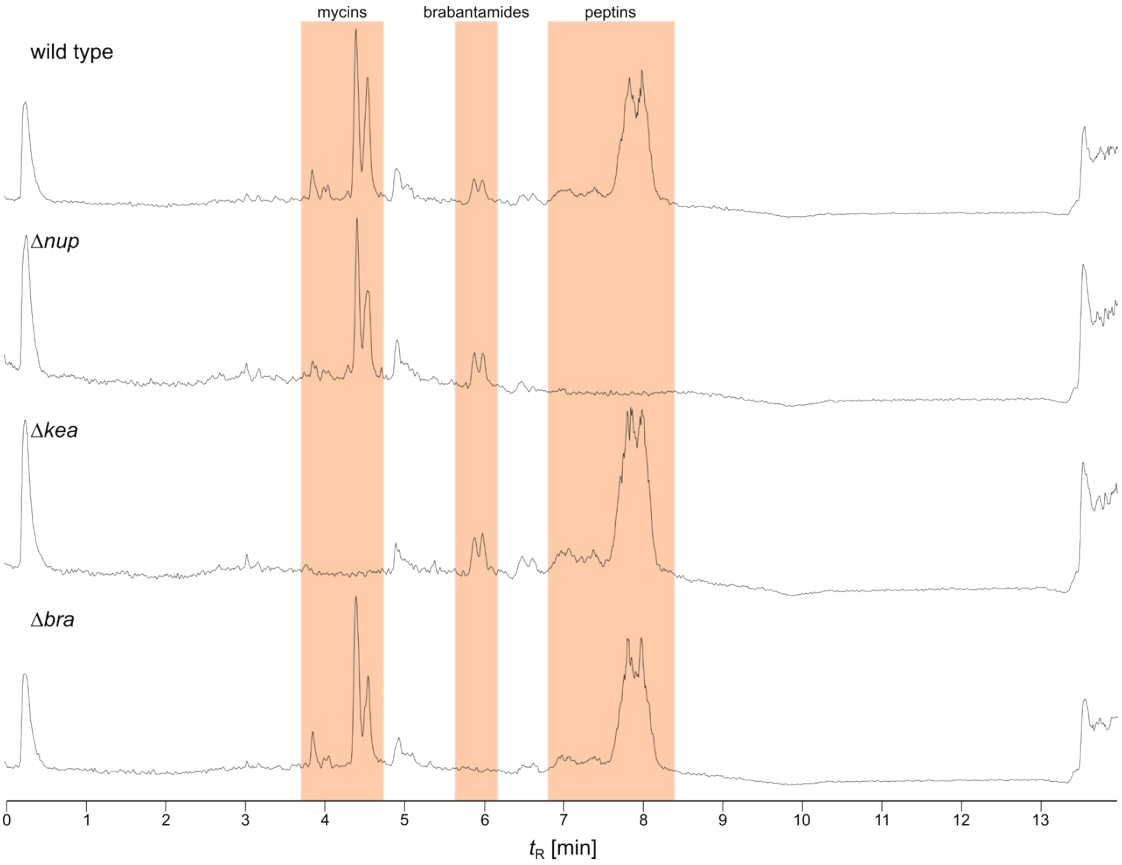

Figure S11 Total ion chromatograms (positive mode) of extracts of wild type 4A2e and gene deletion mutants cultivated in modified Davis medium. All chromatogram profiles are displayed at the same scale.

Regulation of nonribosomal peptide biosynthesis

Overnight cultures of wild type (WT) *Pseudomonas nunensis* 4A2e and the respective gene deletion mutants were used to inoculate 10 mL modified Davis medium in 250 mL Erlenmeyer flasks, and cultures were incubated on a gyratory shaker (22 °C, 180 rpm) for two days. A 500 µL aliquot of each bacterial suspension was mixed with MeOH (500 µL) and centrifuged (21,000 x *g*, 5 min). The resulting supernatant was filtered (PTFE, 0.22 µm) and subjected to LCMS analysis using the standard method.

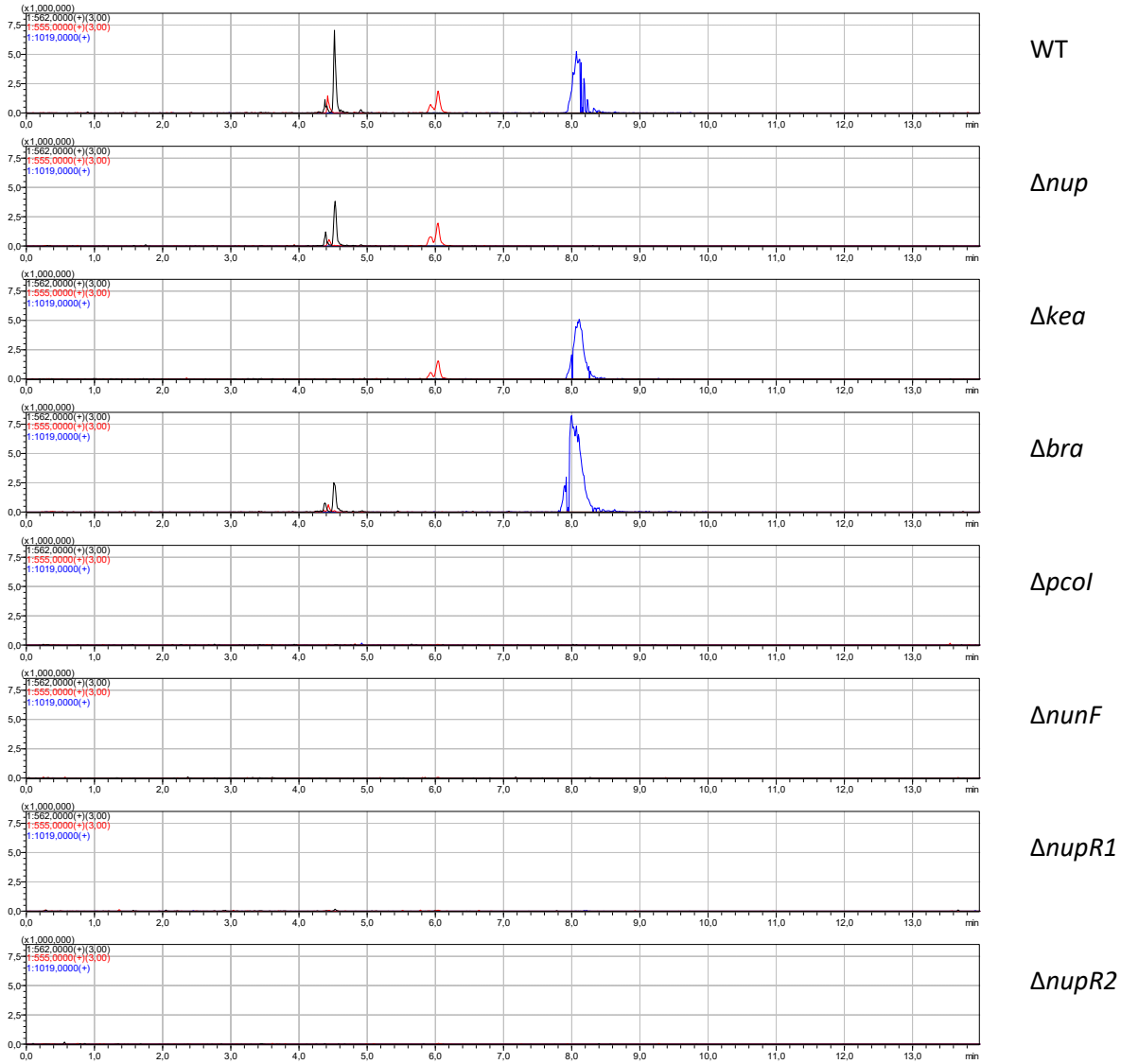

Figure S12 Regulation of NRP biosynthesis. Extracted ion chromatograms for keanumycin D (*m/z* 562 $[M+2H]^{2+}$, black), brabantamide A (*m/z* 555 $[M+H]^{+}$, red), and nunapeptin C (*m/z* 1019 $[M+2H]^{2+}$, blue) for wild type 4A2e and gene deletion mutants.

For further identification of the putative signal of the autoinducer synthase PcoI, we compared extracted ion chromatograms of different homoserine lactones for the wild type and the Δ*pcoI* mutant and found *N*-hexanoyl-homoserine lactone to be the most likely candidate. Hence, we extracted both wild type and Δ*pcoI* cultures (modified Davis medium, 100 mL respectively) after two days with *i*PrOH/$CHCl_3$ (1:1 (v/v), 600 mL), dried the organic layers with anhydrous Na_2SO_4, and concentrated the extracts *in vacuo*. LCMS analysis showed the presence of a molecule (*m/z* 200.1 in pos. mode) in the wild type extract, which was absent in the mutant, and shared the same retention time (t_R = 1.44 min) with a synthetic standard of *N*-hexanoyl-L-homoserine lactone (Figure S12).

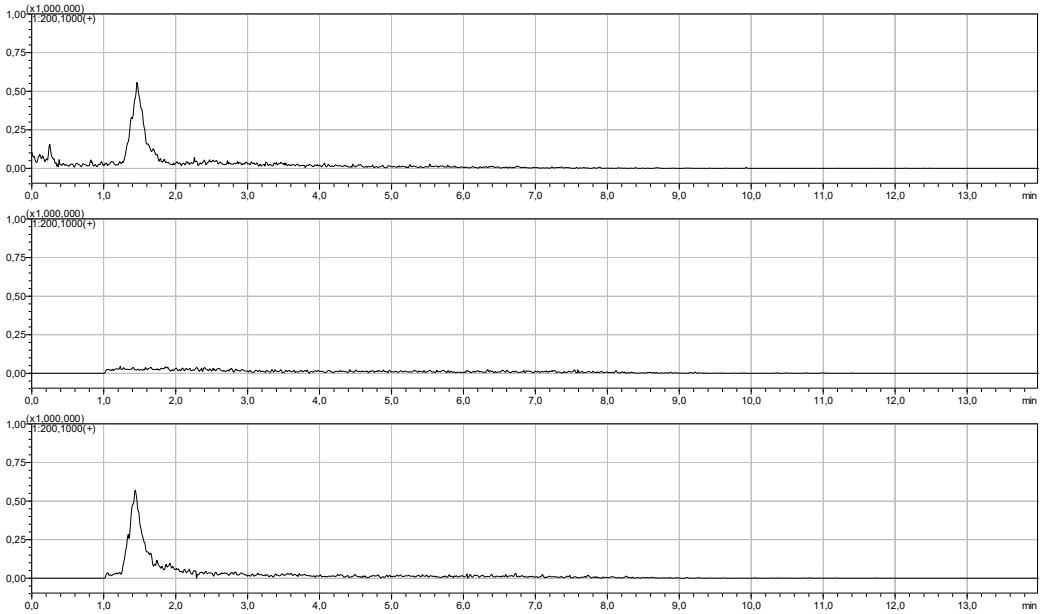

Figure S13 Identification of *N*-hexanoyl-L-homoserine lactone (C6-HSL) as autoinducer in 4A2e. Extracted ion chromatograms of C6-HSL (*m/z* 200.1 $[M+H]^+$, t_R = 1.44 min) for WT, Δ*pcoI* and synthetic C6-HSL.

To restore nonribosomal peptide biosynthesis in the Δ*pcoI* mutant, we spiked the culture medium with synthetic C6-HSL. Aliquots of overnight cultures (200 µL from 2 mL) of WT and Δ*pcoI* were used to start new cultures (10 mL in 250 mL Erlenmeyer flasks), which were incubated on a gyratory shaker (180 rpm, 22 °C) for 7 hours. 100 µL DMSO was added to WT and a Δ*pcoI* culture, while 100 µL of a C6-HSL stock (100 µM in DMSO) was added to a second Δ*pcoI* culture. Cultivation was continued for another 18 h and aliquots (500 µL) of the respective cultures analysed as described above.

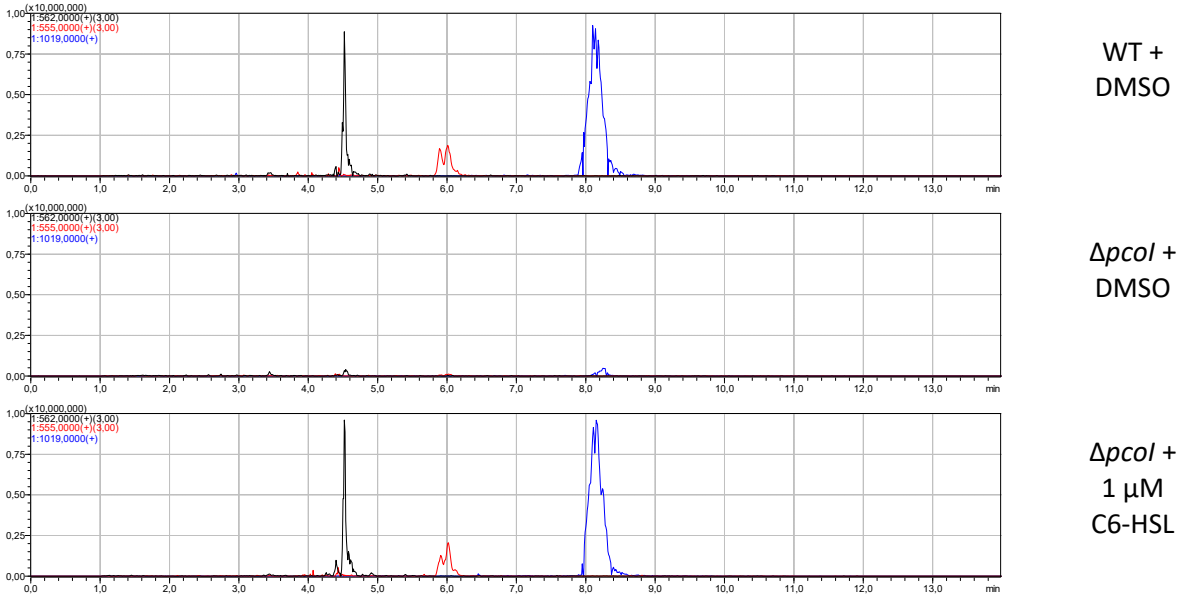

Figure S14 Restoration of NRP production in Δ*pcoI*. Extracted ion chromatograms for keanumycin D (*m/z* 562 $[M+2H]^{2+}$, black), brabantamide A (*m/z* 555 $[M+H]^+$, red), and nunapeptin C (*m/z* 1019 $[M+2H]^{2+}$, blue) for WT, Δ*pcoI*, and Δ*pcoI* supplemented with synthetic C6-HSL.

Plaque assays with WT 4A2e and gene deletion mutants

The edibility of WT 4A2e and various gene deletion mutants was tested in a 24-well plate format as previously described.[18,21,22] Bacteria were grown in SM/5 broth at 28 °C overnight, and 30 µL of a bacterial suspension was used to inoculate a single well with SM/5 agar, respectively. Plates were left to dry in a laminar flow hood for ca. 2 h.

Amoebae were grown in submerged *Klebsiella aerogenes* cultures in SM/5 broth (120 rpm, 22 °C) for 2 days, until amoebae reached the late exponential phase. Cells were harvested, and washed by repeated centrifugation (500 x *g*, 5 min) and resuspension in cold Sörensen's buffer until the supernatant remained clear. The cell concentration was adjusted to 2,000 cells/µL and 5 µL of the respective suspension was used to seed a single well with bacterial lawn. Subsequently, assays were incubated at 22 °C for 14 d. The assays were performed in biological triplicates of technical duplicates.

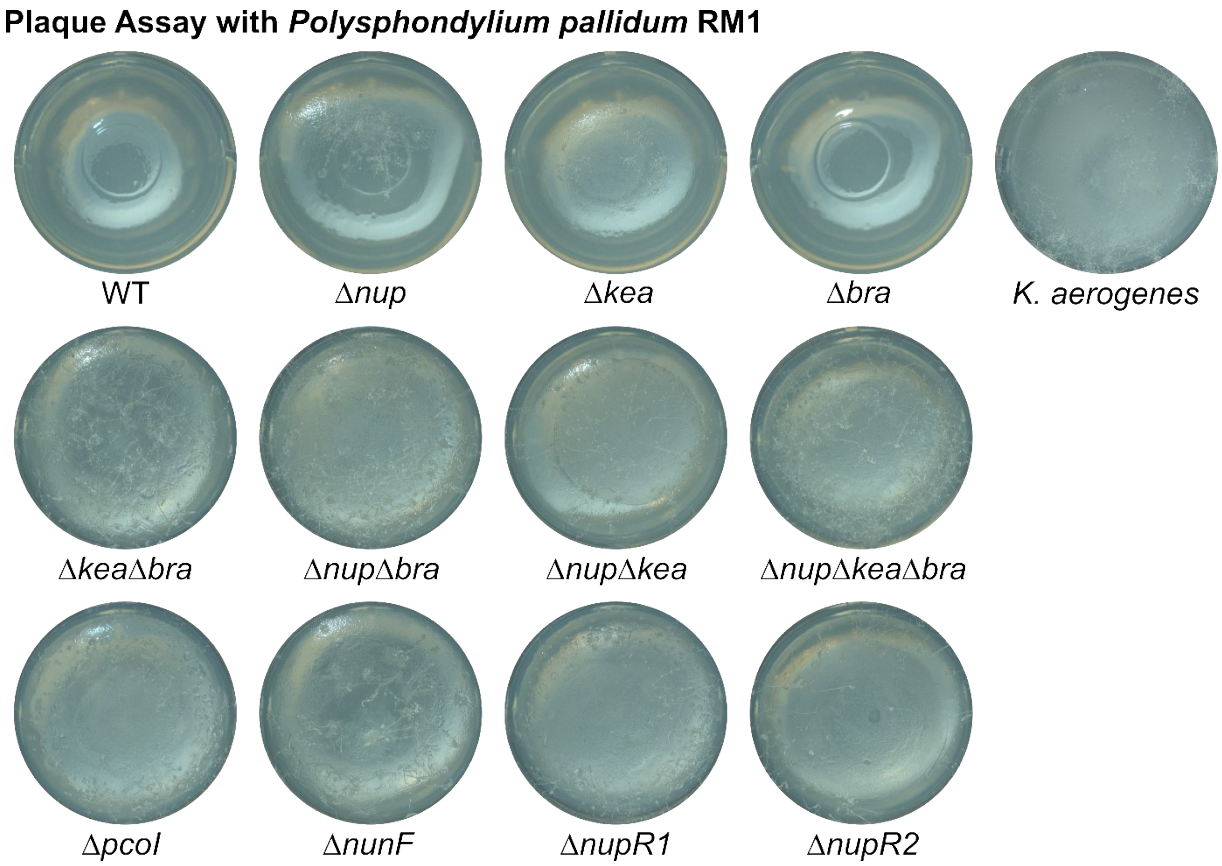

Figure S15 Edibility assays with *Polysphondylium pallidum* RM1.

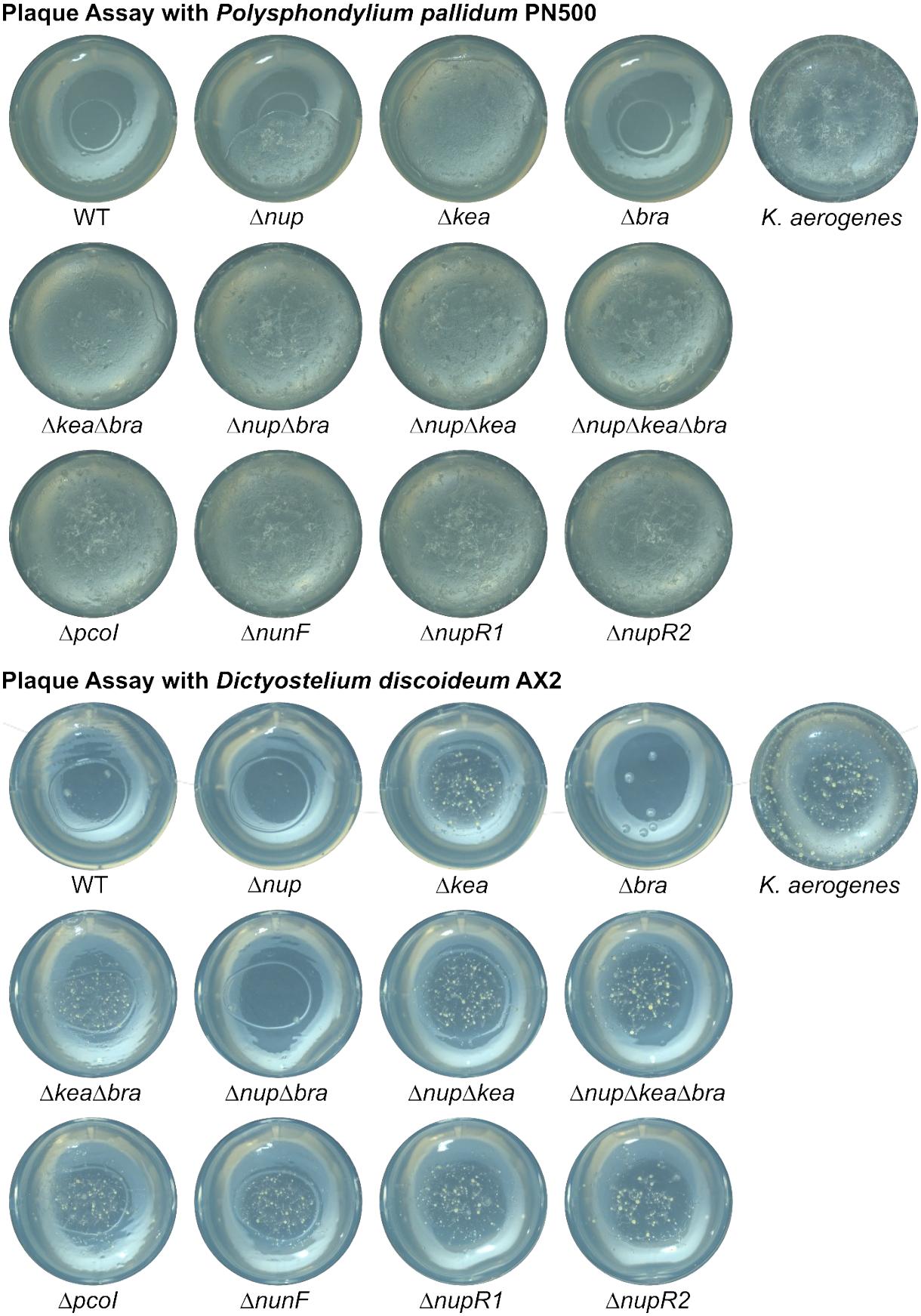

Figure S16 Edibility assays with *Polysphondylium pallidum* PN500 and *Dictyostelium discoideum* AX2.

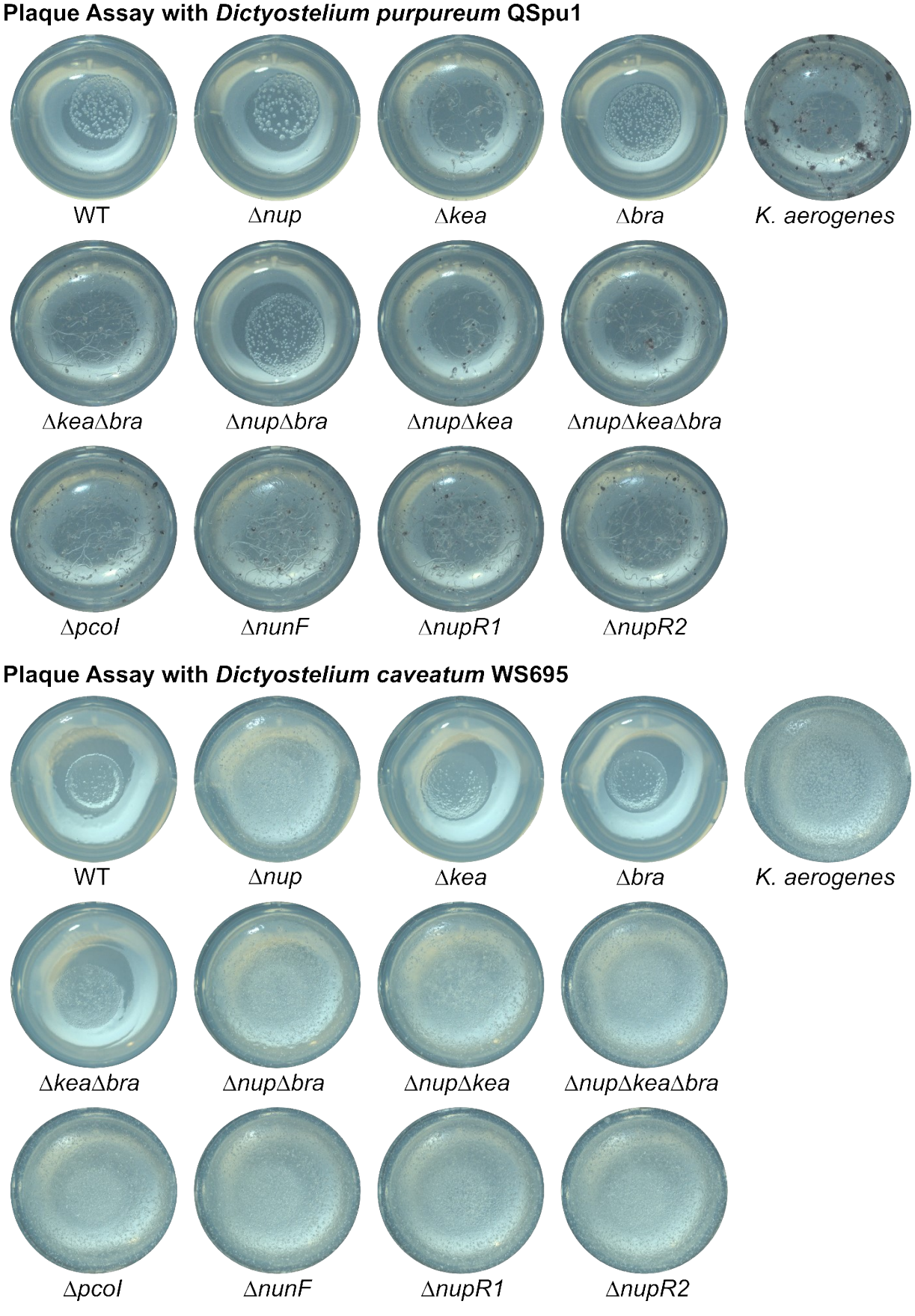

Figure S17 Edibility assays with *Dictyostelium purpureum* QSpu1 and *Dictyostelium caveatum* WS695.

Growth inhibition assays

Growth inhibition of *Dictyostelium discoideum* AX2

The amoebicidal activity of the lipopeptides was evaluated as previously described.[22] Briefly, *Dictyostelium discoideum* AX2 cells were cultivated in 96-well plates (3,000 cells/well) containing HL5 + 1% DMSO (200 µL/well) and a specific amount of compound (starting from 50 µg/mL for peptins and brabantamide A, and from 0.5 µg/mL for keanumycin D; 2-fold serial dilution). Dilution series were performed in triplicates and plates incubated at 22 °C for 72 h. Cell concentrations were determined using a CASY® Cell Counter + Analyser System (Model TT, Roche Innovatis AG) equipped with a 60 µm capillary and the evaluation cursor set to 7.5 – 17.5 µm. The concentration of viable cells (including standard deviation) was plotted against the logarithmic concentration of the compounds and the IC_{50} values were determined using PRISM (GraphPad, version 5.03). The presented values are results of three biological replicates.

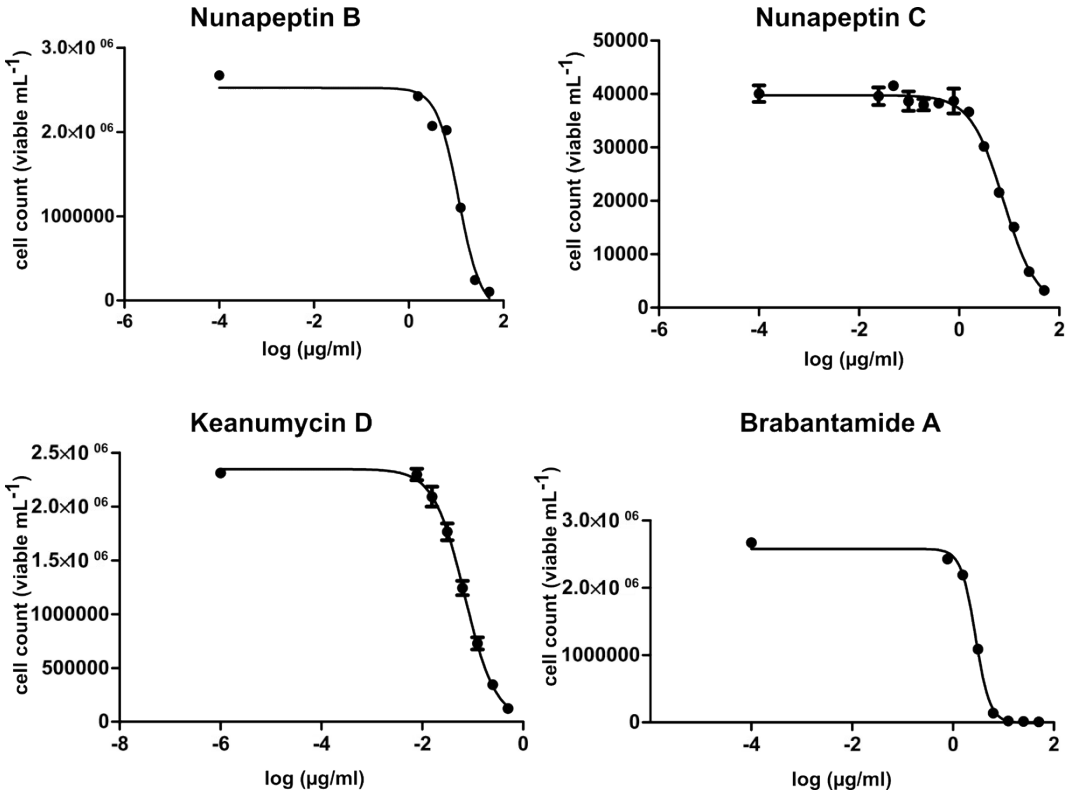

Figure S18 Dose-response curves for the amoebicidal activity of nonribosomal lipopeptides against *Dictyostelium discoideum* AX2.

Growth inhibition of *Acanthamoeba castellanii* and *A. comandoni*

The amoebicidal activity of the lipopeptides against *Acanthamoeba castellanii* and *A. comandoni* was determined as previously described for keanumycin A.[19] Briefly, *Acanthamoeba* cells were cultivated in 96-well plates (1,250 cells/well) containing PYG medium + 1% DMSO (100 µL/well) and a specific amount of compound (starting from 50 µg/mL; 2-fold serial dilution). Dilution series were performed in triplicates and plates incubated at 28 °C for 96 h. Cell viability was determined by a resazurin-based assay. A freshly prepared aqueous resazurin solution (20 µL, 1 mM, resazurin sodium salt) was added to every well, and plates were incubated at 28 °C for 3 h. A plate reader (Tecan, Infinite M200 PRO, excitation at λ = 560 nm, emission at λ = 590 nm) was used to determine the fluorescence emission. The fluorescence intensity (including standard deviation) was plotted against the logarithmic concentration of the compounds and the IC_{50} values were determined using PRISM (GraphPad, version 5.03). The presented values are results of three biological replicates.

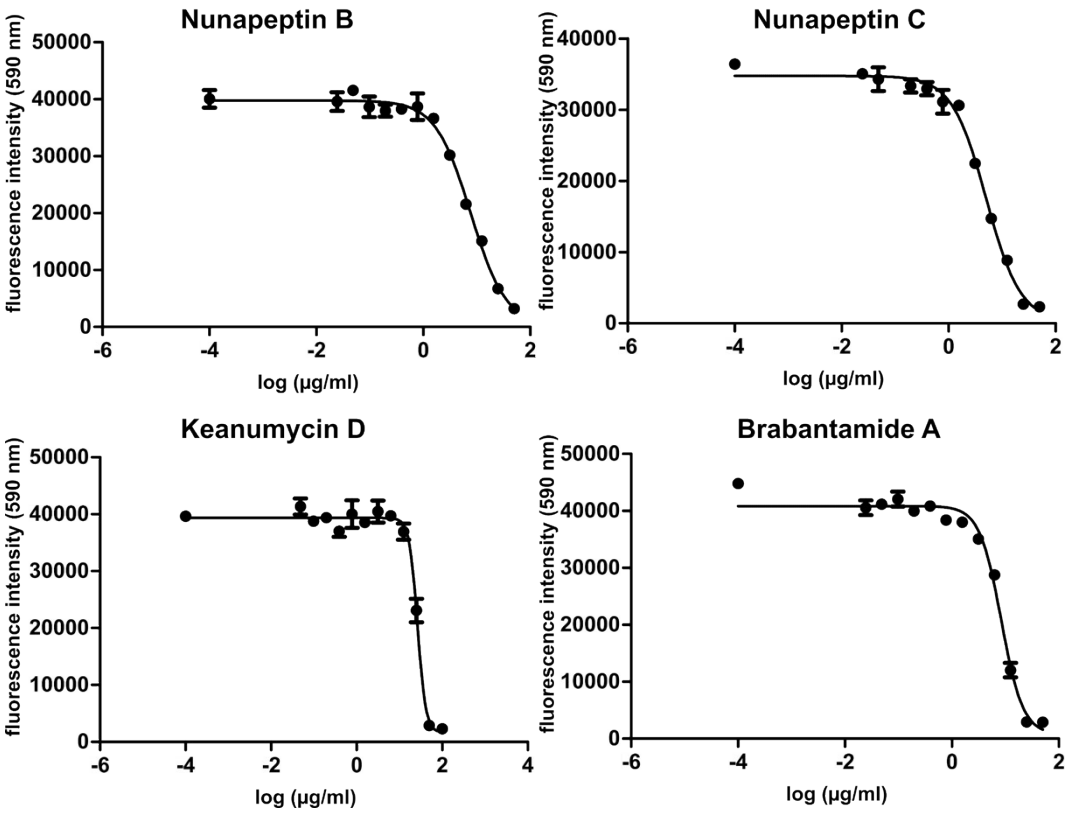

Figure S19 Dose-response curves for the amoebicidal activity of nonribosomal lipopeptides against *Acanthamoeba castellanii.*

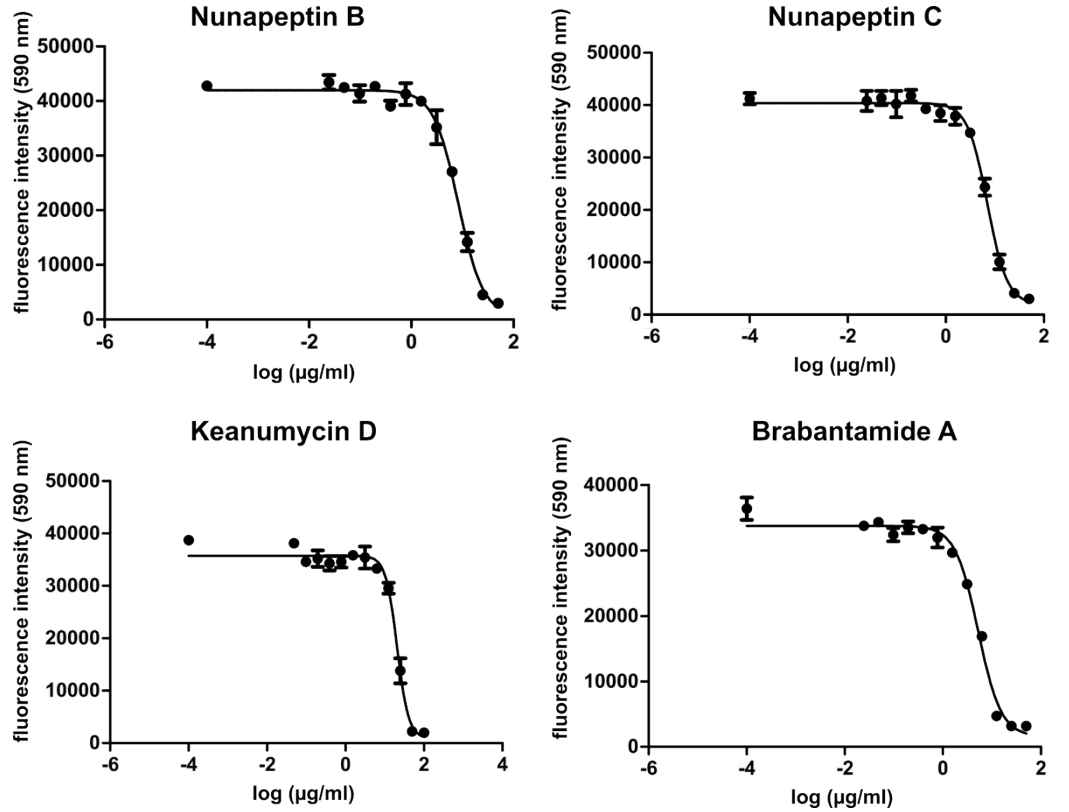

Figure S20 Dose-response curves for the amoebicidal activity of nonribosomal lipopeptides against *Acanthamoeba comandoni*.

Table S6 Amoebicidal activity of nonribosomal lipopeptides against amoebae. Average IC_{50} values are the result of three independent biological replicates.

	Average IC_{50}			
Organism	Nunapeptin B	Nunapeptin C	Keanumycin D	Brabantamide A
Dictyostelium discoideum AX2	11.5 µg/mL 5.7 µM	6.2 µg/mL 3.1 µM	83 ng/mL 74 nM	2.6 µg/mL 4.7 µM
Acanthamoeba castellanii	7.2 µg/mL 3.5 µM	5.3 µg/mL 2.6 µM	25.6 µg/mL 22.8 µM	8.1 µg/mL 14.6 µM
Acanthamoeba comandoni	8.1 µg/mL 4.0 µM	6.8 µg/mL 3.3 µM	23.2 µg/mL 20.6 µM	4.9 µg/mL 8.9 µM

Bacteria–nematode co-cultivation assay

Aliquots of overnight cultures of WT 4A2e and the respective gene deletion mutants were used to inoculate co-cultivation agar plates, which were subsequently incubated at 28 °C overnight. Starved nematodes were washed from NGM agar plates by flooding the plates with sterile K-medium (3 x 4.5 mL) and the suspension was transferred into a 15 mL conical tube. Worms were gently pelleted by centrifugation (250 x *g*, 2 min). The supernatant was removed and the nematodes washed by repeated resuspension in K-medium and centrifugation, until the supernatant remained clear. The concentration was adjusted to 400 – 800 animals/mL. Then, the nematode suspension (100 µL) was added to the bacterial lawn, and the plates incubated at 22 °C in a humid environment for 10 d. Thereafter, worms were gently washed of the agar by flooding the plate with K-medium (3 x 4.5 mL) and the suspension was transferred into a 15 mL conical centrifuge tube. Nematodes were washed by repeated centrifugation (250 x *g*, 2 min) and resuspension in K-medium, until the supernatant remained clear. An aliquot of the suspension was transferred to a nematode counting dish and the number of viable worms counted manually using a stereo microscope.

The nematode count for each strain was calculated based on the average of three technical replicates. For statistical analysis, the data of each experiment was normalised to the minimum and maximum nematode count. One-way ANOVA followed by Tukey's post-hoc test was performed with normalised data of four independent experiments (Supplementary table 4).

Isolation of nonribosomal lipopeptides

A pre-culture of *Pseudomonas nunensis* 4A2e in modified Davis medium (400 mL) was used to inoculate a batch fermenter (40 L) and incubated at 22 °C for 48 h. The biomass was separated from the supernatant by centrifugation (9,000 x *g*, 20 min) and freeze-dried. The supernatant was extracted with Amberlite XAD-4 resin (Alfa Aesar), which was then rinsed with deionised water and washed with MeOH. The supernatant was extracted three times in total. MeOH fractions were pooled and concentrated under reduced pressure. The residue was dissolved in a minimal amount of MeOH and dried on Isolute® HM-N (Biotage), which was loaded on a Sfär C18 cartridge (Biotage, 60 g, 100 Å, 30 µm, 85 mL column volume (CV)) and fractionated using a flash chromatography system (Biotage Isolera Prime) and the following method: flow rate of 50 mL/min; 3 CV: 10% MeCN in water containing 0.1% formic acid; 12 CV: linear gradient from 10% to 100% MeCN in water containing 0.1% formic acid; 3 CV: 100% MeCN containing 0.1% formic acid. Fractions containing keanumycin D, brabantamide A, and nunapeptin B and C were identified by LCMS, combined respectively and concentrated under reduced pressure. The lyophilised biomass was extracted with MeOH and the organic solvent separated by centrifugation (12,000 x *g*, 15 min, PPCO centrifuge bottles). The biomass was extracted twice, supernatants were combined and solvents removed *in vacuo*. The residue was dissolved in a minimal amount of warm MeOH and the solution stored in a PPCO centrifuge tube (Thermo Fisher, 50 mL) at –20 °C overnight. Precipitate was removed by centrifugation (20,000 x *g*, 5 min, –10 °C), the supernatant concentrated under reduced pressure, and the residue subjected to flash fractionation as described above.

Nunapeptins were further purified by preparative HPLC equipped with a Luna® C18(2) column (Phenomenex, 250 x 21.4 mm, 100 Å, 5 µm) and the following method: flow rate of 20 mL/min; 0 – 5 min: 10% MeCN in water containing 0.1% trifluoroacetic acid; 5 – 45 min: linear gradient from 10% to 100% MeCN in water containing 0.1% trifluoroacetic acid; 45 – 55 min: 100% MeCN containing 0.1% trifluoroacetic acid.

Nunapeptin B

^{1}H NMR (600 MHz, DMSO-d_6): δ 9.72 (s, 1H), 9.29 (s, 1H), 9.23 (d, *J* = 5.9 Hz, 1H), 9.20 (s, 1H), 9.11 (s, 1H), 8.33 (d, *J* = 7.1 Hz, 1H), 8.11 (d, *J* = 5.4 Hz, 1H), 8.07 (d, *J* = 6.8 Hz, 1H), 8.00 (br. s, 1H), 7.93 (d, *J* = 7.1 Hz, 1H), 7.87 (d, *J* = 7.7 Hz, 1H), 7.83 (d, *J* = 7.5 Hz, 1H), 7.76 (d, *J* = 8.6 Hz, 1H), 7.73 (m, 3H), 7.69 (d, *J* = 8.7 Hz, 1H), 7.59 (m, 2H), 7.52 (d, *J* = 8.3 Hz, 1H), 7.48 (d, *J* = 7.1 Hz, 1H), 7.45 (d, *J* = 8.0 Hz, 1H), 7.40 (d, *J* = 9.6 Hz, 1H), 6.43 (q, *J* = 7.0 Hz, 1H), 6.24 (q, *J* = 7.0 Hz, 1H), 5.99 (br. s, 1H), 5.53 (m, 2H), 4.89 (m, 1H), 4.43 (dd, *J* = 9.6, 4.9 Hz, 1H), 4.39 (m, 1H), 4.34 (m, 3H), 4.24 (m, 5H), 4.13 (m, 6H), 3.99 (m, 1H), 3.86

(d, *J* = 10.9, 3.3 Hz, 1H), 3.83 (m, 1H), 3.74 (t, *J* = 10.4 Hz, 2H), 3.62 (m, 4H), 3.53 (t, *J* = 6.1 Hz, 1H), 2.81 (m, 2H), 2.30 (m, 3H), 2.18 (m, 1H), 2.02 (m, 6H), 1.83 (m, 4H), 1.69 (d, *J* = 7.1 Hz, 3H), 1.66 (d, *J* = 7.1 Hz, 3H), 1.62 (d, *J* = 7.1 Hz, 3H), 1.50 (m, 4H), 1.31 (m, 6H), 1.23 (m, 26H), 1.14 (d, *J* = 6.0 Hz, 3H), 1.11 (m, 1H), 1.03 (m, 1H), 0.91 (dd, *J* = 11.6, 6.7 Hz, 6H), 0.83 (m, 35H) ppm.

^{13}C NMR (150 MHz, DMSO-d_6): δ 174.7, 172.8, 172.5, 172.4, 172.2, 172.1, 171.9, 171.8, 171.4, 170.7, 170.6, 170.0, 169.5, 168.8, 166.9, 164.2, 163.9, 163.6, 163.0, 135.3, 131.4, 131.0, 130.1, 128.8, 126.9, 118.7, 104.4, 70.7, 61.6, 61.0, 60.7, 58.7, 58.4, 57.7, 57.61, 57.56, 57.1, 56.8, 55.6, 55.3, 52.0, 49.5, 49.3, 49.2, 49.1, 49.0, 48.63, 48.59, 48.2, 37.2, 36.2, 35.6, 34.3, 31.1, 30.6, 30.24, 30.21, 30.1, 29.3, 28.6, 28.4, 27.1, 25.6, 24.7, 24.4, 24.0, 22.1, 19.3, 19.2, 19.1, 18.20, 18.15, 18.1, 17.8, 17.7, 17.6, 17.5, 17.3, 17.1, 16.7, 16.4, 15.7, 14.5, 13.9, 13.0, 12.8, 12.0, 11.8, 11.5 ppm.

HRMS (ESI, *m/z*): calculated for $C_{94}H_{157}N_{23}O_{26}$ $[M+2H]^{2+}$ 1012.0830; found 1012.0823.

Optical rotation $[\alpha]_D^{22}$: –64.7 (*c* 0.34 in MeOH).

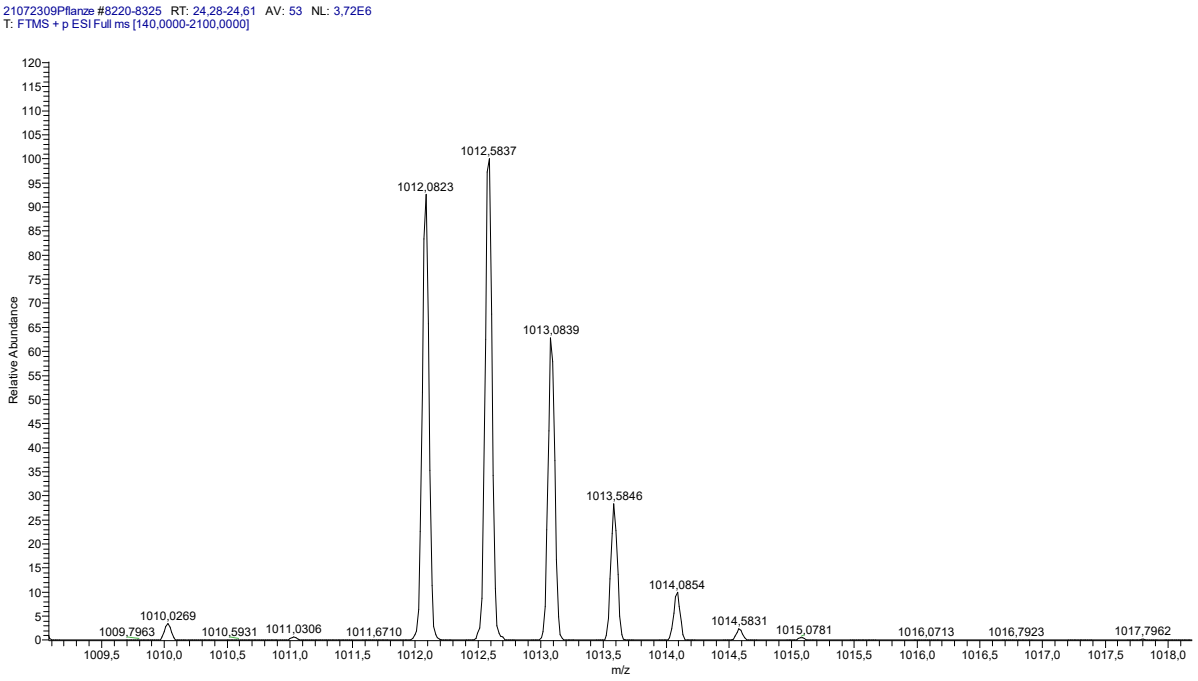

Figure S21 HRMS spectrum of nunapeptin B. HRMS (ESI, *m/z*): calculated for $C_{94}H_{157}N_{23}O_{26}$ $[M+2H]^{2+}$ 1012.0830; found 1012.0823.

Nunapeptin C

^{1}H NMR (600 MHz, DMSO-d_6): δ 9.71 (s, 1H), 9.26 (s, 1H), 9.24 (d, *J* = 6.4 Hz, 1H), 9.16 (s, 1H), 9.09 (s, 1H), 8.31 (d, *J* = 7.0 Hz, 1H), 8.06 (m, 2H), 8.02 (br. s, 1H), 7.90 (d, *J* = 7.3 Hz, 1H), 7.83 (m, 3H), 7.74 (m, 4H), 7.67 (d, *J* = 8.6 Hz, 1H), 7.58 (d, *J* = 6.8 Hz, 2H), 7.47 (m, 3H), 7.39 (d, *J* = 9.6 Hz, 1H), 6.43 (q, *J* = 7.1 Hz, 1H), 6.26 (q, *J* = 7.0 Hz, 1H), 5.98 (br. s, 1H), 5.53 (m, 2H), 4.90 (m, 1H), 4.40 (m, 3H), 4.33 (m, 3H), 4.24 (m, 6H), 4.14 (m, 7H), 3.98 (m, 1H), 3.88 (dd, *J* = 11.0, 3.6 Hz, 1H), 3.84 (m, 1H), 3.76 (t, *J* = 10.4 Hz, 1H), 3.63 (m, 3H), 3.53 (t, *J* = 6.4 Hz, 3H), 2.81 (m, 2H), 2.30 (m, 3H), 2.20 (m, 2H), 2.11–1.94 (m, 6H), 1.84 (m, 4H), 1.70 (d, *J* = 7.1 Hz, 3H), 1.66 (d, *J* = 7.1 Hz, 3H), 1.63 (d, *J* = 7.1 Hz, 3H), 1.52 (m, 3H), 1.31 (m, 7H), 1.24 (m, 29H), 1.15 (d, *J* = 6.0 Hz, 3H), 1.10 (m, 2H), 0.92 (dd, *J* = 11.4, 6.8 Hz, 7H), 0.84 (m, 37H) ppm.

^{13}C NMR (150 MHz, DMSO-d_6): δ 174.6, 172.7, 172.42, 172.37, 172.2, 172.0, 171.9, 171.7, 171.3, 170.7, 170.6, 170.4, 169.91, 169.87, 169.4, 168.7, 166.8, 164.0, 163.9, 163.5, 162.7, 135.3, 131.3, 130.8, 130.0, 128.6, 127.1, 118.6, 104.5, 70.5, 61.4, 60.9, 60.7, 58.7, 58.5, 57.8, 57.7, 57.1, 56.6, 55.5, 51.9, 49.4, 49.2, 49.1, 49.0, 48.9, 48.7, 48.2, 37.1, 36.0, 34.3, 30.9, 30.3, 29.93, 29.86, 29.1, 28.7, 28.4, 28.2, 27.1, 25.4, 24.6, 24.3, 21.8, 19.4, 19.1, 19.0, 18.1, 18.0, 17.9, 17.7, 17.43, 17.36, 17.3, 17.2, 17.1, 16.9, 16.4, 16.2, 14.4, 13.7, 12.7, 12.6, 11.8, 11.3 ppm.

HRMS (ESI, *m/z*): calculated for $C_{95}H_{159}N_{23}O_{26}$ $[M+2H]^{2+}$ 1019.0908; found 1019.0895.

Optical rotation $[\alpha]_D^{22}$: –67.9 (*c* 0.53 in MeOH).

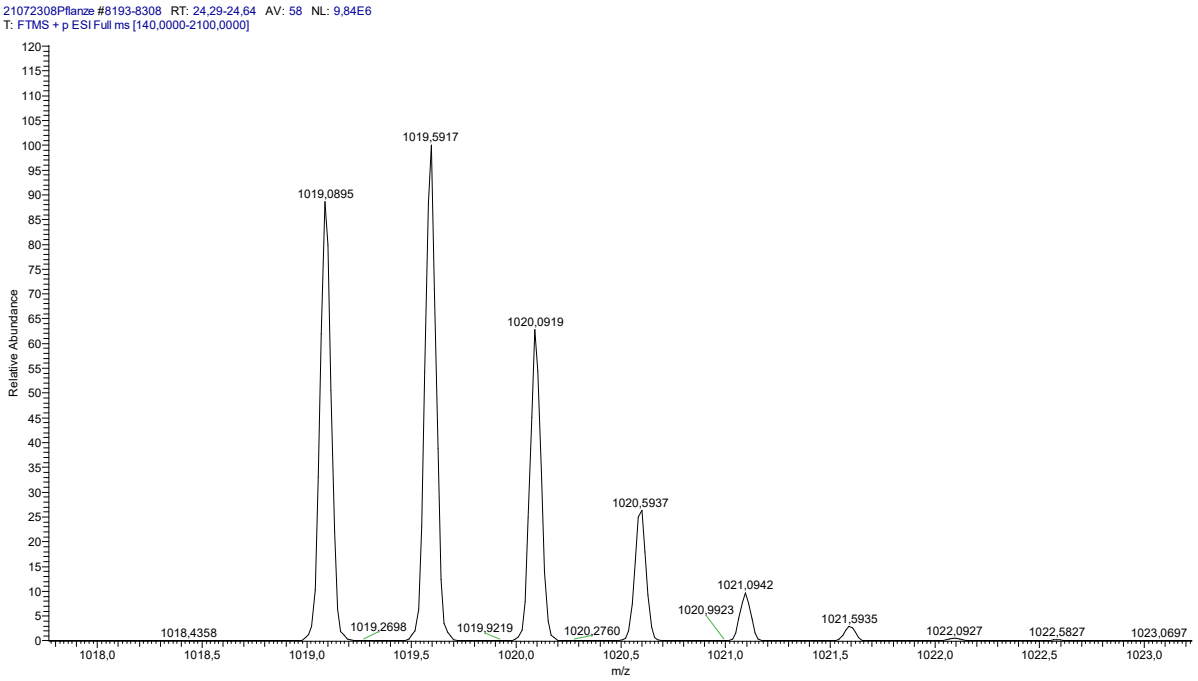

Figure S22 HRMS spectrum of nunapeptin C. HRMS (ESI, *m/z*): calculated for $C_{95}H_{159}N_{23}O_{26}$ $[M+2H]^{2+}$ 1019.0908; found 1019.0895.

Brabantamide A was further purified by preparative HPLC equipped with a Luna® C18(2) column (Phenomenex, 250 x 21.4 mm, 100 Å, 5 µm) and the following method: flow rate of 20 mL/min; 0 – 5 min: 10% MeCN in water containing 0.1% formic acid; 5 – 45 min: linear gradient from 10% to 100% MeCN in water containing 0.1% formic acid; 45 – 55 min: 100% MeCN containing 0.1% formic acid.

Brabantamide A

^{1}H NMR (300 MHz, CD_3OD): δ 6.25 (d, *J* = 1.8 Hz, 1H), 4.99 (m, 1H), 4.79 (d, *J* = 1.4 Hz, 1H), 4.17 (m, 1H), 3.75 (m, 1H), 3.60 (m, 3H), 3.36 (m, 1H), 3.28 (m, 1H), 2.69 (m, 3H), 2.10 (m, 2H), 1.60 (m, 3H), 1.32 (m, 18H), 1.21 (d, *J* = 6.2 Hz, 3H), 0.90 (t, *J* = 6.6 Hz, 3H) ppm.

^{13}C NMR (75 MHz, CD_3OD): δ 173.6, 168.8, 166.4, 158.2, 100.0, 98.0, 74.9, 73.8, 72.6, 72.3, 70.3, 66.2, 47.0, 44.0, 34.5, 33.1, 31.2, 30.80, 30.76, 30.74, 30.70, 30.5, 27.2, 25.8, 23.7, 18.0, 14.5 ppm.

HRMS (ESI, *m/z*): calculated for $C_{28}H_{47}N_2O_9$ $[M+H]^+$ 555.3276; found 555.3273.

Optical rotation $[\alpha]_D^{22}$: +37.5 (*c* 0.4 in MeOH).

All data are in agreement with previously reported data.[23] Slight differences in the ^{1}H NMR data, however, are a result of using different values for the residual solvent signal of CD_3OD as internal standard.

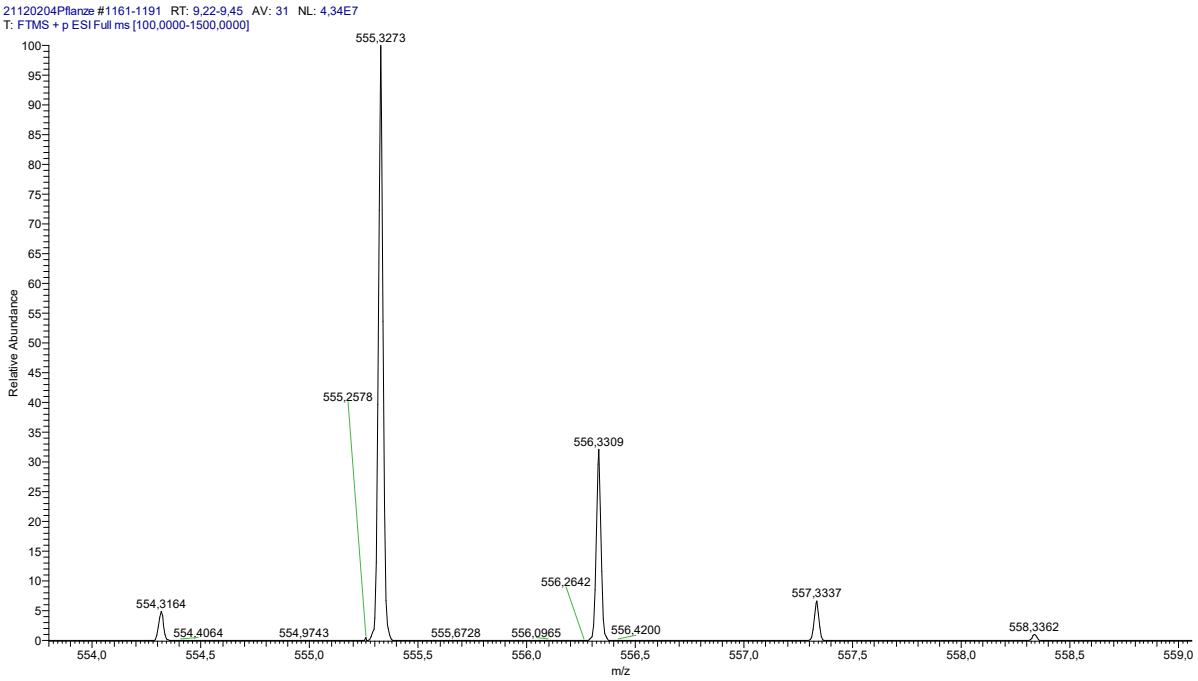

Figure S23 HRMS spectrum of brabantamide A. HRMS (ESI, *m/z*): calculated for $C_{28}H_{47}N_2O_9$ $[M+H]^+$ 555.3276; found 555.3273.

The keanumycin D-containing fraction was further subjected to size exclusion chromatography on Sephadex LH-20 (Cytiva). The column (1000 x 10 mm) was operated with gravity flow and pure MeOH as mobile phase. Fractions containing keanumycin D were identified by LCMS, combined, and solvents removed *in vacuo*. Further purification was accomplished by preparative HPLC equipped with a Luna® C18(2) column (Phenomenex, 250 x 21.4 mm, 100 Å, 5 µm) and the following method: flow rate of 20 mL/min; 0 – 5 min: 25% MeCN in water containing 0.1% trifluoroacetic acid; 5 – 35 min: linear gradient from 25% to 50% MeCN in water containing 0.1% trifluoroacetic acid; 35 – 40 min: linear gradient from 50% to 100% MeCN in water containing 0.1% trifluoroacetic acid; 40 – 50 min: 100% MeCN containing 0.1% trifluoroacetic acid. Finally, keanumycin D was obtained after semipreparative HPLC equipped with a Jupiter® Proteo column (Phenomenex, 250 x 10 mm, 90 Å, 4 µm) and the following method: flow rate of 5 mL/min; 0 – 5 min: 25% MeCN in water containing 0.1% trifluoroacetic acid; 5 – 35 min: linear gradient from 25% to 50% MeCN in water containing 0.1% trifluoroacetic acid; 35 – 40 min: linear gradient from 50% to 100% MeCN in water containing 0.1% trifluoroacetic acid; 40 – 50 min: 100% MeCN containing 0.1% trifluoroacetic acid.

Keanumycin D

^{1}H NMR (600 MHz, DMSO-d_6): δ 6.80 (q, *J* = 7.1 Hz, 1H), 5.05 (m, 2H), 4.96 (m, 1H), 4.37 (td, *J* = 6.4, 2.1 Hz, 2H), (dd, *J* = 9.3, 4.9 Hz, 2H), 4.26 (m, 1H), 4.10 (m, 3H), 3.94 (m, 2H), 3.77 (m, 2H), 3.65 (m, 2H), 3.58 (m, 3H), 3.52 (m, 2H), 3.03 (m, 6H), 2.35 (m, 3H), 2.24 (m, 3H), 2.21–2.01 (m, 8H), 1.78 (d, *J* = 7.1 Hz, 2H), 1.60 (m, 2H), 1.46 (m, 4H), 1.37 (m, 2H), 1.29 (m, 16H), 0.90 (t, *J* = 7.1 Hz, 3H) ppm.

HRMS (ESI, *m/z*): calculated for $C_{47}H_{81}ClN_{11}O_{18}$ $[M+H]^+$ 1122.5444; found 1122.5433.

Optical rotation $[\alpha]_D^{22}$: +23.1 (*c* 0.13 in MeOH).

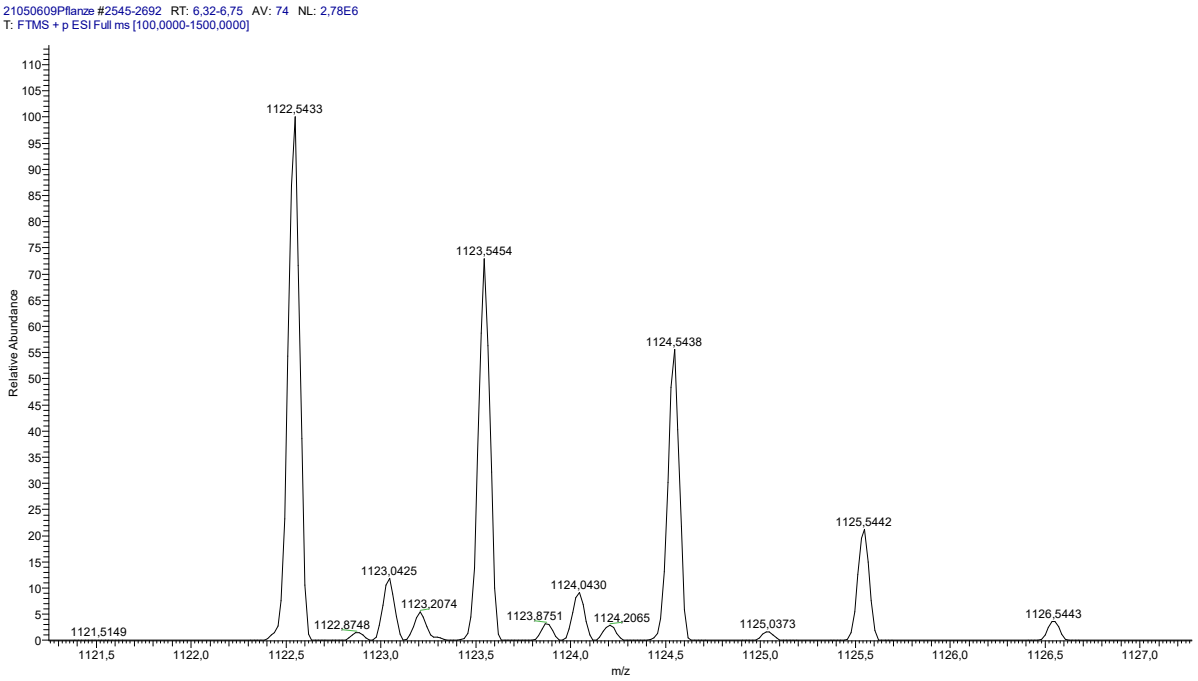

Figure S24 HRMS spectrum of keanumycin D. HRMS (ESI, *m/z*): calculated for $C_{47}H_{81}ClN_{11}O_{18}$ $[M+H]^+$ 1122.5444; found 1122.5433.

Sequence analysis of nonribosomal peptides

Analysis of nunapeptin B

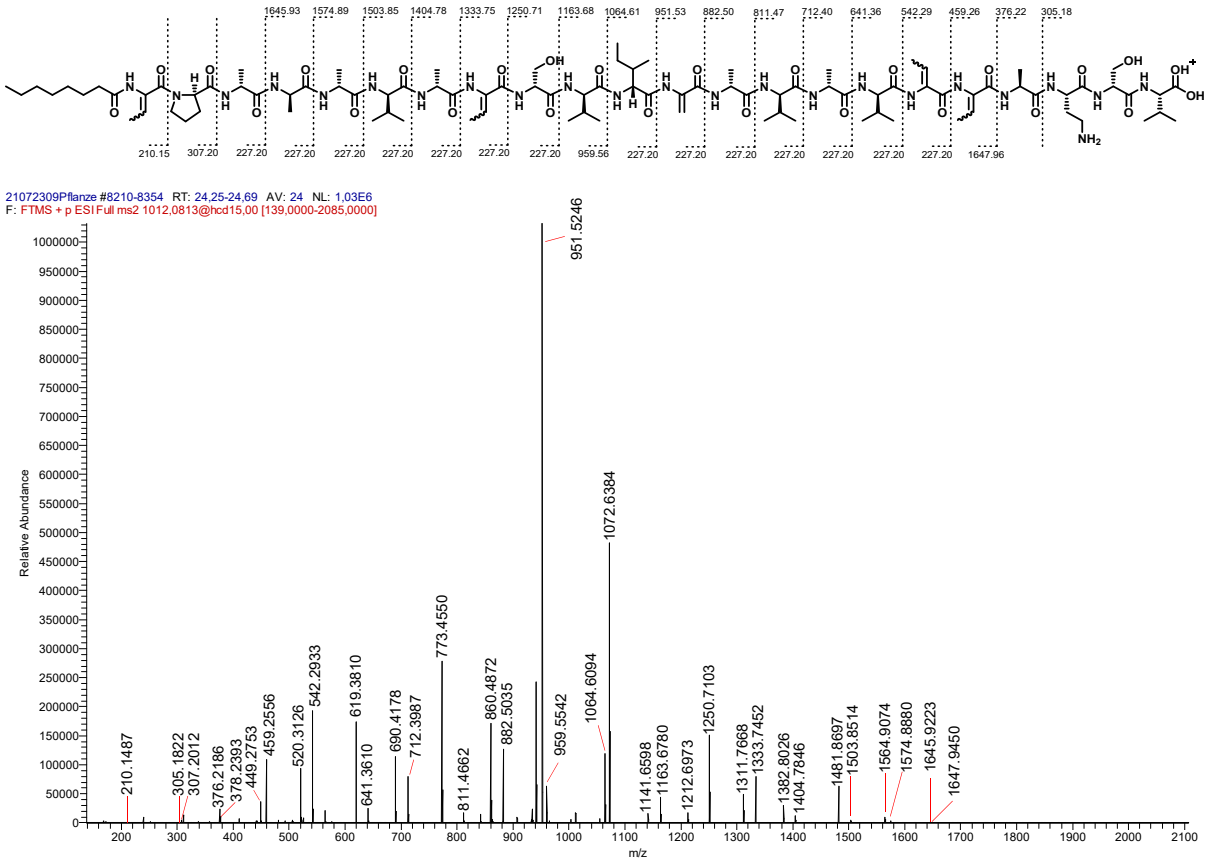

Figure S25 Amino acid sequence analysis of nunapeptin B via $HRMS^2$.

Analysis of nunapeptin C

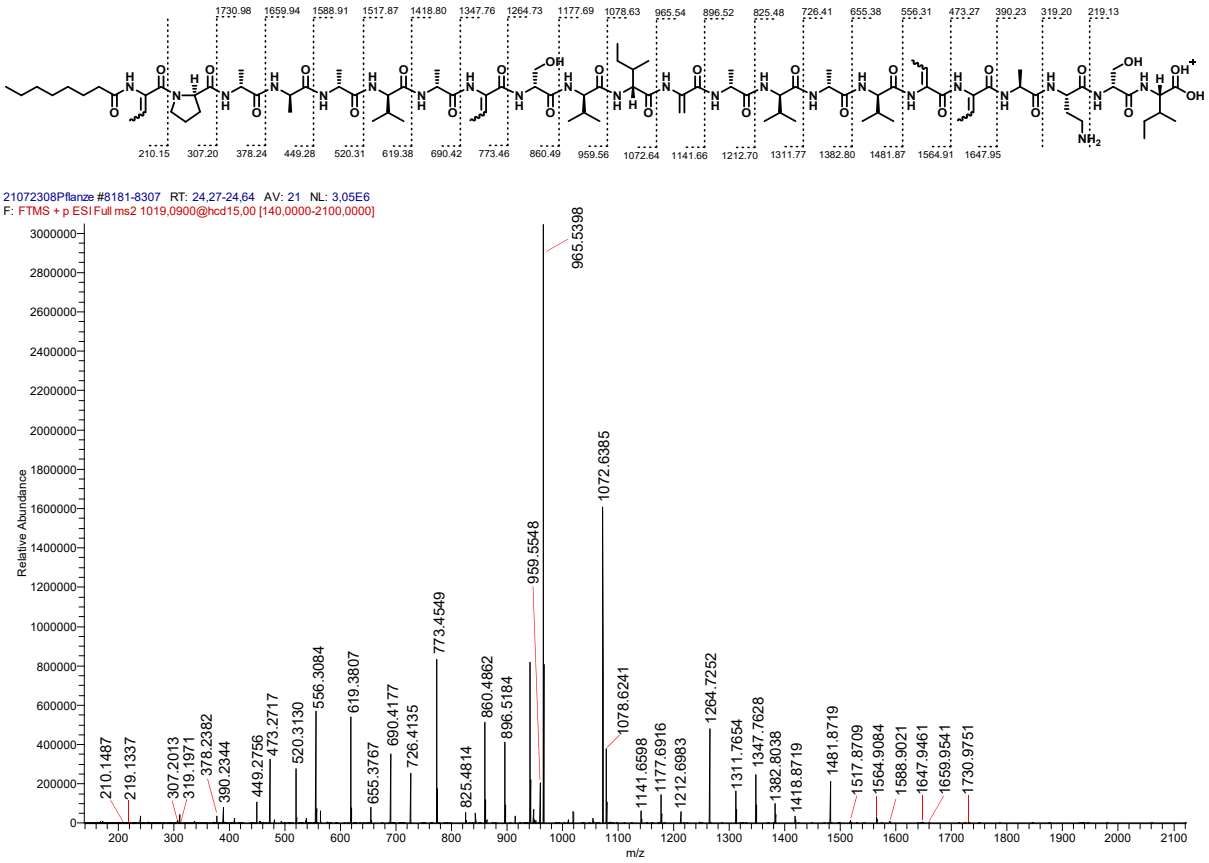

Figure S26 Amino acid sequence analysis of nunapeptin C via HRMS^2.

Analysis of keanumycin D

For HRMS^2 analysis, keanumycin D was hydrolysed by the addition of 1 M aq. NH_4HCO_3 (20 µL) to a solution of the lipopeptide (50 µg) in MeOH (100 µL). The reaction was shaken at 37 °C for 16 h and diluted to a final concentration of 0.1 mg/mL prior to analysis. Unexpectedly, a C-terminal methyl ester of the linearised lipopeptide had formed and the chloride substituent was mostly unaffected under these reaction conditions, in contrast to our previous work on keanumycin A – C.[19]

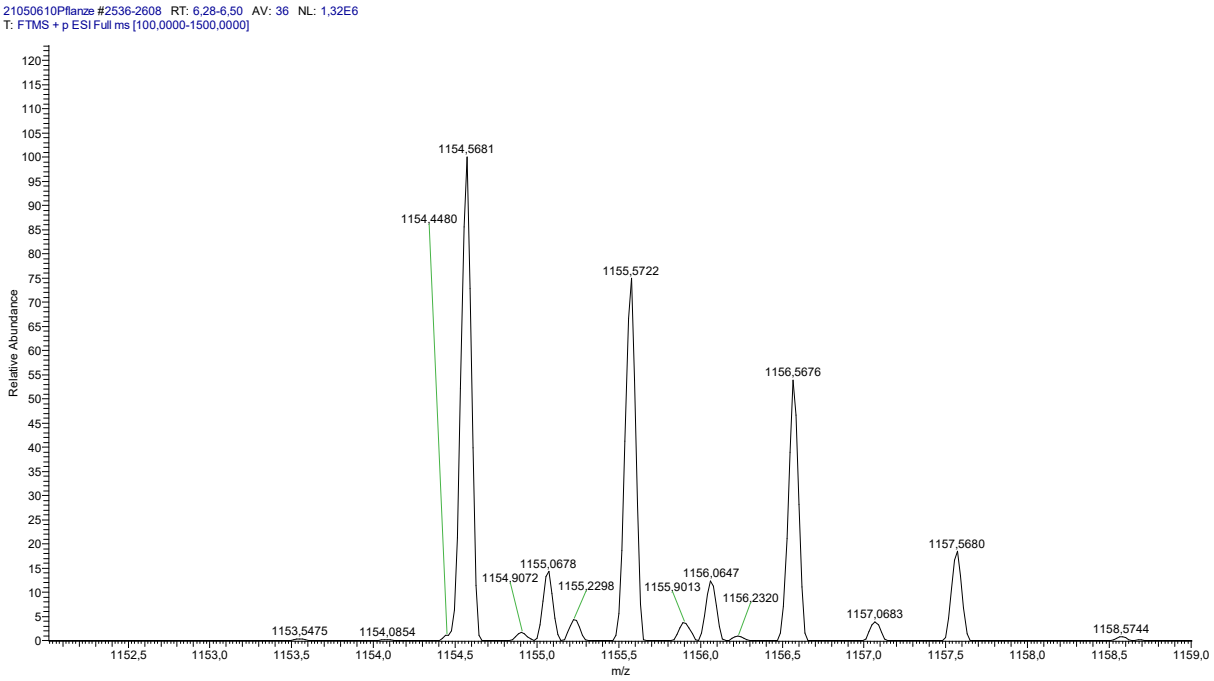

Figure S27 HRMS spectrum of linearised keanumycin D methyl ester. HRMS (ESI, *m/z*): calculated for $C_{48}H_{85}ClN_{11}O_{19}$ $[M+H]^+$ 1154.5706; found 1154.5681.

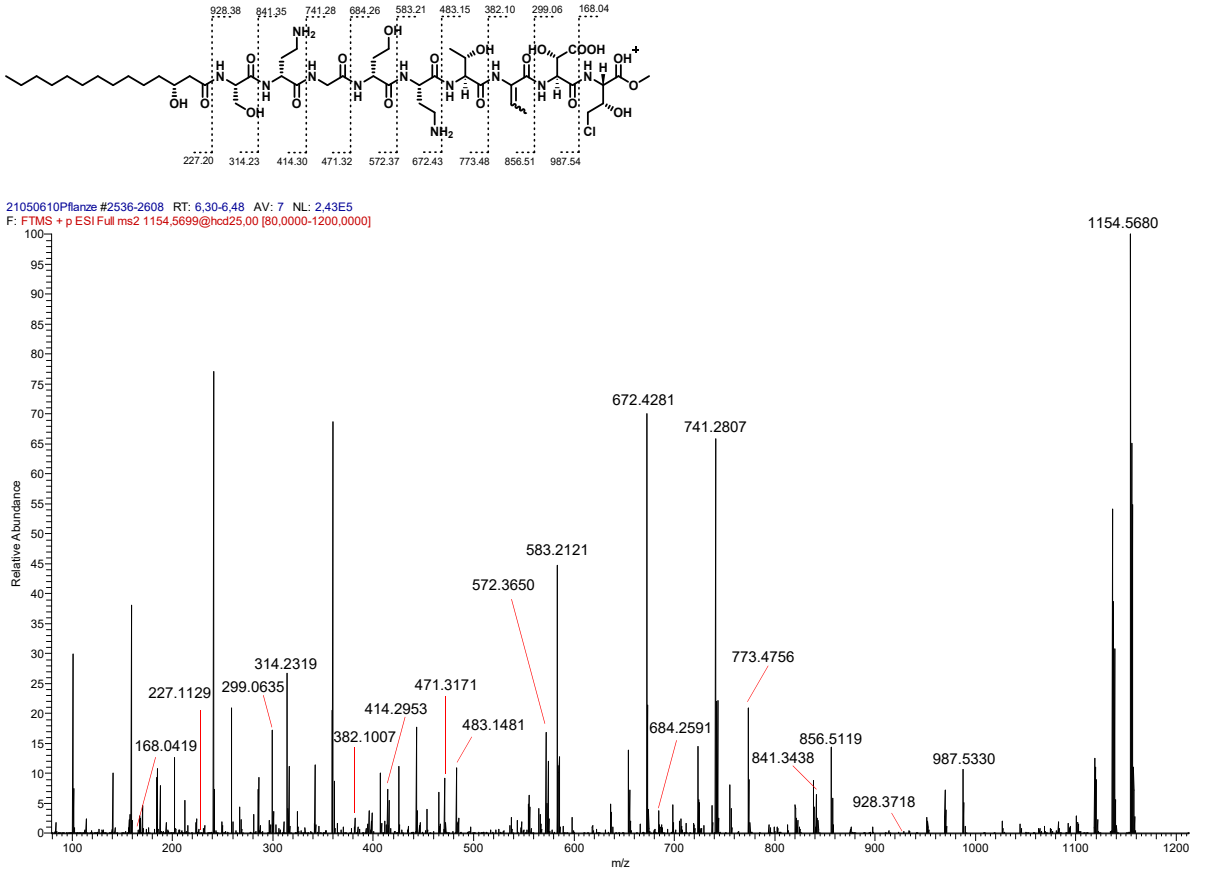

Figure S28 Amino acid sequence analysis of linearised keanumycin D methyl ester via $HRMS^2$.

Synthesis of protected 4-chloro-L-threonine

Synthesis of protected L-vinylglycine (11)

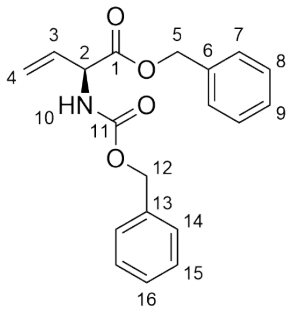

A solution of *N*-Cbz-L-glutamic acid 1-benzyl ester (500 mg, 1.4 mmol, 1.0 eq.) in benzene (17 mL) was degassed by passing a gentle stream of argon through the solution for 30 min. $Cu(OAc)_2$ monohydrate (134 mg, 0.7 mmol, 0.5 eq.) was added and the suspension stirred for 1 h. Freshly preparred $Pb(OAc)_4$ (1.2 g, 2.7 mmol, 2.0 eq.) was added in small portions and the reaction refluxed overnight. When a TLC control showed the absence of starting material, the suspension was filtered through a pad of Celite. The filtrate was diluted with EtOAc and washed with water and brine. The organic layer was dried with anhydrous $MgSO_4$ and concentrated *in vacuo*. The product was obtained after flash chromatography (9:1 – 4:1 (v/v) cyclohexane/EtOAc) as a white wax (147 mg, 34% yield).

^{1}H NMR (500 MHz, $CDCl_3$): δ 7.38 – 7.34 (m, 10H, 7-H – 9-H, 14-H – 16-H), 5.95 (m, 1H, 3-H), 5.70 (d, *J* = 7.3 Hz, 1H, 10-H), 5.39 (dd, *J* = 17.2, 1.3 Hz, 1H, 4-H), 5.29 (dd, *J* = 10.4, 1.4 Hz, 1H, 4-H), 5.21 (s, 2H, 5-H), 5.16 (s, 2H, 12-H), 5.05 (m, 1H, 2-H) ppm.

^{13}C NMR (125 MHz, $CDCl_3$): δ 170.3 (C-1), 155.6 (C-11), 136.2, 135.2 (C-6, C-13), 132.3 (C-3), 128.6, 128.50, 128.46, 128.2, 128.1 (C-7 – C-9, C-114 – C-16), 117.8 (C-4), 67.4, 67.1 (C-5, C-12), 56.3 (C-2) ppm.

HRMS (ESI, *m/z*): calculated for $C_{19}H_{20}NO_4$ $[M+H]^+$ 326.1387; found 326.1389.

Optical rotation $[\alpha]_D^{22}$: –2.0 (*c* 1.0 in $CHCl_3$).

Synthesis of protected epoxide (12)

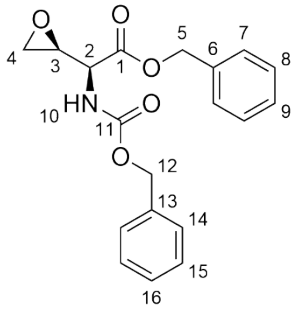

To a solution of protected vinylglycine (75 mg, 0.23 mmol, 1.0 eq.) in CH_2Cl_2 (3 mL) was added 50% *m*CPBA (400 mg, 1.16 mmol, 5.0 eq.) and the reaction stirred in an argon atmosphere at r.t. for 6 d until TLC analysis showed the absence of starting material. The reaction was cooled to 0 °C, diluted with CH_2Cl_2 (3 mL), and stopped by the addition of a 10% (w/v) Na_2SO_3 solution in water (3 mL). The mixture was extracted with CH_2Cl_2 (2 x 5 mL) and combined organic layers were washed with phosphate buffer (2 x 5 mL, 0.1 M, pH 7.0), dried over anhydrous Na_2SO_4 and concentrated *in vacuo*. The crude product was recrystallised from *n*-hexane/EtOAc (8:1) to yield white crystals (72 mg, 92% yield).

^{1}H NMR (500 MHz, DMSO-d_6): δ 8.04 (d, *J* = 8.2 Hz, 1H, 10-H), 7.37 – 7.32 (m, 10H, 7-H – 9-H, 14-H – 16-H), 5.17 (dd, *J* = 16.6, 12.7 Hz, 2H, 5-H), 5.06 (s, 2H, 12-H), 4.09 (dd, J = 7.9, 6.5 Hz, 1H, 2-H), 3.31 (hidden under water peak, 1H, 3-H), 2.83 (m, 1H, 4-H), 2.73 (m, 1H, 4-H) ppm.

^{13}C NMR (125 MHz, DMSO-d_6): δ 169.3 (C-1), 156.1 (C-11), 136.8, 135.7 (C-6, C-13), 128.4, 128.3, 128.0, 127.8, 127.7, 127.6 (C-7 – C-9, C-14 – C-16), 66.3, 65.7 (C-5, C-12), 56.2 (C-2), 50.5 (C-3), 44.9 (C-4) ppm.

HRMS (ESI, *m/z*): calculated for $C_{19}H_{20}NO_5$ $[M+H]^+$ 342.1336; found 342.1338.

Optical rotation $[\alpha]_D^{22}$: –4.0 (*c* 1.0 in MeOH).

Synthesis of protected 4-chloro-L-threonine (13)

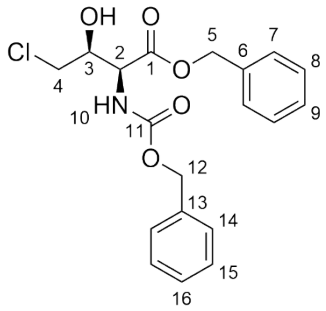

The protected epoxide (33 mg, 0.1 mmol, 1.0 eq.) was dissolved in a solution of Li_2CuCl_4 in THF (1.9 mL, 0.1 M, 0.2 mmol, 2.0 eq.) and stirred at r.t. under an argon atmosphere overnight. The reaction was stopped by the addition of a saturated $NaHCO_3$ solution in water (5 mL) and subsequently diluted with water (5 mL). The suspension was extracted with Et_2O (3 x 20 mL), combined organic layers were dried over anhydrous Na_2SO_4 and concentrated *in vacuo*. The product was obtained after recrystallisation from *n*-hexane/EtOAc (4:1) as white crystals (18 mg, 50% yield).

^{1}H NMR (500 MHz, DMSO-d_6): δ 7.38 – 7.31 (m, 10H, 7-H – 9-H, 14-H – 16-H), 5.67 (d, *J* = 6.9 Hz, 1H, -OH), 5.17 (s, 2H, 5-H), 5.09 (d, *J* = 12.7 Hz, 1H, 12-H), 5.05 (d, *J* = 12.7 Hz, 1H, 12-H), 4.49 (dd, *J* = 9.1, 2.9 Hz, 1H, 2-H), 4.17 (m, 1H, 3-H), 3.62 (dd, *J* = 10.9, 6.7 Hz, 1H, 4-H), 3.51 (dd, *J* = 10.9, 6.6 Hz, 1H, 4-H) ppm.

^{13}C NMR (125 MHz, DMSO-d_6): δ 170.2 (C-1), 156.5 (C-11), 136.8, 135.8 (C-6, C-13), 128.4, 128.3, 128.0, 127.8, 127.7, 127.6 (C-7 – C-9, C-14 – C-16), 70.8 (C-3), 66.3, 65.7 (C-5, C-12), 56.5 (C-2), 45.0 (C-4) ppm.

HRMS (ESI, *m/z*): calculated for $C_{19}H_{21}ClNO_5$ $[M+H]^+$ 378.1103; found 378.1106.

Optical rotation $[\alpha]_D^{22}$: –13.0 (*c* 1.0 in MeOH).

Marfey's analysis of nonribosomal peptides

Marfey's analysis was performed as previously described.[18,19]

500 µg of nunapeptin B and C, respectively, and approximately 100 µg of keanumycin D were hydrolysed by the addition of 6 N HCl (200 µL) and heating to 100 °C for 12 h. The solvent was removed *in vacuo* and the residue dissolved in water (100 µL). 1 M aq. $NaHCO_3$ (40 µL) and 0.5% (w/v) Marfey's reagent (1-fluoro-2,4-dinitrophenyl-5-L-alanine amide, FDAA) in acetone (200 µL) were added and the reaction shaken at 40 °C for 1 h. The reaction was stopped by the addition of 2 M HCl (20 µL) and then filtered (PTFE, 0.22 µm). Amino acid standards were dissolved in water (100 µL, 5 µmol) and treated analogously.

Amino acid standards and derivatized peptides were analysed using a UHPLC-MS (Phenomenex Luna® C18(2), 150 x 2 mm, 100 Å, 5 µm) with the following method: flow rate of 0.2 mL/min; 0 – 5 min: 10% (v/v) MeCN in water containing 0.1% formic acid; 5 – 35 min: linear gradient from 10% to 50% (v/v) MeCN in water containing 0.1% formic acid; 35 – 36.5 min: linear gradient from 50% to 100% (v/v) MeCN in water containing 0.1% formic acid; 36.5 – 46.5 min: 100% MeCN containing 0.1% formic acid.

Marfey's analysis of nunapeptins

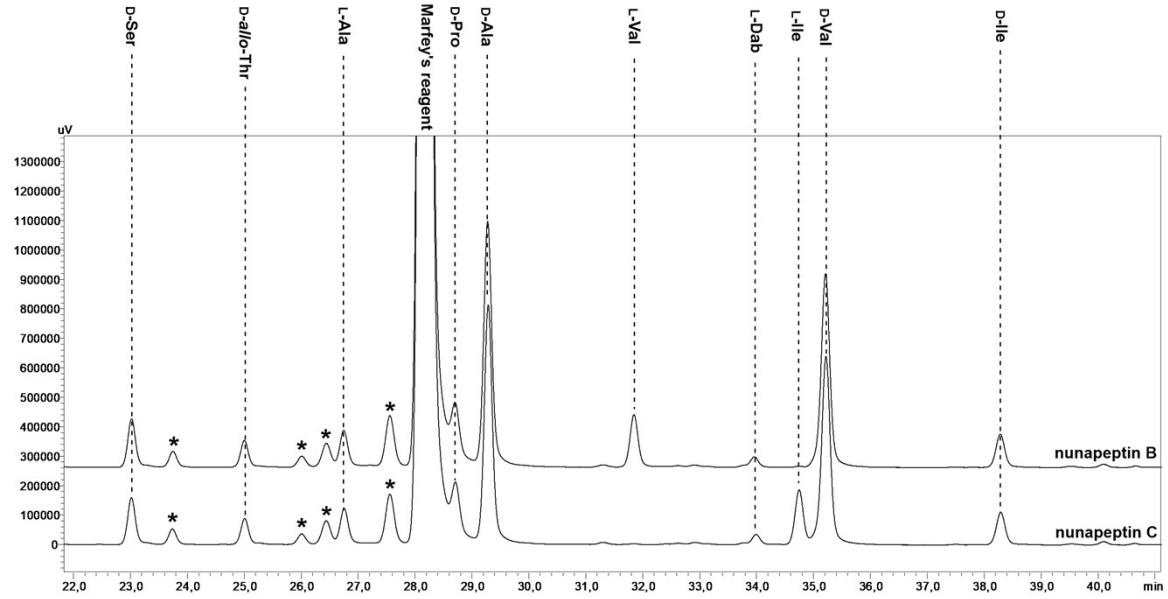

Figure S29 Marfey's analysis of nunapeptin B and C. Asterisks indicate unidentified peaks.

Marfey's analysis of nunapeptin B and C allowed to determine the following amino acid compositions:

2x D-Ser (t_R = 23.0 min); 1x D-*allo*-Thr (t_R = 23.0 min); 1x L-Ala (t_R = 26.8 min); 1x D-Pro (t_R = 28.7 min); 6x D-Ala (t_R = 29.3 min); 1x L-Val for nunapeptin B (t_R = 31.8 min); 1x L-Dab (t_R = 34.0 min); 1x L-Ile for nunapeptin C (t_R = 34.8 min); 4x D-Val (t_R = 35.2 min); 1x D-Ile (t_R = 38.3 min).

The difference between nunapeptin B and C is the presence of a single L-valine in nunapeptin B, which is substituted with L-isoleucine in nunapeptin C. Using this approach, it is not possible to distinguish between L-isoleucine and L-*allo*-isoleucine or D-isoleucine and D-*allo*-isoleucine, respectively.

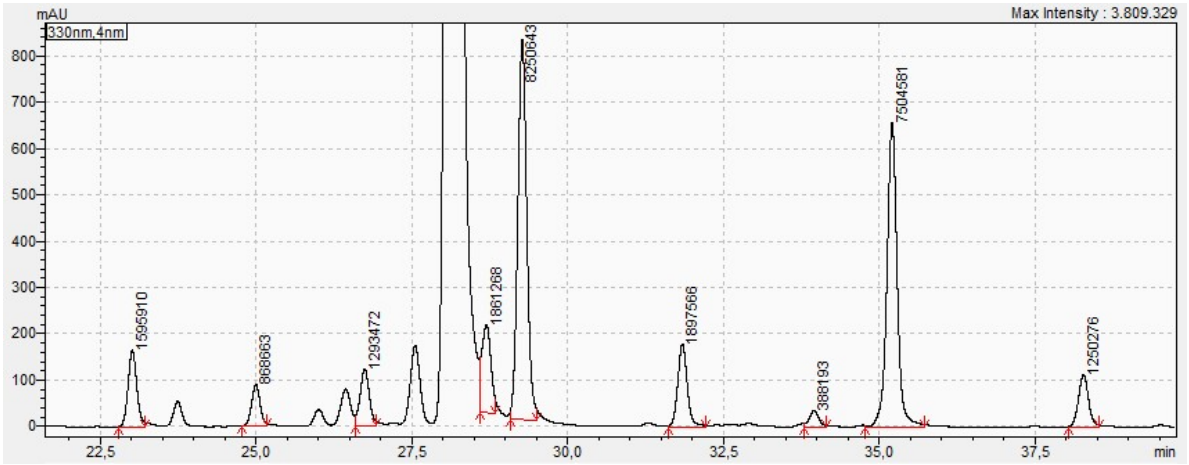

Figure S30 HPLC profile of hydrolysed and FDAA-derivatized nunapeptin B (λ = 330 nm).

Table S7 Integration areas for Marfey's analysis of nunapeptin B.

Amino Acid	Retention Time [min]	Area under the peak
D-Ser	23.0	1,595,910
D-*allo*-Thr	25.0	868,663
L-Ala	26.7	1,293,472
D-Pro	28.7	1,861,268
D-Ala	29.3	8,250,643
L-Val	31.8	1,897,566
L-Dab	34.0	388,193
D-Val	35.2	7,504,581
D-Ile	38.3	1,250,276

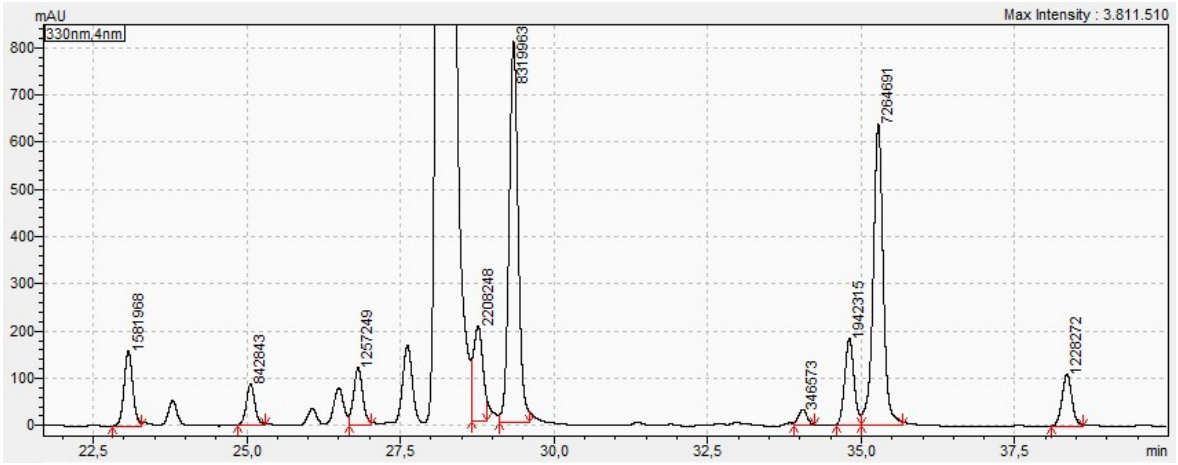

Figure S31 HPLC profile of hydrolysed and FDAA-derivatized nunapeptin C (λ = 330 nm).

Table S8 Integration areas for Marfey's analysis of nunapeptin C.

Amino Acid	Retention Time [min]	Area under the peak
D-Ser	23.1	1,581,968
D-*allo*-Thr	25.1	842,843
L-Ala	26.8	1,257,249
D-Pro	28.8	2,208,248
D-Ala	29.3	8,319,963
L-Dab	34.0	346,573
L-Ile	34.8	1,942,315
D-Val	35.3	7,264,691
D-Ile	38.3	1,228,272

Marfey's analysis of keanumycin D

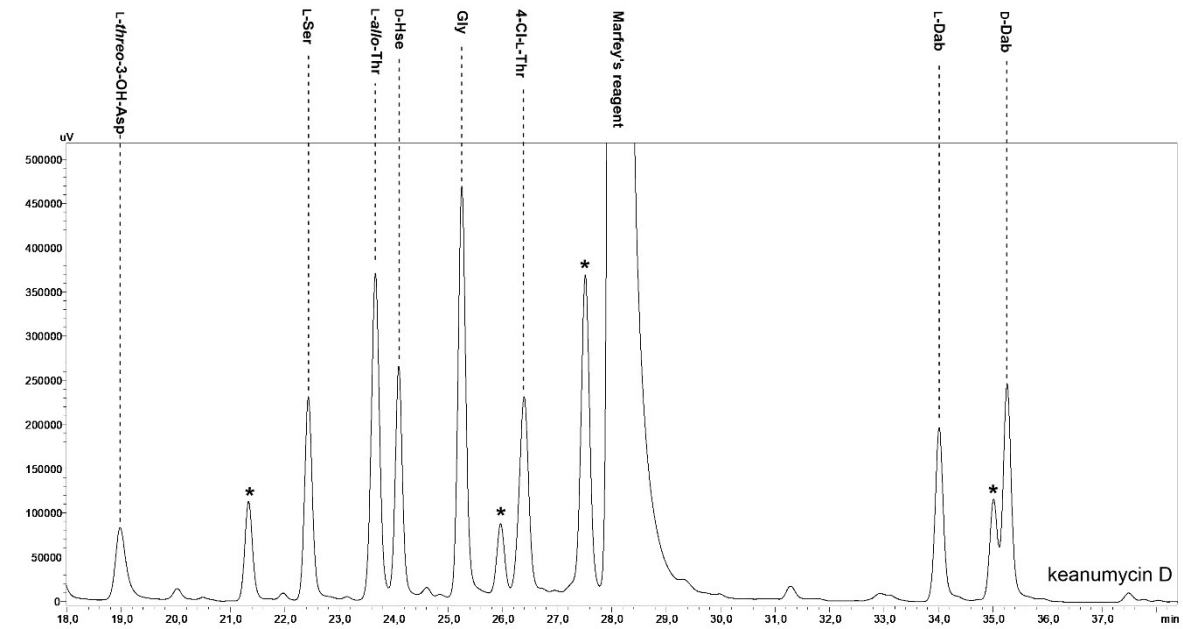

Figure S32 Marfey's analysis of keanumycin D. Asterisks indicate unidentified peaks.

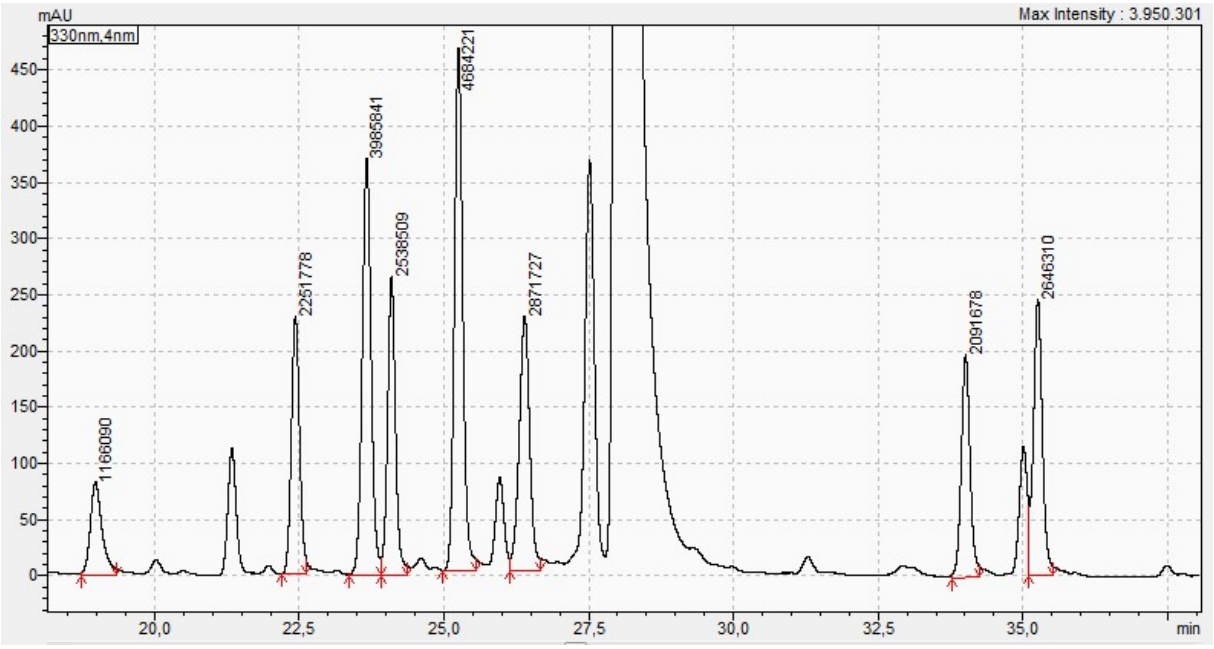

Figure S33 HPLC profile of hydrolysed and FDAA-derivatized keanumycin D (λ = 330 nm).

Table S9 Integration areas for Marfey's analysis of keanumycin D.

Amino Acid	Retention Time [min]	Area under the peak
L-threo-3-OH-Asp	19.0	1,166,090
L-Ser	22.4	2,251,778
L-*allo*-Thr	23.7	3,985,841
D-Hse	24.1	2,538,509
Gly	25.3	4,684,221
4-Cl-L-Thr	26.4	n/a
L-Dab	34.0	2,091,678
D-Dab	35.3	2,646,310

Marfey's analysis of keanumycin D allowed to determine the following amino acid compositions:

1x L-*threo*-3-OH-Asp (t_R = 19.0 min); 1x L-Ser (t_R = 22.4 min); 1x L-*allo*-Thr (t_R = 23.7 min); 1x D-Hse (t_R = 24.1 min); 1x Gly (t_R = 25.3 min); 1x 4-Cl-L-Thr (t_R = 26.4 min); 1x L-Dab (t_R = 34.0 min); 1x D-Dab (t_R = 35.3 min).

It has to be noted, that 4-Cl-L-Thr (*m/z* 406.1 in pos. mode) was found to coelute with an unidentified impurity (*m/z* 271.2 in pos. mode) and was only identified in the MS chromatogram. Therefore, we are unable to report a peak area for 4-Cl-L-Thr unambiguously.

Stable isotope labelling of nunapeptin C

An overnight culture of WT 4A2e was used to inoculate 100 mL of stable isotope labelling medium in a 1 L Erlenmeyer flask which was shaken at 22 °C for 28 h. The broth was extracted with EtOAc (250 mL), the organic layer washed with brine, dried over anhydrous Na_2SO_4, and concentrated *in vacuo*. The residue was dissolved in a minimal amount of MeOH and loaded on Isolute HM-N. The dried Isolute material was loaded on a pre-equilibrated (10% MeOH in water) C18 HyperSep SPE column (Thermo Scientific, 1 g, 6 mL), and gradually washed with 10%, 50%, and 100% MeOH in water (25 mL, each). Fractions were concentrated *in vacuo* and analysed via LCMS for the presence of nunapeptins, which were only found in the 100% MeOH fraction. This residue was finally purified using semipreparative HPLC (Phenomenex Luna® C18(2), 5 µm, 100 Å, 250 x 10 mm) and the following method: flow rate of 5 mL/min; 0 – 5 min: 10% (v/v) MeCN in water containing 0.1% formic acid; 5 – 45 min: linear gradient from 10% to 100% (v/v) MeCN in water containing 0.1% formic acid; 45 – 55 min: 100% MeCN containing 0.1% formic acid. A nunapeptin C-containing fraction (t_R = 45.4 min) was further subjected to $HRMS^2$ analysis.

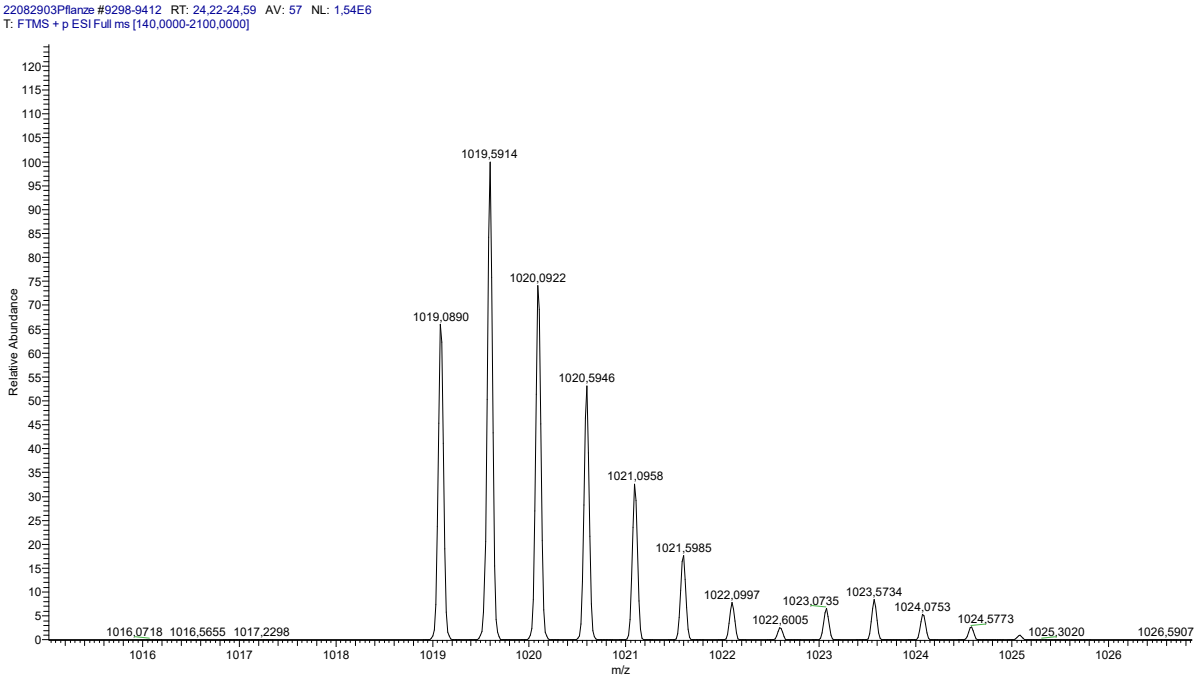

Figure S34 HRMS analysis of nunapeptin C-d_1. HRMS (ESI, *m/z*): calculated for $C_{95}H_{158}DN_{23}O_{26}$ $[M+2H]^{2+}$ 1019.5939; found 1019.5914.

Under these experimental conditions, we obtained a mixture of non-labelled, monoisotopic (*m/z* 1019.0890) nunapeptin C and isotopologues (*m/z* 1019.5914). To distinguish the selective incorporation of L-alanine-2-d_1 into the peptide backbone from random distribution of isotopes in other isotopologues (*e.g.* $C_{94}{}^{13}CH_{159}N_{23}O_{26}$ or $C_{95}H_{159}N_{22}{}^{15}NO_{26}$), we compared the relative intensities of monoisotopic ions and isotopic ions observed for the fragmentation of *m/z* 1019.5914 for nunapeptin C isolated from stable isotope labelling medium and labelling control medium.

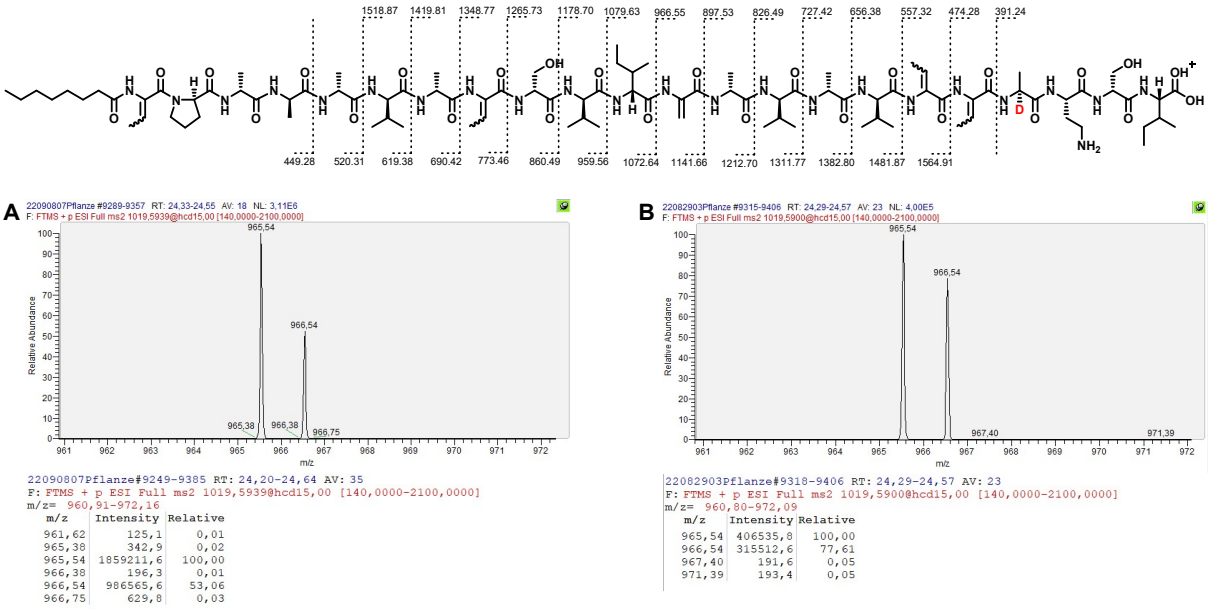

Figure S35 Example for the comparison of relative fragment ion intensities of monoisotopic nunapeptin C and isotopologues. A) Nunapeptin C from labelling control medium, B) Nunapeptin C from stable isotope labelling medium.

Table S10 Comparison of the relative intensities of C-terminal.

m/z of monoisotopic ions	*m/z* of isotopic ions	relative intensity for labelling control medium [%]	relative intensity for stable isotope labelling medium [%]
1517.87	1518.87	95	65
1418.80	1419.80	96	186
1347.76	1348.76	90	122
1264.73	1265.73	81	119
1177.69	1178.69	73	106
1078.62	1079.63	63	91
965.54	966.54	53	78
896.52	897.52	46	68
825.48	826.48	37	51
726.41	727.42	33	53
655.38	656.38	29	35
556.31	557.31	23	39
473.27	474.27	18	34
390.23	391.24	12	24

Table S11 Comparison of the relative intensities of N-terminal fragment ions.

m/z of monoisotopic ions	*m/z* of isotopic ions	relative intensity for labelling control medium [%]	relative intensity for stable isotope labelling medium [%]
449.28	450.28	19	7
520.31	521.32	22	19
619.38	620.39	30	28
690.42	691.42	37	31
773.46	774.46	41	36
860.49	861.49	49	44
959.55	960.56	60	50
1072.64	1073.64	71	63
1141.66	1142.66	82	65
1212.70	1213.70	79	56
1311.77	1312.77	105	83
1382.80	1383.80	112	104
1481.87	1482.87	137	109
1564.91	1565.91	165	138

The comparison of the intensities found for N-terminal fragment ions shows that the incorporation of heavier isotopes in **3** from labelling control medium is greater than in **3** from stable isotope labelling medium for all fragment ions assigned. For C-terminal fragment ions however, an enrichment of heavier isotopes is observed, indicating the presence of the deuterated alanine in these fragments. Since the enrichment is found in almost all fragment ions, even the smaller ones with a lower *m*/*z*, we conclude that they all must share the deuterated amino acid. This is only possible for the alanine on position 19, which is in agreement with the bioinformatic prediction. Hence, Ala19 must be L-configured.

Determination of the ring size of nunapeptins

During ESI-MS^2 analysis, the lactone moiety of both nunapeptins fragmented to give the free carboxylic acid of the C-terminal amino acid and dehydrobutyrine (Dhb) instead of the initial D-*allo*-threonine. Due to the presence of three additional dehydrobutyrines in the peptide backbone, it was difficult to deduce the correct position of D-*allo*-threonine from the analysis of the native nunapeptins alone. Therefore, we decided to mask the original dehydroamino acids by catalytic hydrogenation. This would result in the observation of a single remaining dehydrobutyrine moiety in the peptide backbone, when analysed via ESI-MS^2.

In a Schlenk tube, nunapeptin C (ca. 1 mg) was stirred with Pd/C in MeOH (2 mL) in a hydrogen atmosphere. The reaction was stirred at r.t. overnight and subsequently filtered through a pad of Celite. The solvent was removed *in vacuo* and the residue analysed with HRMS^2. As expected, we observed an increase of 8 Da (hydrogenation of 3 x Dhb and 1 x Dha) in the product and a single Dhb upon MS^2 analysis at position 18. Hence, nunapeptins must contain a 16-membered lactone motif, which is in agreement with the previous reports on nunapeptins.[17]

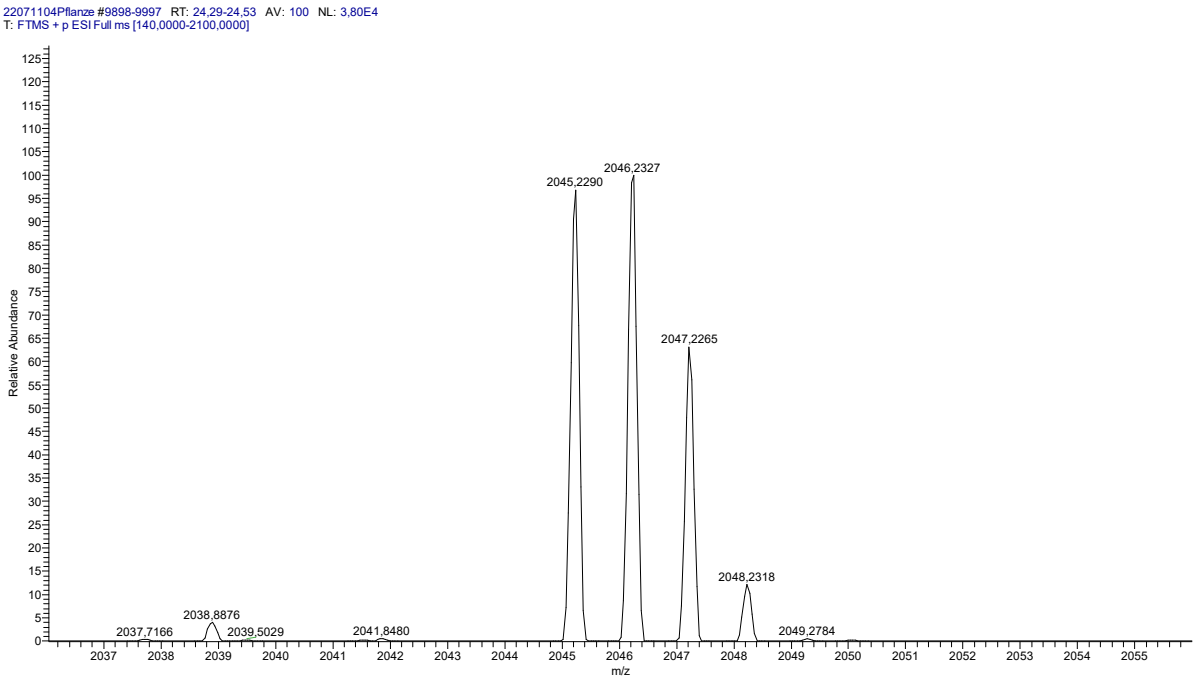

Figure S36 HRMS spectrum of reduced nunapeptin C. HRMS (ESI, *m*/*z*): calculated for $C_{95}H_{166}N_{23}O_{26}$ $[M+H]^+$ 2045.2369; found 2045.2290.

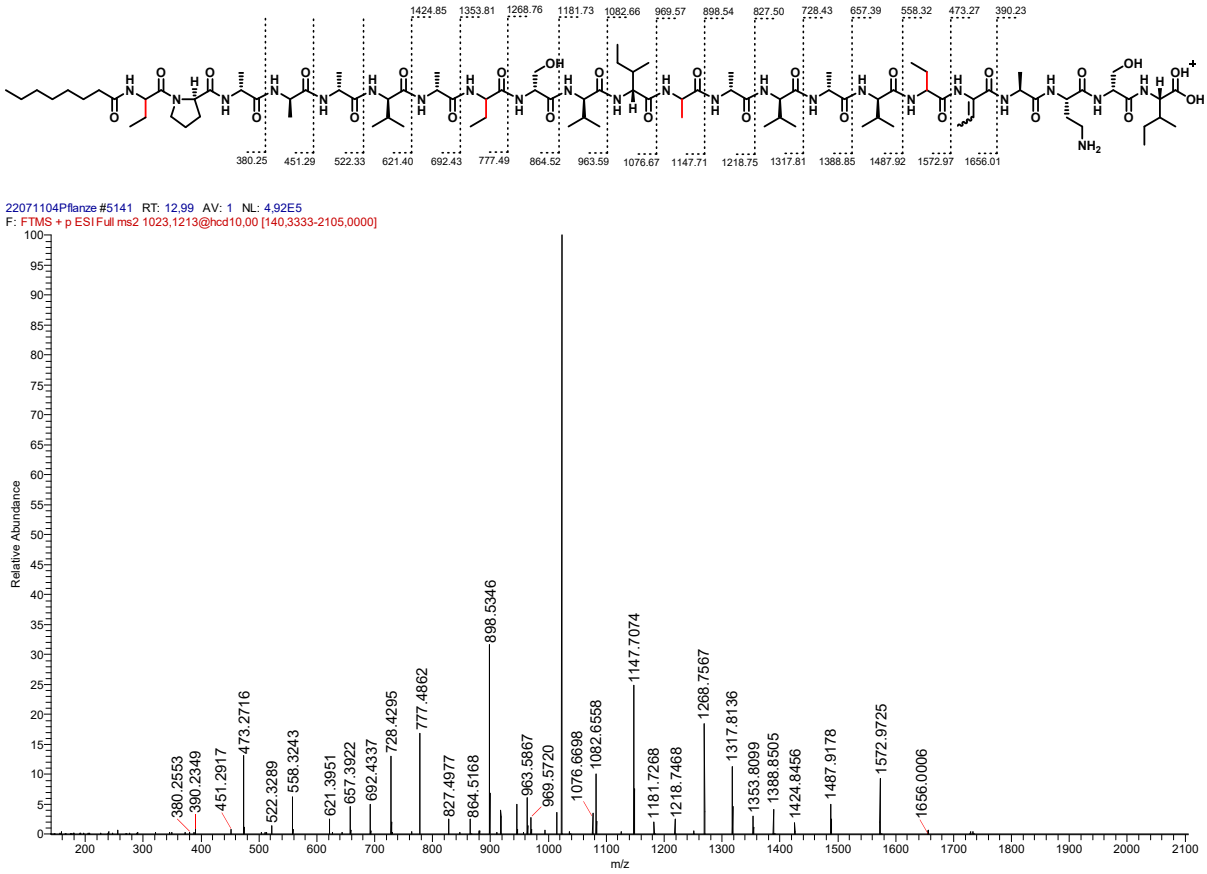

Figure S37 Amino acid sequence analysis of reduced nunapeptin C via HRMS^2.

Determination of the absolute configuration of the 3-hydroxytetradecanoic acid residue in keanumycin D

Synthesis of methyl 3-oxotetradecanoate (8)

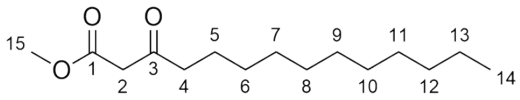

Meldrum's acid (721 mg, 5.0 mmol, 1.0 eq.) was dissolved in 20 mL CH_2Cl_2 with anhydrous pyridine (810 µL, 10.0 mmol, 2.0 eq.) and cooled to 0 °C. Lauroyl chloride (1.31 mL, 5.5 mmol, 1.1 eq.) was added dropwise and the reaction slowly warmed to r.t. After 1 h at r.t., toluene (5 mL) was added and the solvents were removed *in vacuo*. The residual oil was dissolved in MeOH (15 mL) and refluxed overnight. Solvents were removed *in vacuo* and the product purified by flash chromatography (98:2 – 95:5 (v/v) cyclohexane/EtOAc) to yield 886 mg (63% yield) of white needles.

^{1}H NMR (300 MHz, $CDCl_3$): δ 3.60 (s, 3H, 15-H), 3.33 (s, 2H, 2-H), 2.42 (t, *J* = 7.4 Hz, 2H, 4-H), 1.47 (m, 2H, 5-H), 1.15 (m, 16H, 6-H to 13-H), 0.76 (t, *J* = 6.6 Hz, 3H, 14-H) ppm.

^{13}C NMR (75 MHz, $CDCl_3$): δ 202.5 (C-3), 167.5 (C-1), 52.0 (C-15), 48.8 (C-2), 42.8 (C-4), 31.8, 29.5, 29.4, 29.3, 29.2, 28.9 (C-6 to C-13), 23.3 (C-5), 22.6, 13.9 (C-14) ppm.

HRMS (ESI, *m/z*): calculated for $C_{15}H_{29}O_3$ $[M+H]^+$ 257.2111; found 257.2106.

Synthesis of methyl (*R*)-3-hydroxytetradecanoate (9)

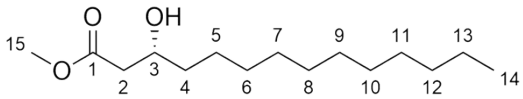

Preparation of catalyst: (*R*)-BINAP (10.5 mg, 17 µmol, 0.024 eq.) and (COD)Ru(2-methylallyl)$_2$ (4.4 mg 0.014 µmol, 0.020 eq.) were suspended in degassed acetone (700 µL) in a 10 mL Schlenk-tube. Then, 180 µL degassed MeOH and 48% aq. HBr (5 µL,

30.9 mmol, 44 eq.) were added and the reaction stirred at r.t. for 45 min. The solvents are removed *in vacuo* and the tube flushed with argon gas.

A solution of methyl 3-oxotetradecanoate (180 mg, 0.7 mmol, 1.0 eq.) in degassed MeOH (2 mL) was added to freshly prepared hydrogenation catalyst in the Schlenk-tube. A balloon with hydrogen gas was connected to the tube, the vessel flushed with hydrogen thoroughly, and the reaction stirred at 55 °C for 3 h. Solvents were removed *in vacuo* and the product obtained after flash chromatography (10:1 – 4:1 (v/v) cyclohexane/EtOAc) as a colourless resin (146 mg, 81% yield).

^{1}H NMR (600 MHz, $CDCl_3$): δ 3.97 (m, 1H, 3-H), 3.68 (s, 3H, 15-H), 2.97 (s, 1H, -OH), 2.47 (dd, *J* = 16.4, 3.1 Hz, 1H, 2-H), 2.39 (dd, *J* = 16.4, 9.1 Hz, 1H, 2-H), 1.51 – 1.37 (m, 3H), 1.31 – 1.22 (m, 17H), 0.85 (t, *J* = 7.0 Hz, 3H, 14-H) ppm.

^{13}C NMR (150 MHz, $CDCl_3$): δ 173.6 (C-1), 68.1 (C-3), 51.8 (C-15), 41.2 (C-2), 36.7, 32.0, 29.74, 29.72, 29.67, 29.61, 29.4, 25.6, 22.8 (C-4 to C-13), 14.2 (C-14) ppm.

HRMS (ESI, *m/z*): calculated for $C_{15}H_{31}O_3$ $[M+H]^+$ 259.2268; found 259.2264.

Optical rotation $[\alpha]_D^{22}$: –14.0 (*c* 1.0 in $CHCl_3$).

Synthesis of methyl (*S*)-3-hydroxytetradecanoate (10)

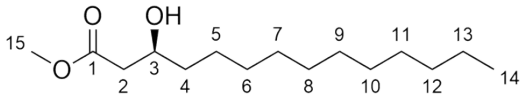

Synthesis of methyl (*S*)-3-hydroxytetradecanoate was performed in the same manner as mentioned above, but using (*S*)-BINAP instead of (*R*)-BINAP, to yield a faint brownish resin (147 mg, 80% yield).

^{1}H NMR (600 MHz, $CDCl_3$): δ 3.96 (m, 1H, 3-H), 3.66 (s, 3H, 15-H), 3.01 (s, 1H, -OH), 2.48 (dd, *J* = 16.4, 3.2 Hz, 1H, 2-H), 2.38 (dd, *J* = 16.4, 9.1 Hz, 1H, 2-H), 1.50 – 1.36 (m, 3H), 1.28 – 1.21 (m, 17H), 0.84 (t, *J* = 7.1 Hz, 3H, 14-H) ppm.

^{13}C NMR (150 MHz, $CDCl_3$): δ 173.5 (C-1), 68.0 (C-3), 51.7 (C-15), 41.3 (C-2), 36.6, 32.0, 29.72, 29.69, 29.65, 29.59, 29.4, 25.6, 22.7 (C-4 to C-13), 14.2 (C-14) ppm.

HRMS (ESI, *m/z*): calculated for $C_{15}H_{31}O_3$ $[M+H]^+$ 259.2268; found 259.2265.

Optical rotation $[\alpha]_D^{22}$: +16.0 (*c* 1.0 in $CHCl_3$).

Synthesis of methyl (3*R*)-3-(((*R*)-3,3,3-trifluoro-2-methoxy-2-phenylpropanoyl)oxy)tetradecanoate (7)

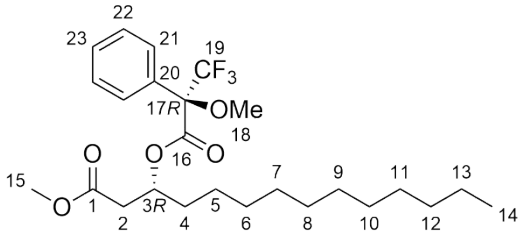

Methyl (*R*)-3-hydroxytetradecanoate (17.4 mg, 67 µmol, 1.0 eq.) was dissolved in CH_2Cl_2 and pyridine (1 mL, anhydrous, 1:1 (v/v)), (*S*)-MTPA-Cl (16 µL, 88 µmol, 1.3 eq.) was added neat and the solution stirred at r.t. for 1 h. After complete consumption of starting material, the reaction was stopped by addition of 0.1 M HCl (3 mL) and extracted three times with CH_2Cl_2 (4 mL, respectively). Combined organic layers are dried over anhydrous Na_2SO_4, filtered, toluene (5 mL) was added and the solvents were removed *in vacuo*. Product was obtained after flash chromatography (98:2 – 95:5 (v/v) cyclohexane/EtOAc) as a colourless resin (27.7 mg, 87% yield).

^{1}H NMR (600 MHz, $CDCl_3$): δ 7.53 (m, 2H, -Ph), 7.39 (m, 3H, -Ph), 5.48 (m, 1H, 3-H), 3.66 (s, 3H, 15-H), 3.54 (s, 3H, 18-H), 2.69 (dd, *J* = 16.0, 8.3 Hz, 1H, 2-H), 2.61 (dd, *J* = 16.0, 4.6 Hz, 1H, 2-H), 1.69 – 1.59 (m, 2H, 4-H), 1.31 – 1.19 (m, 18H, 5-H to 13-H), 0.88 (t, *J* = 7.1 Hz, 3H, 14-H) ppm.

^{13}C NMR (150 MHz, $CDCl_3$): δ 170.7 (C-1), 166.1 (C-16), 132.4 (C-20), 129.7, 128.5, 127.4 (C-21 to C-23), 123.4 (*J* = 288.6 Hz, -CF_3), 73.5 (C-3), 55.6 (C-18), 52.0 (C-15), 38.7 (C-2), 33.7 (C-4), 32.1, 29.7, 29.6, 29.50, 29.48, 29.3, 24.7, 22.8 (C-5 to C-13), 14.3 (C-14) ppm.

HRMS (ESI, *m/z*): calculated for $C_{25}H_{38}F_3O_5$ $[M+H]^+$ 475.2666; found 475.2663.

Synthesis of methyl (3*S*)-3-(((*R*)-3,3,3-trifluoro-2-methoxy-2-phenylpropanoyl)oxy)tetradecanoate (6)

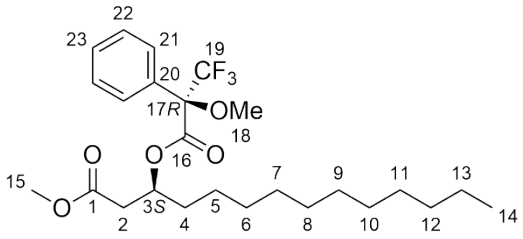

Synthesis of the (*R*)-Mosher ester of methyl (*S*)-3-hydroxytetradecanoate was performed the same way as described above. Methyl (*S*)-3-hydroxytetradecanoate (20.3 mg, 79 µmol) was esterified to yield the title compound (22.9 mg, 61% yield) as a colourless resin.

^{1}H NMR (600 MHz, $CDCl_3$): δ 7.53 (m, 2H, -Ph), 7.39 (m, 3H, -Ph), 5.48 (m, 1H, 3-H), 3.58 (s, 3H, 15-H), 3.53 (s, 3H, 18-H), 2.64 (dd, *J* = 16.0, 8.2 Hz, 1H, 2-H), 2.57 (dd, *J* = 16.0, 4.9 Hz, 1H, 2-H), 1.70 (m, 2H, 4-H), 1.35 – 1.25 (m, 18H, 5-H to 13-H), 0.88 (t, *J* = 7.1 Hz, 3H, 14-H) ppm.

^{13}C NMR (150 MHz, $CDCl_3$): δ 170.5 (C-1), 166.0 (C-16), 132.3 (C-20), 129.7, 128.5, 127.6 (C-21 to C-23), 123.4 (*J* = 288.6 Hz, -CF_3), 73.6 (C-3), 55.5 (C-18), 51.9 (C-15), 38.6 (C-2), 33.9 (C-4), 32.0, 29.7, 29.6, 29.54, 29.47, 29.4, 25.1, 22.8 (C-5 to C-13), 14.3 (C-14) ppm.

HRMS (ESI, *m/z*): calculated for $C_{25}H_{38}F_3O_5$ $[M+H]^+$ 475.2666; found 475.2661.

Derivatisation of the 3-hydroxytetradecanoate residue of keanumycin D

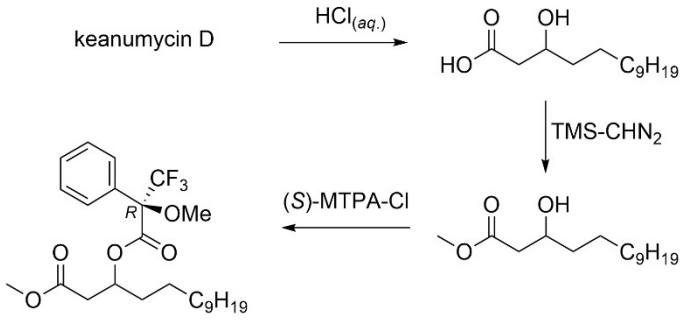

Approximately 150 µg of keanumycin D were hydrolysed with 6 N HCl (200 µL) and heating to 100 °C for 12 h. Solvents were removed *in vacuo* and the residue dissolved in anhydrous MeOH (200 µL). Trimethylsilyldiazomethane (200 µL, ca. 0.6 M in hexane, 0.12 mmol) was added dropwise at r.t. until a faint yellow colour persisted and the suspension was stirred for an additional 15 min. The reaction was stopped by addition of formic acid (5 µL). Toluene (1 mL) was added and the solvents were removed *in vacuo*. The residue was suspended in CH_2Cl_2 and pyridine (200 µL, anhydrous, 1:1 (v/v)) and (*S*)-MTPA-Cl (100 µL, 88 µmol, 1.3 eq.) was added neat in small batches and the reaction stirred at r.t. for 35 min before it was stopped by the addition of MeOH (200 µL). Solvents were removed *in vacuo* and the residue dissolved in $CHCl_3$ (100 µL) prior to GCMS analysis.

GCMS analysis of MTPA-derivatised 3-hydroxytetradecanoate methyl esters

GCMS analysis was performed on a TRACE 1310 GC (Thermo Scientific) coupled with a TSQ 9000 electron impact-triple quadrupole mass spectrometer (Thermo Scientific). A 4 mm GC inlet liner with quartz wool and a BPX5 capillary column (SGE, 30 m, 0.25 mm ID, 0.25 µm film) were used. The column was operated with helium carrier gas (0.6 mL/min) and split injection (split flow: 15 mL/min, ratio 1:25). The injector temperature was set to 250 °C, the GC temperature was set to 200 °C

(isothermic program for 4h), MS transfer line was set to 300 °C, the ion source temperature was set to 200 °C. Total ion current (TIC) values were recorded in the mass range of 45 – 600 amu.

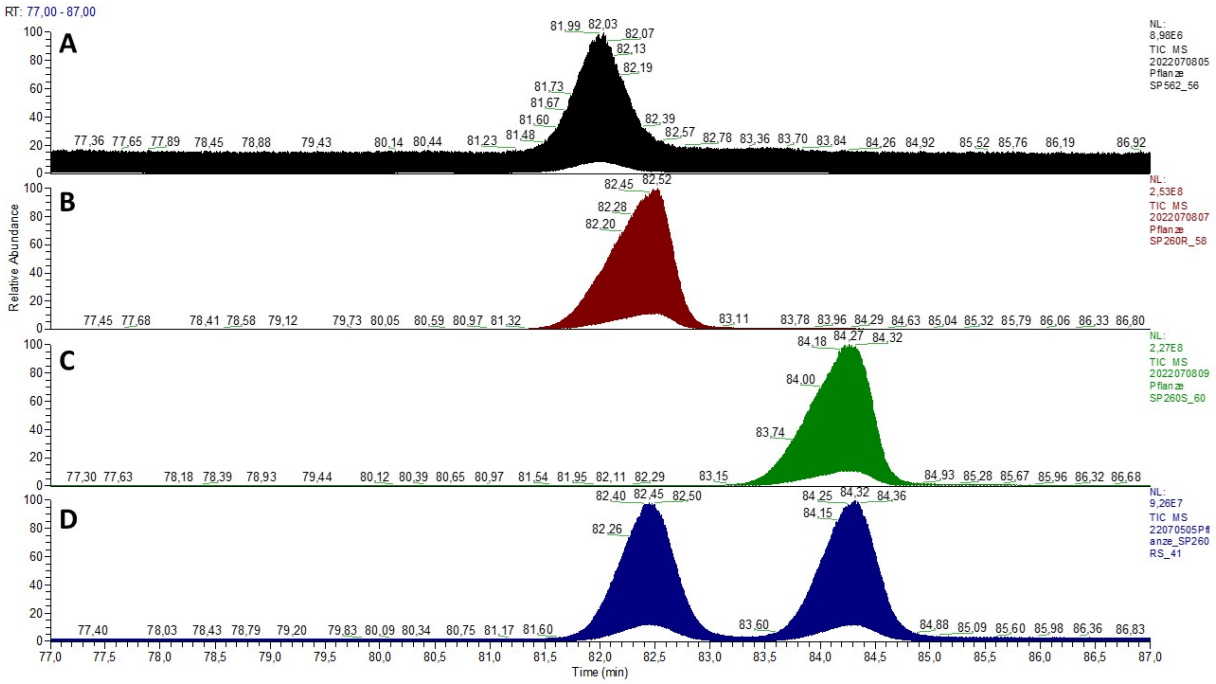

Figure S38 Elucidation of the absolute configuration of 3-hydroxytetradecanoic acid in keanumycin D. Total ion chromatograms of A) derivatised 3-hydroxytetradecanoic acid from keanumycin D; B) MTPA ester of (*R*)-configured standard **7**; C) MTPA ester of (*S*)-configured standard **6**; D) 1:1 mixture of (*R*)- and (*S*)-configured standards **7** and **6**.

LCMS analysis of hydrolysed nunapeptin C

Nunapeptin C (ca. 500 µg) was resuspended in 1N NaOH (100 µL) and heated at 80 °C for 16 h. After cooling the reaction to r.t., an aliquot (10 µL) was analysed on a Shimadzu Nexera X3 UHPLC connected to a Shimadzu single quadrupole mass spectrometer (LCMS-2020). The UHPLC was equipped with a Phenomenex Kinetex Phenyl-Hexyl column (50 x 2.1 mm, 1.7 µm, 100 Å) and the column oven set to 40 °C. The scan range of MS was set to *m/z* 140 to 300, a scan speed of 7500 u/s and an event time of 300 ms. The interface temperature was set to 350 °C, the desolvation line temperature to 250 °C and the heat block temperature to 400 °C. The nebulising gas flow was set to 1.5 L/min and dry gas flow to 15 L/min. The following method was used: flow rate of 0.7 mL/min; 0 – 0.5 min: 10% MeCN in water; 0.5 – 8.5 min: linear gradient from 10% to 100% MeCN in water. A commercial standard of octanoic acid (*m/z* 143.1 in negative mode) was treated equally.

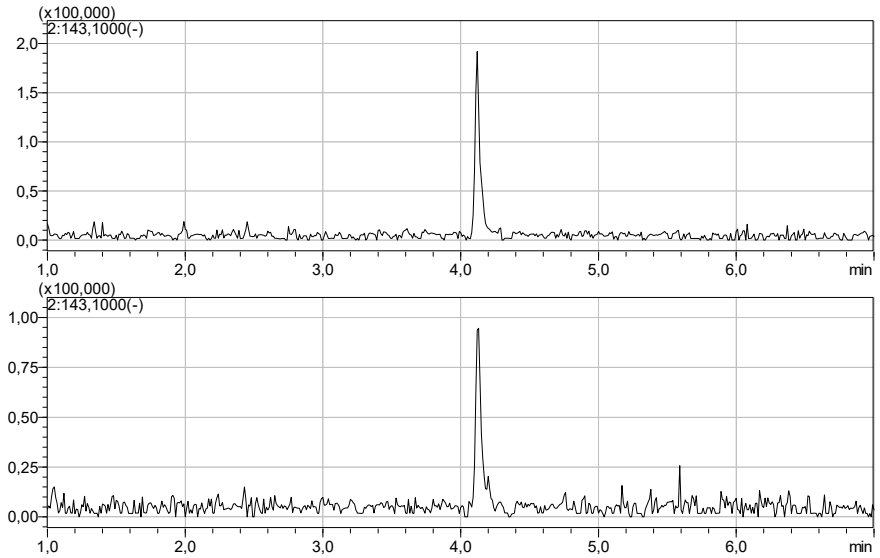

hydrolysed nunapeptin C (**3**)

commercial standard of octanoic acid

Figure S39 Extracted ion chromatograms of the *N*-acyl lipid from hydrolysed nunapeptin B and a commercial standard of octanoic acid (*m/z* 143.1 $[M-H]^-$, t_R = 4.1 min).

HCN production in *Pseudomonas nunensis* 4A2e

The ability of 4A2e to produce HCN was tested as recently described by Pacheco-Moreno *et al*.[24] An overnight culture of wild type 4A2e was used to inoculate different solid media (LB, SM/5, NGM, co-cultivation agar, and modified Davis medium agar) in a 48-well plate. A Feigl-Anger reagent paper was prepared by soaking a Whatman 3MM chromatography paper in Feigl-Anger reagent (copper(II) ethyl acetoacetate (5 mg/mL) and 4,4'-methylenebis(*N*,*N*-dimethylaniline) (5 mg/mL) in $CHCl_3$) followed by evaporation of the solvent. The paper was placed under the plate lid and the plate was incubated at 22 °C for 2 d. An aqueous solution of KCN (100 µL, 0.25 mg/mL) served as positive control. The production of HCN was scored by the intensity of the blue staining on the paper. It was highest on LB, whilst co-cultivation agar, modified Davis medium, and SM/5 showed medium production; and little production was observed on NGM agar. In addition, comparison of wild type 4A2e with a gene deletion mutant (Δ*nup*Δ*kea*Δ*bra*) impaired in the production of **1**–**4**, and regulatory mutants showed no evident difference in HCN production.

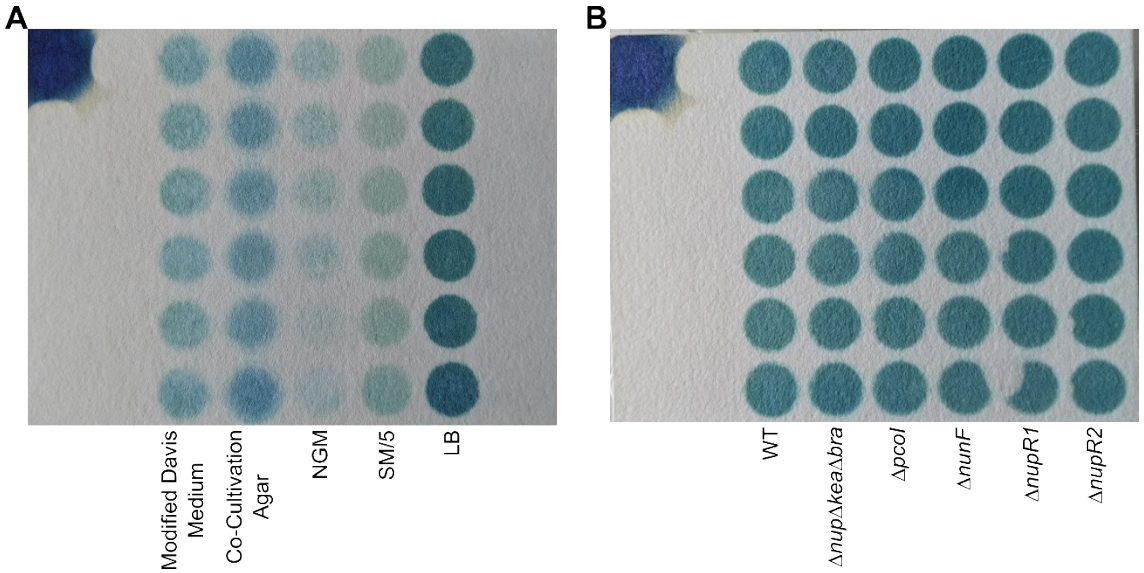

Figure S40 Investigation of HCN production of 4A2e. A) Comparison of HCN production of wild type 4A2e on different media. B) Comparison of HCN production of wild type 4A2e and different mutants on LB agar.

References

1 T. Stiernagle, *WormBook*, 2006, DOI: 10.1895/wormbook.1.101.1.
2 A. Pires da Silva, *WormBook*, 2013, DOI: 10.1895/wormbook.1.114.2.
3 L. R. Hmelo, B. R. Borlee, H. Almblad, M. E. Love, T. E. Randall, B. S. Tseng, C. Lin, Y. Irie, K. M. Storek, J. J. Yang, R. J. Siehnel, P. L. Howell, P. K. Singh, T. Tolker-Nielsen, M. R. Parsek, H. P. Schweizer and J. J. Harrison, *Nat. Protoc.*, 2015, **10**, 1820–1841.
4 L. Medlin, H. J. Elwood, S. Stickel and M. L. Sogin, *Gene*, 1988, **71**, 491–499.
5 R. Floyd, E. Abebe, A. Papert and M. Blaxter, *Mol. Ecol.*, 2002, **11**, 839–850.
6 T. E. Douglas, D. A. Brock, B. Adu-Oppong, D. C. Queller and J. E. Strassmann, in *Dictyostelium discoideum Protocols*, eds. L. Eichinger and F. Rivero, Humana Press, Totowa, NJ, 2013, vol. 983, pp. 113–124.
7 A. Barrière and M.-A. Félix, *WormBook*, 2014, DOI: 10.1895/wormbook.1.115.2.
8 K. Blin, S. Shaw, K. Steinke, R. Villebro, N. Ziemert, S. Y. Lee, M. H. Medema and T. Weber, *Nucleic Acids Research*, 2019, **47**, W81–W87.
9 K. Blin, S. Shaw, H. E. Augustijn, Z. L. Reitz, F. Biermann, M. Alanjary, A. Fetter, B. R. Terlouw, W. W. Metcalf, E. J. N. Helfrich, G. P. van Wezel, M. H. Medema and T. Weber, *Nucleic Acids Research*, 2023, gkad344.
10 S. Lu, J. Wang, F. Chitsaz, M. K. Derbyshire, R. C. Geer, N. R. Gonzales, M. Gwadz, D. I. Hurwitz, G. H. Marchler, J. S. Song, N. Thanki, R. A. Yamashita, M. Yang, D. Zhang, C. Zheng, C. J. Lanczycki and A. Marchler-Bauer, *Nucleic Acids Res.*, 2020, **48**, 265–268.
11 P. A. Kitts, D. M. Church, F. Thibaud-Nissen, J. Choi, V. Hem, V. Sapojnikov, R. G. Smith, T. Tatusova, C. Xiang, A. Zherikov, M. DiCuccio, T. D. Murphy, K. D. Pruitt and A. Kimchi, *Nucleic Acids Res.*, 2016, **44**, D73–D80.
12 V. F. Scalfani, *J. Chem. Educ.*, 2021, **98**, 3904–3914.
13 M. D. Lee, *Bioinformatics*, 2019, **35**, 4162–4164.
14 C. Jain, L. M. Rodriguez-R, A. M. Phillippy, K. T. Konstantinidis and S. Aluru, *Nat Commun*, 2018, **9**, 5114.
15 T. Seemann, *Bioinformatics*, 2014, **30**, 2068–2069.
16 C. L. M. Gilchrist and Y.-H. Chooi, *Bioinformatics*, 2021, **37**, 2473–2475.
17 C. F. Michelsen, J. Watrous, M. A. Glaring, R. Kersten, N. Koyama, P. C. Dorrestein and P. Stougaard, *mBio*, 2015, **6**, e00079-15.

18 J. Arp, S. Götze, R. Mukherji, D. J. Mattern, M. García-Altares, M. Klapper, D. A. Brock, A. A. Brakhage, J. E. Strassmann, D. C. Queller, B. Bardl, K. Willing, G. Peschel and P. Stallforth, *Proc. Natl. Acad. Sci. U.S.A.*, 2018, **115**, 3758–3763.
19 S. Götze, R. Vij, K. Burow, N. Thome, L. Urbat, N. Schlosser, S. Pflanze, R. Müller, V. G. Hänsch, K. Schlabach, L. Fazlikhani, G. Walther, H.-M. Dahse, L. Regestein, S. Brunke, B. Hube, C. Hertweck, P. Franken and P. Stallforth, *J. Am. Chem. Soc.*, 2023, **145**, 2342–2353.
20 C. L. Berry, A. K. C. Brassinga, L. J. Donald, W. G. D. Fernando, P. C. Loewen and T. R. de Kievit, *Can. J. Microbiol.*, 2012, **58**, 1027–1034.
21 R. Froquet, E. Lelong, A. Marchetti and P. Cosson, *Nat. Protoc.*, 2009, **4**, 25–30.
22 M. Klapper, S. Götze, R. Barnett, K. Willing and P. Stallforth, *Angew. Chem. Int. Ed.*, 2016, **55**, 8944–8947.
23 Y. Schmidt, M. van der Voort, M. Crüsemann, J. Piel, M. Josten, H.-G. Sahl, H. Miess, J. M. Raaijmakers and H. Gross, *ChemBioChem*, 2014, **15**, 259–266.
24 A. Pacheco-Moreno, F. L. Stefanato, J. J. Ford, C. Trippel, S. Uszkoreit, L. Ferrafiat, L. Grenga, R. Dickens, N. Kelly, A. D. Kingdon, L. Ambrosetti, S. A. Nepogodiev, K. C. Findlay, J. Cheema, M. Trick, G. Chandra, G. Tomalin, J. G. Malone and A. W. Truman, *eLife*, 2021, **10**, e71900.

NMR Spectra

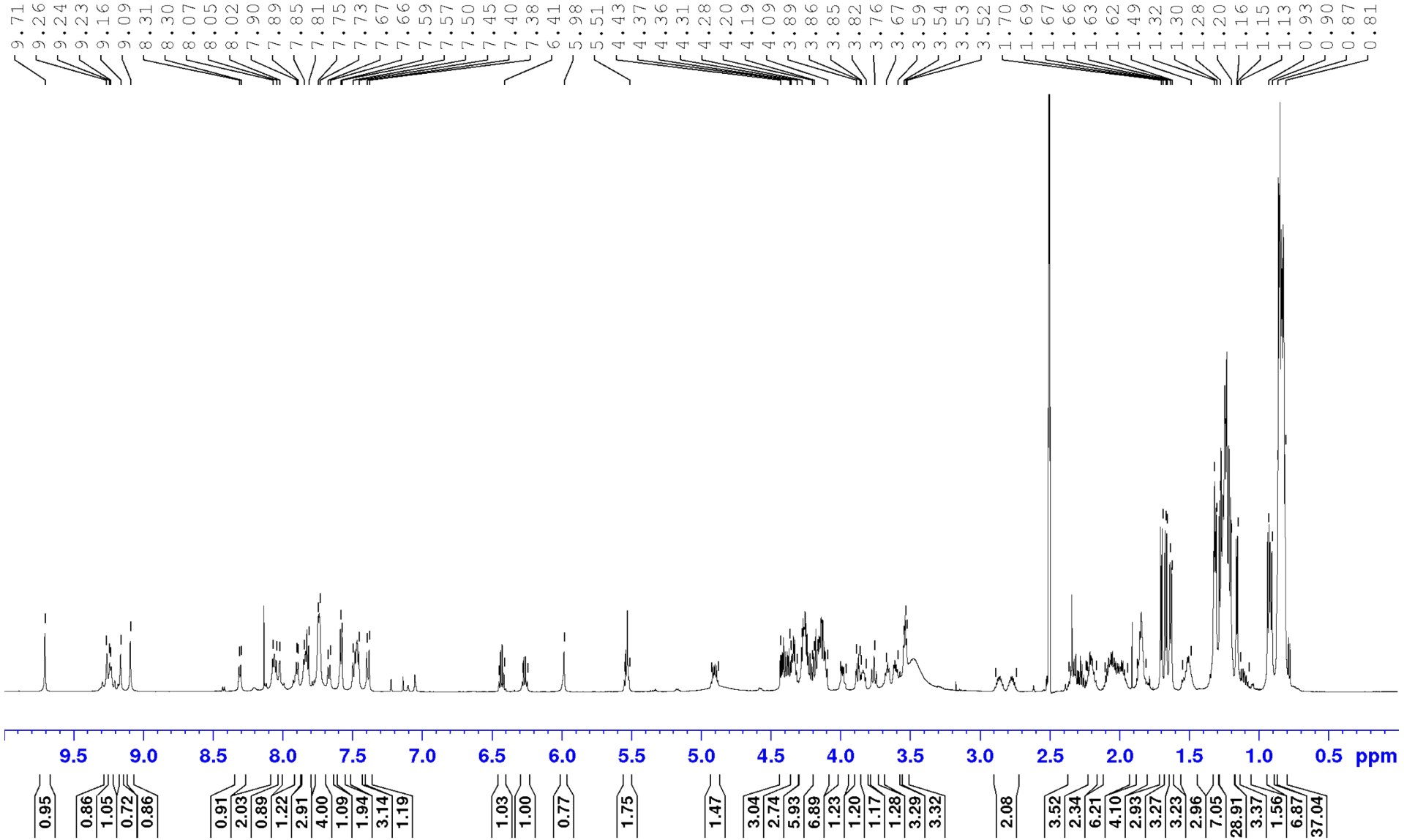

Figure S41 ^{1}H NMR spectrum of nunapeptin B (**2**, 600 MHz, DMSO-d_6).

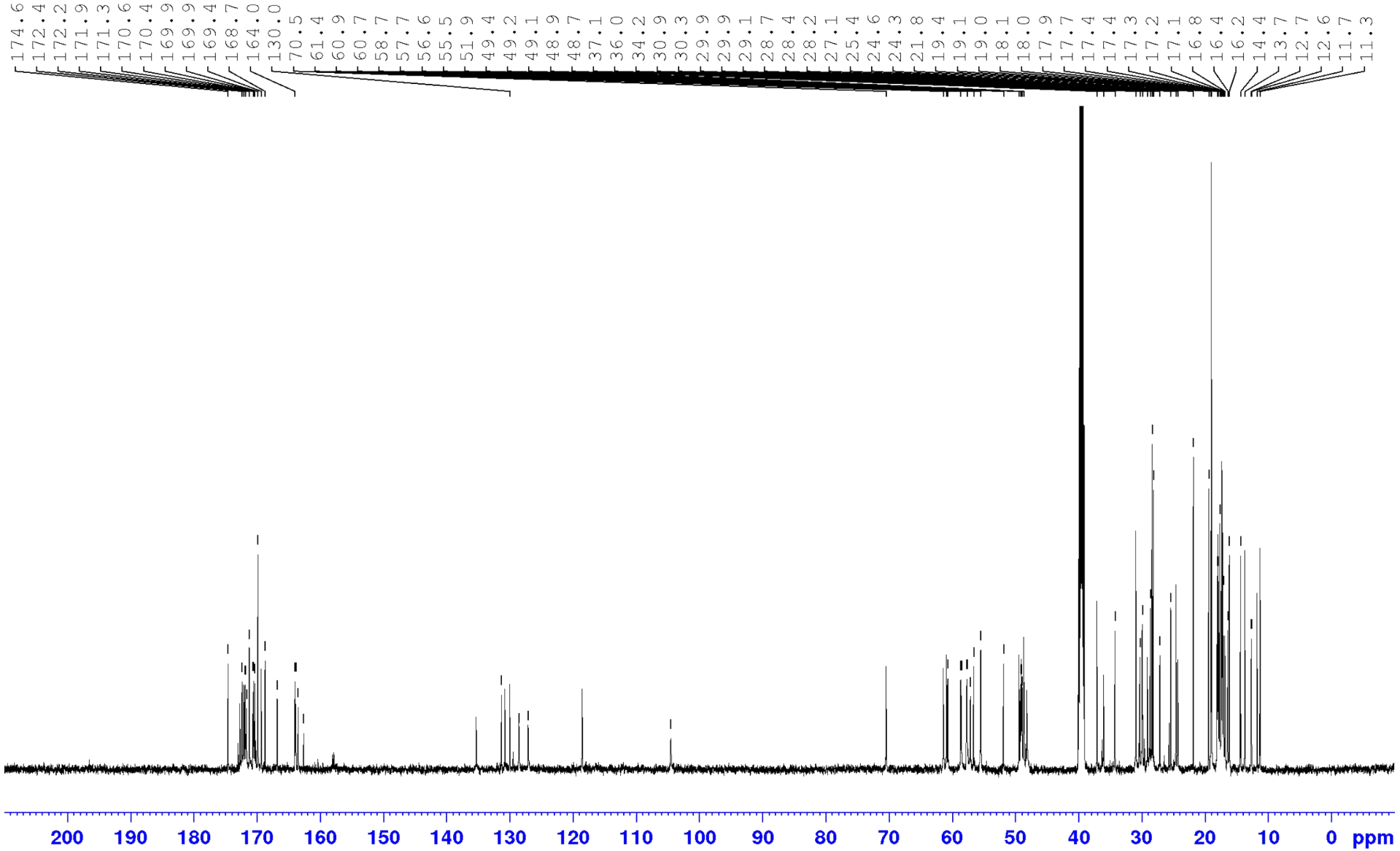

Figure S42 ^{13}C NMR spectrum of nunapeptin B (**2**, 150 MHz, DMSO-d_6).

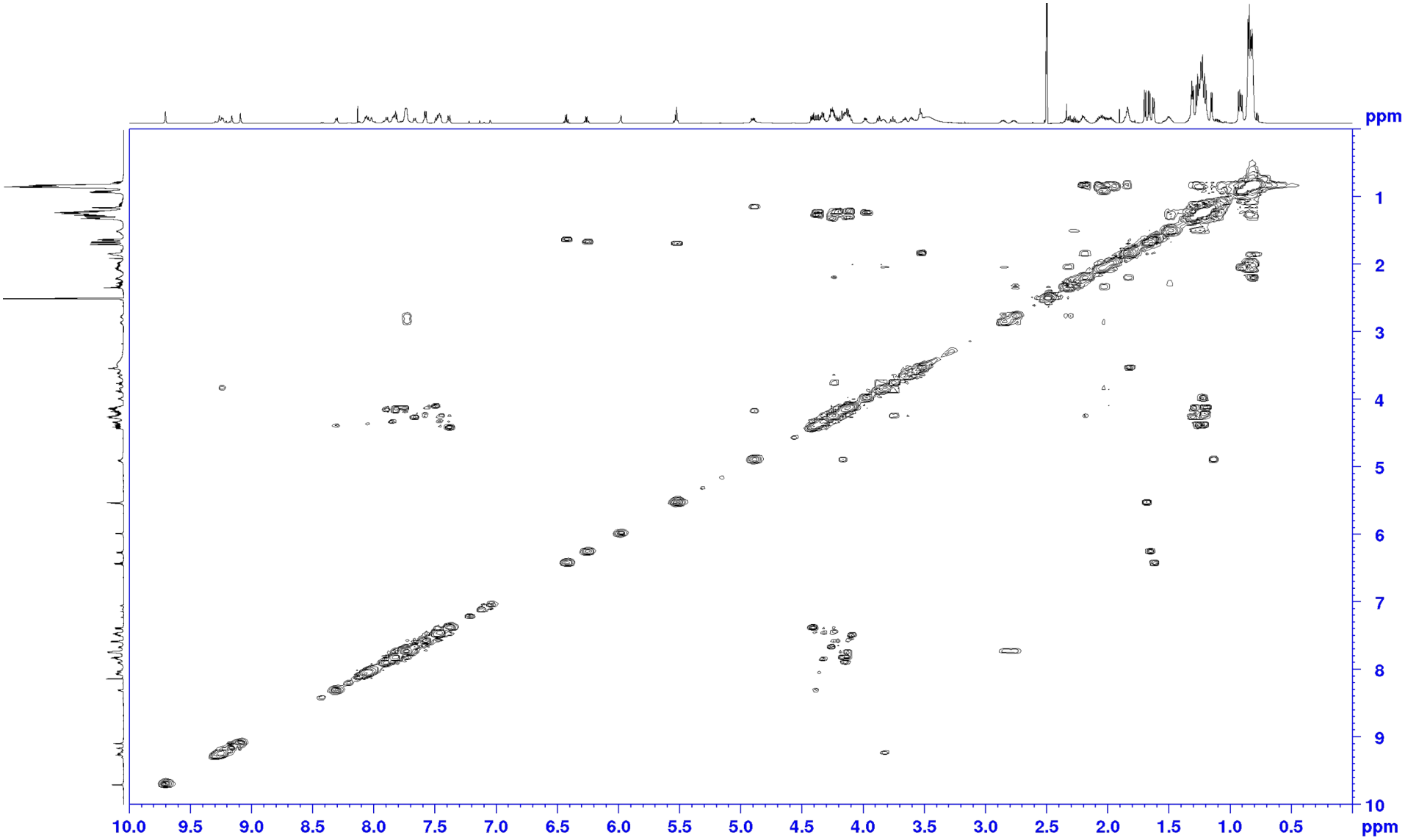

Figure S43 ^{1}H-^{1}H-COSY spectrum of nunapeptin B (**2**, 600 MHz, DMSO-d_6).

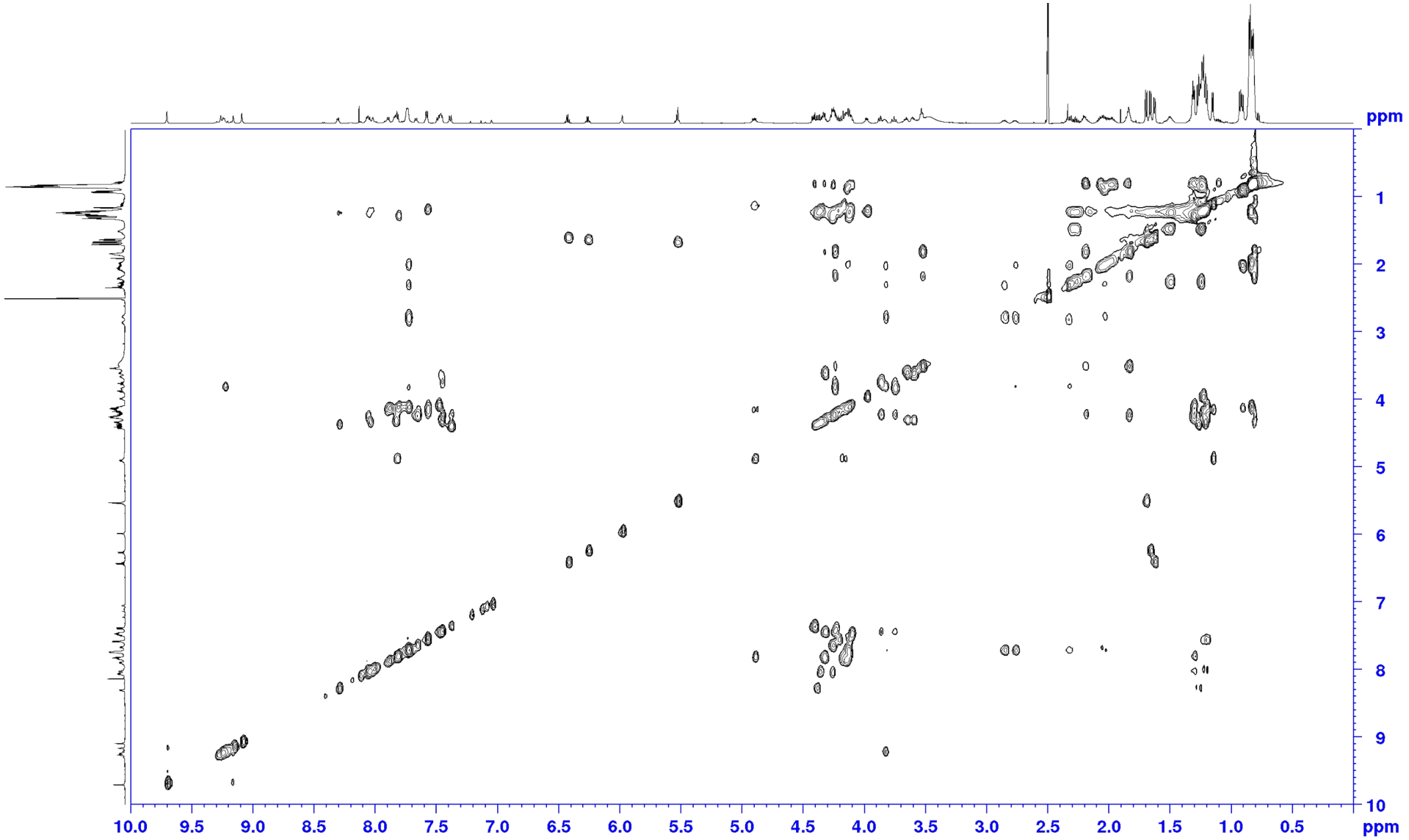

Figure S44 ^{1}H-^{1}H-TOCSY spectrum of nunapeptin B (**2**, 600 MHz, DMSO-d_6).

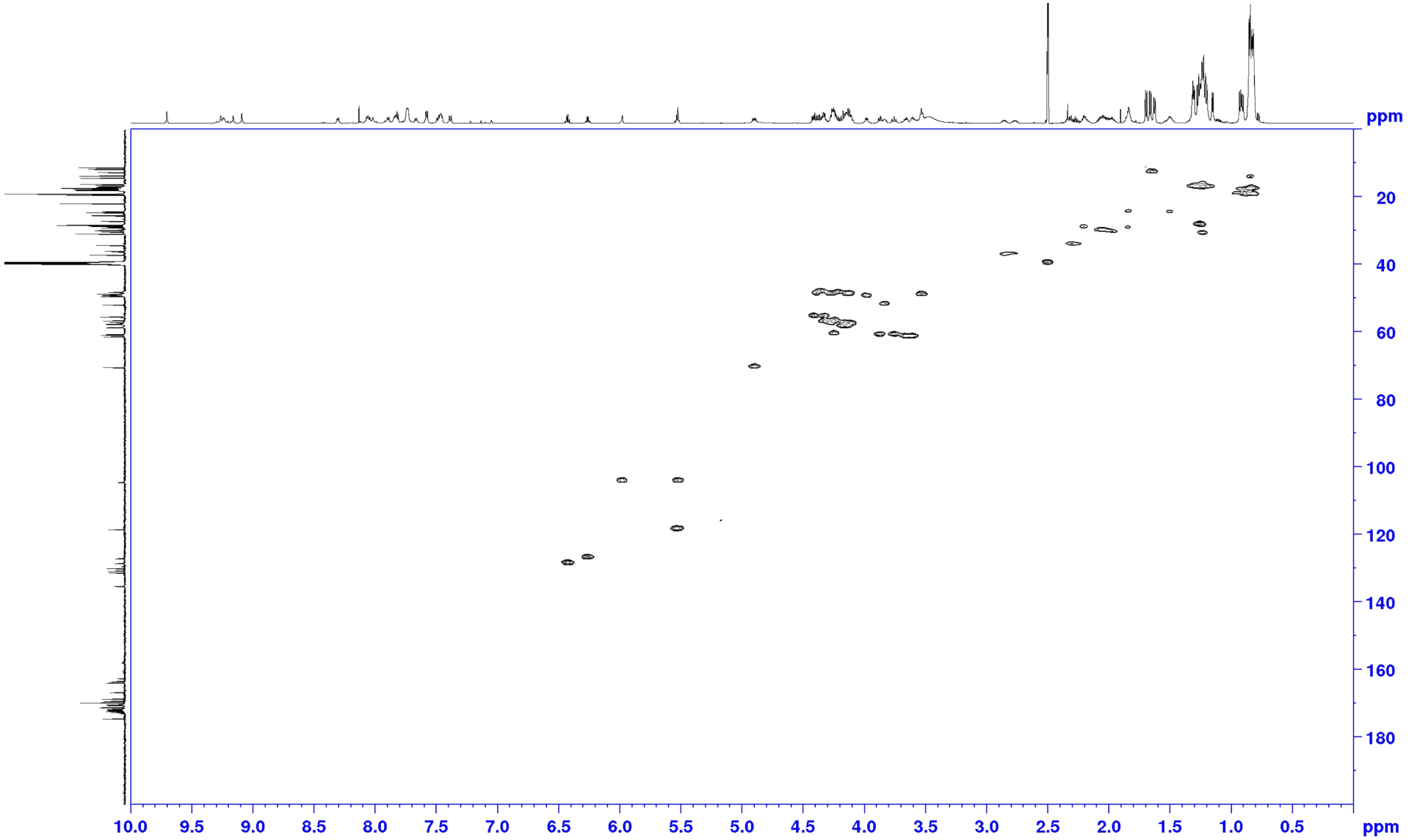

Figure S45 ^{1}H-^{13}C-HSQC spectrum of nunapeptin B (**2**, 600/150 MHz, DMSO-d_6).

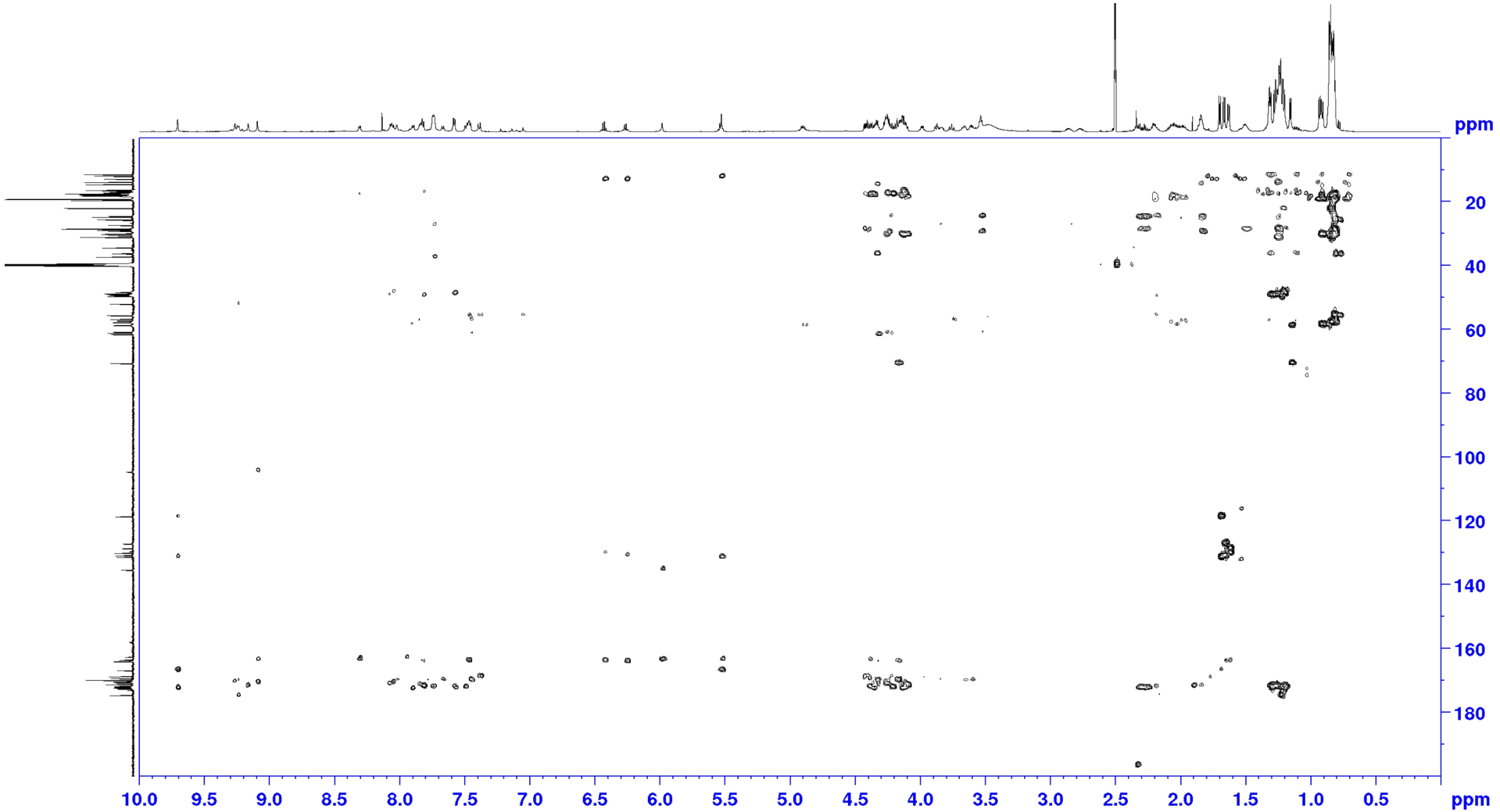

Figure S46 ^{1}H-^{13}C-HMBC spectrum of nunapeptin B (**2**, 600/150 MHz, DMSO-d_6).

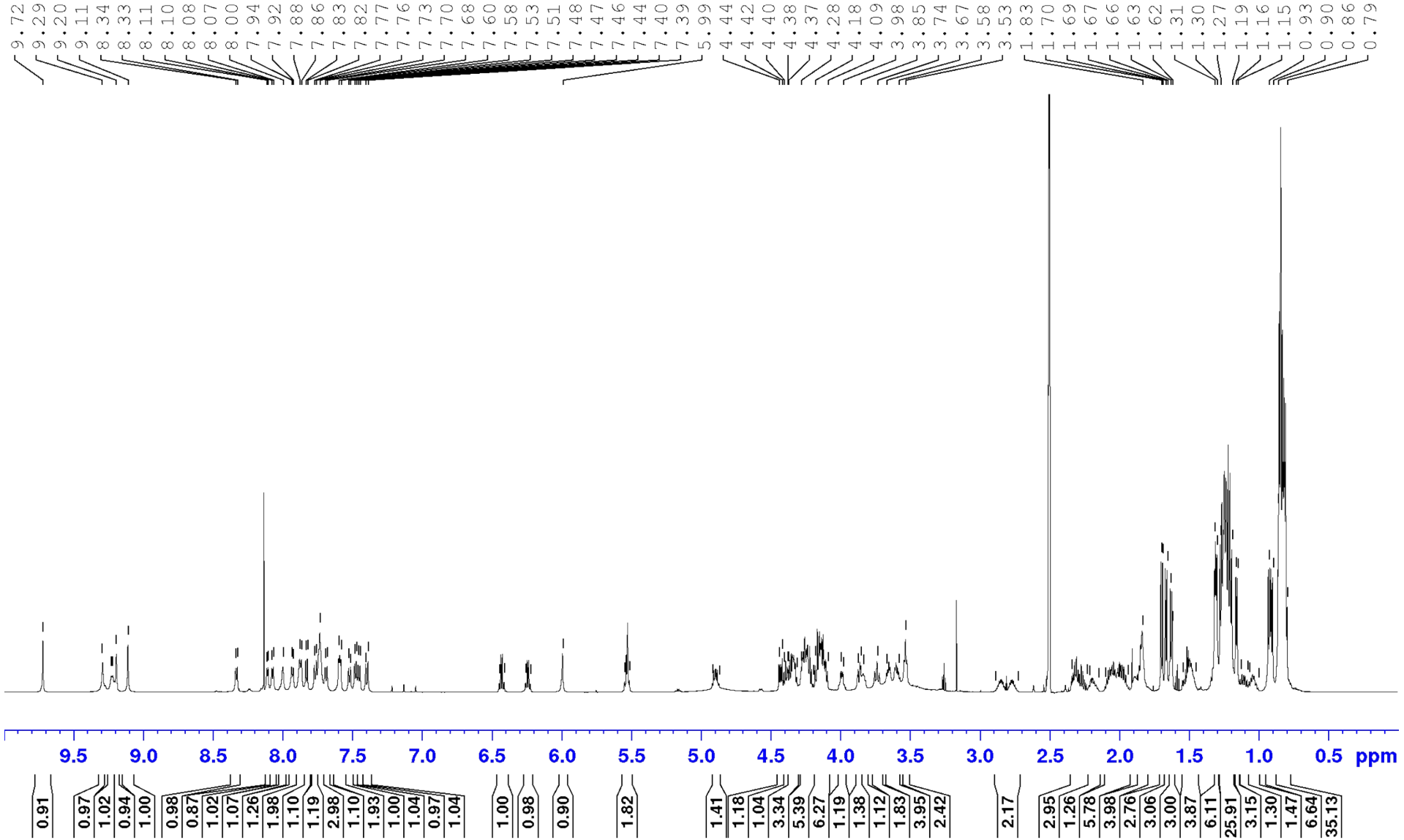

Figure S47 ^{1}H NMR spectrum of nunapeptin C (**3**, 600 MHz, DMSO-d_6).

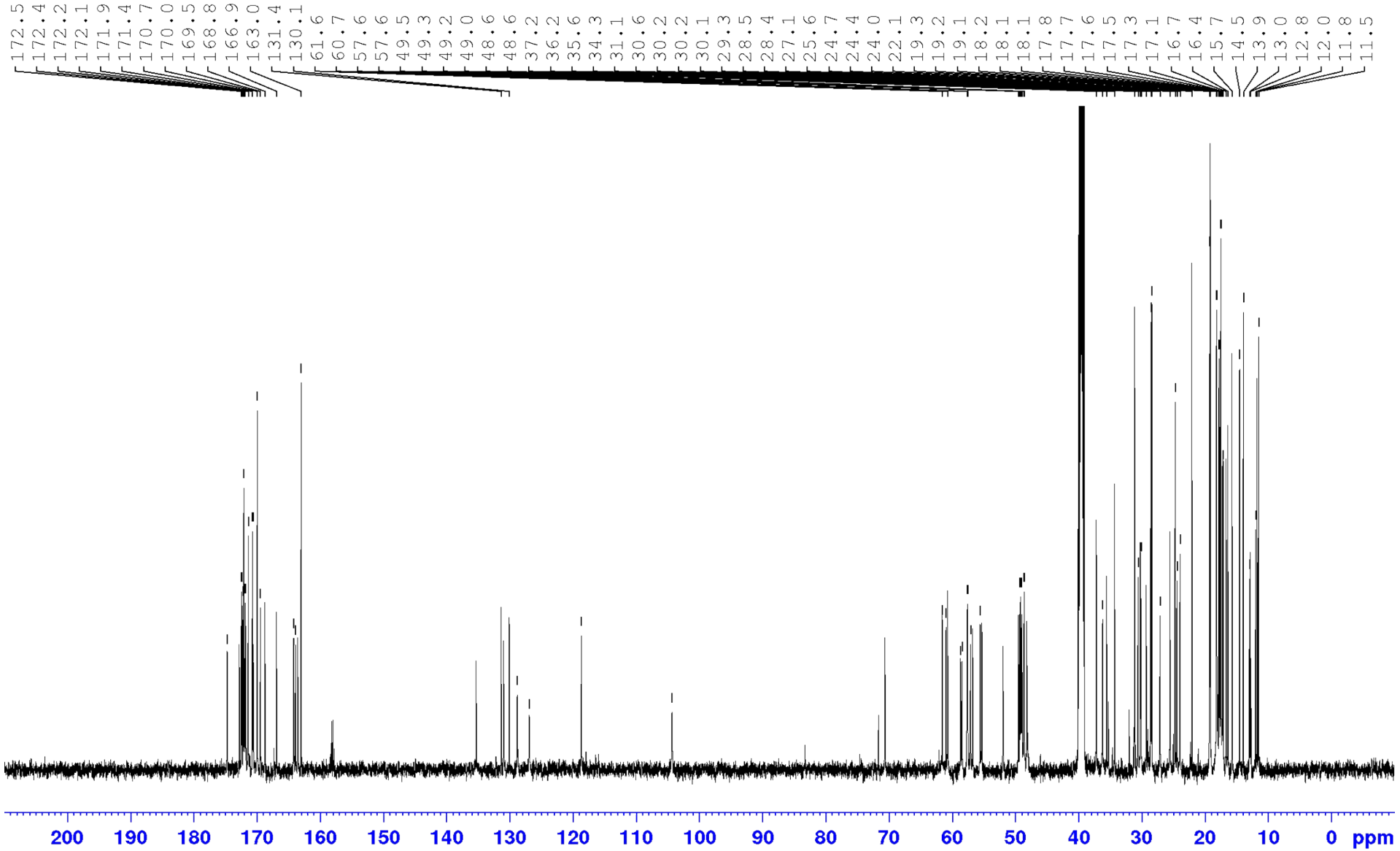

Figure S48 ^{13}C NMR spectrum of nunapeptin C (**3**, 150 MHz, DMSO-d_6).

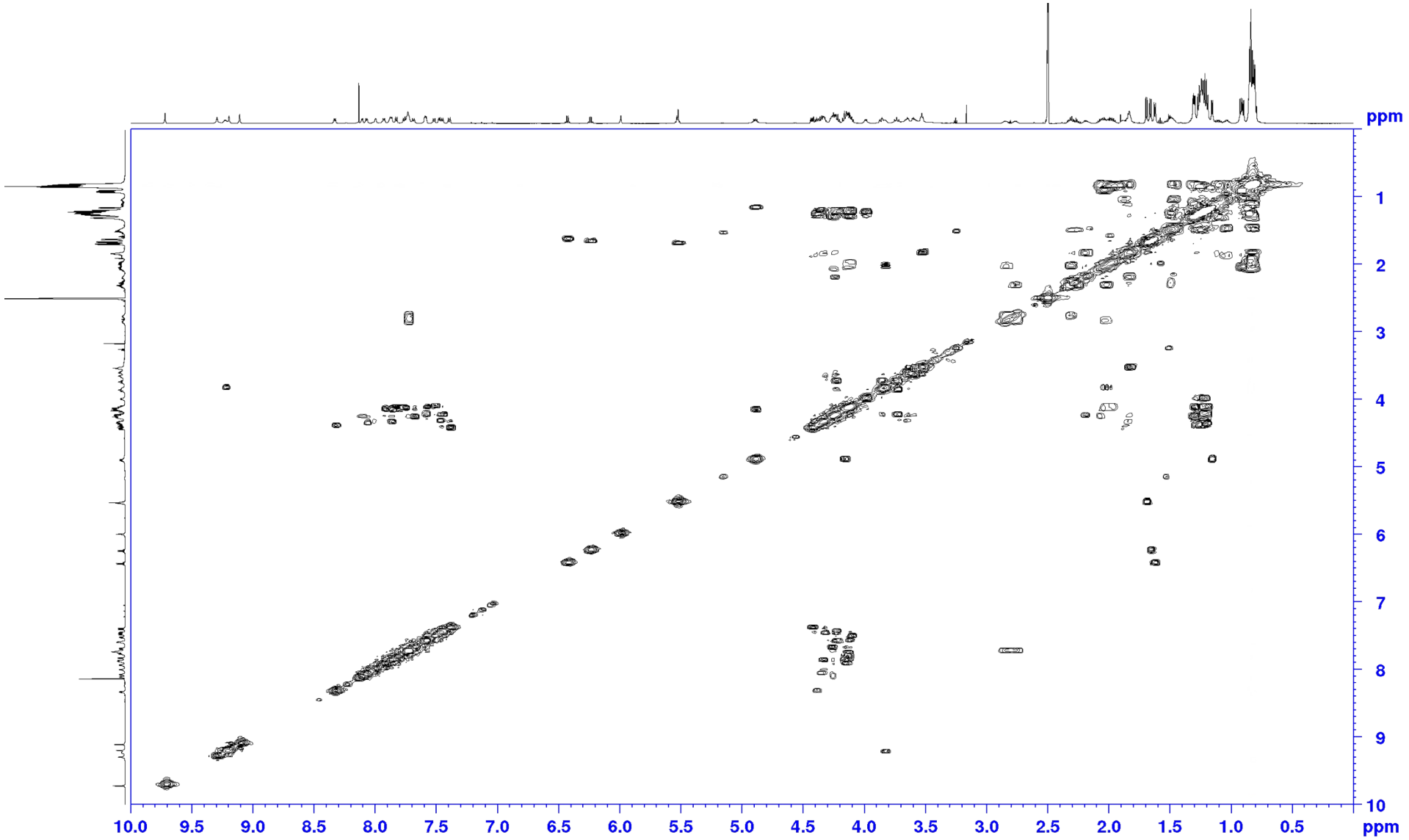

Figure S49 ^{1}H-^{1}H-COSY spectrum of nunapeptin C (**3**, 600 MHz, DMSO-d_6).

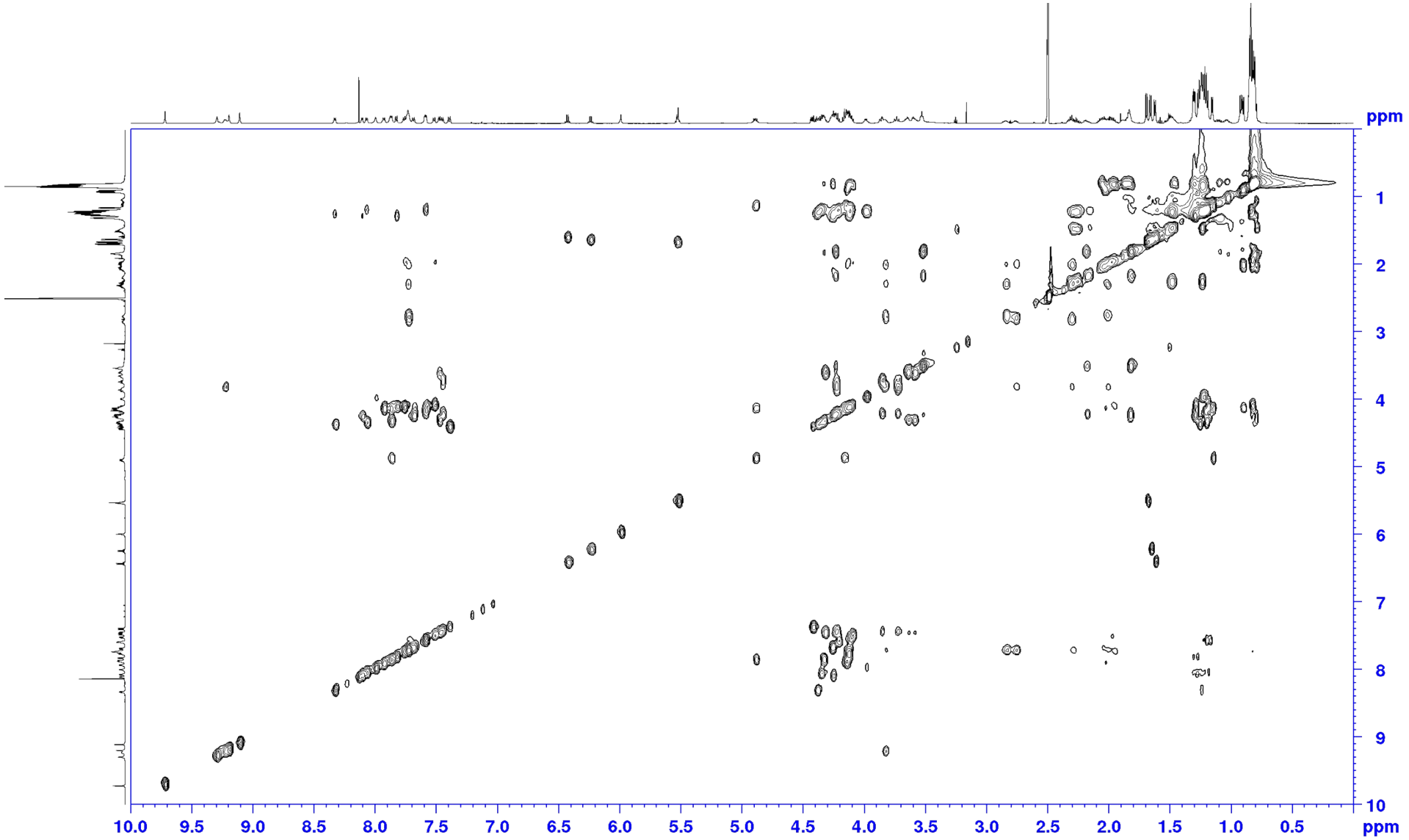

Figure S50 ^{1}H-^{1}H-TOCSY spectrum of nunapeptin C (**3**, 600 MHz, DMSO-d_6).

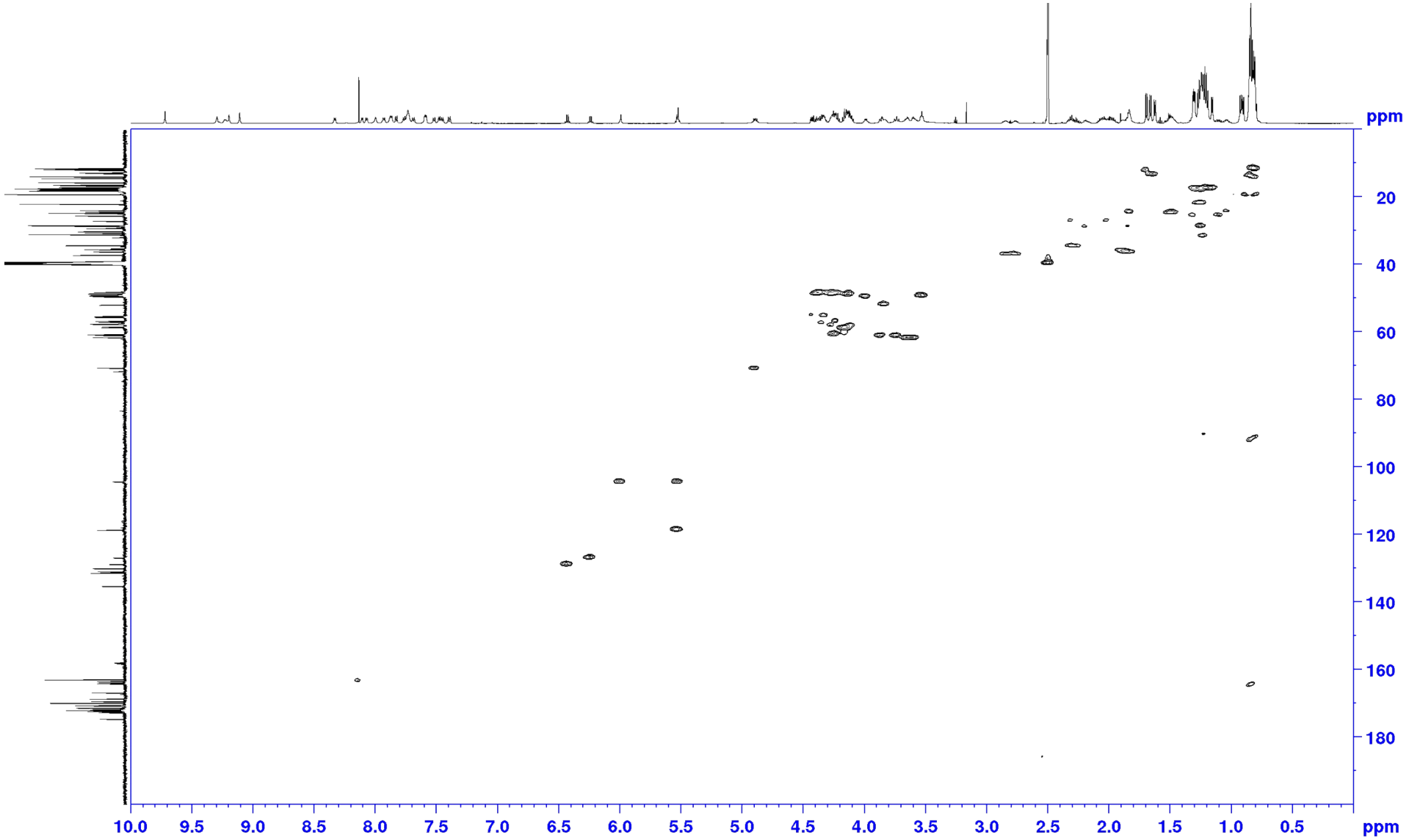

Figure S51 ^{1}H-^{13}C-HSQC spectrum of nunapeptin C (**3**, 600/150 MHz, DMSO-d_6).

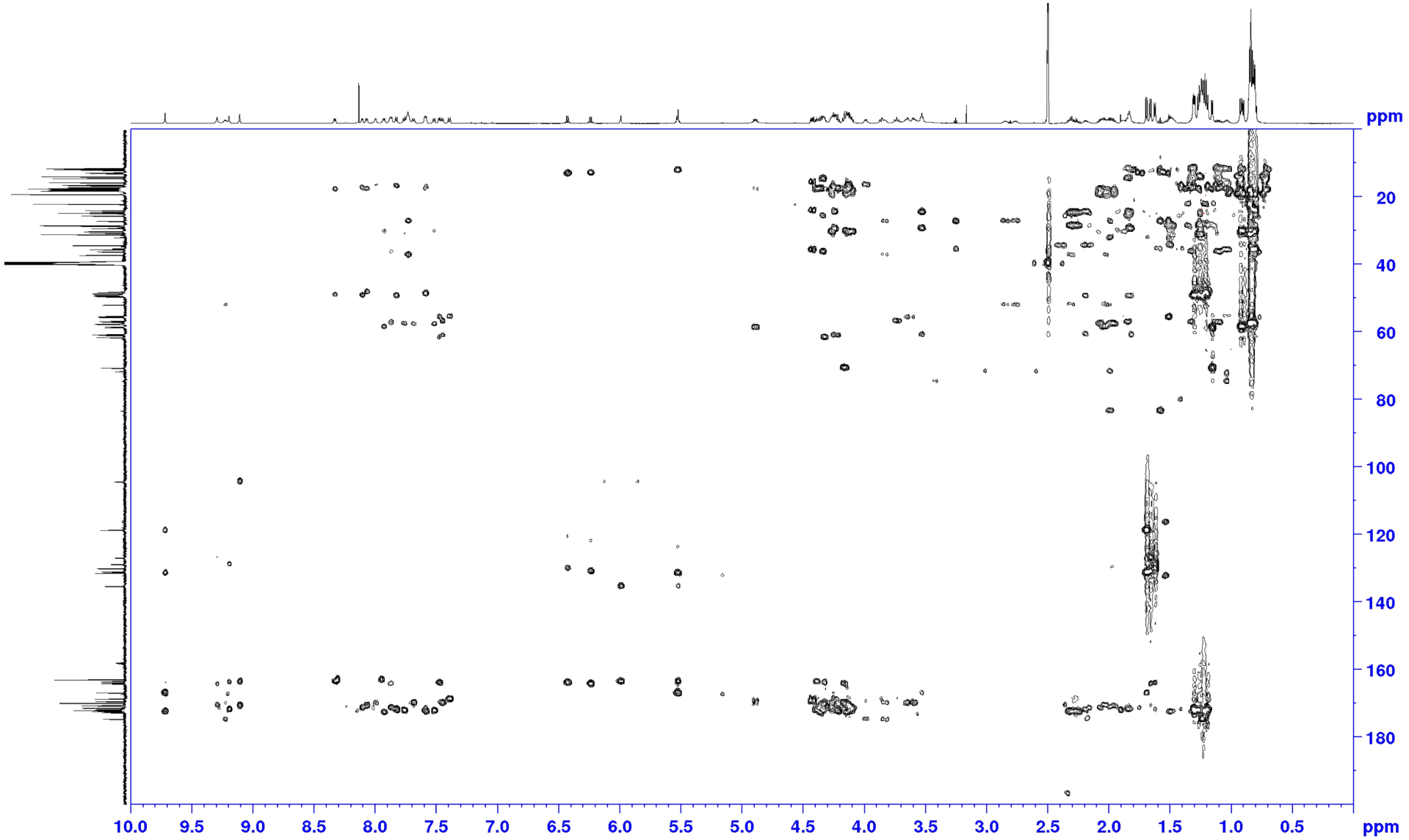

Figure S52 ^{1}H-^{13}C-HMBC spectrum of nunapeptin C (**3**, 600/150 MHz, DMSO-d_6).

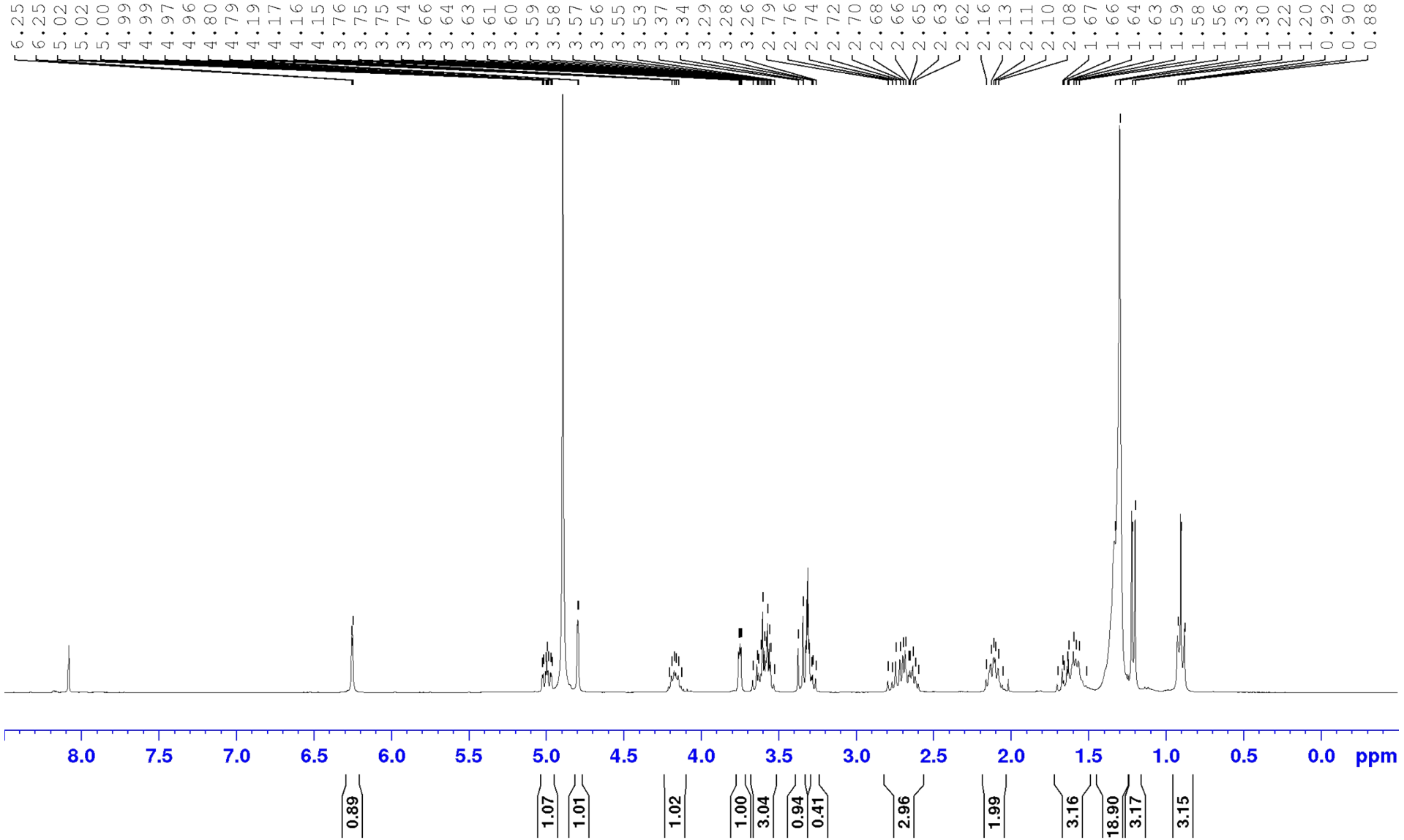

Figure S53 ^{1}H NMR spectrum of brabantamide A (**4**, 300 MHz, CD_3OD).

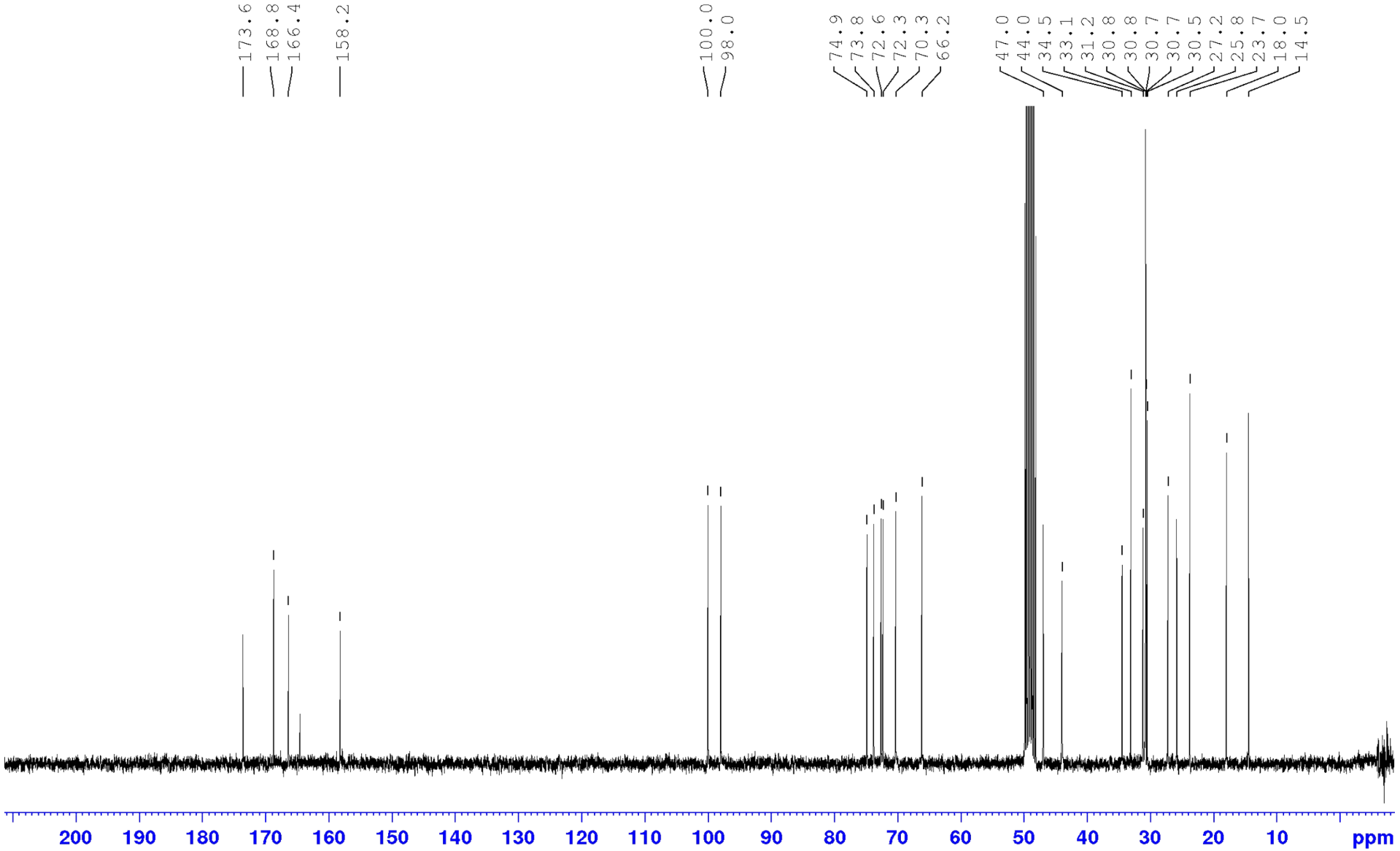

Figure S54 ^{13}C NMR spectrum of brabantamide A (**4**, 75 MHz, CD_3OD).

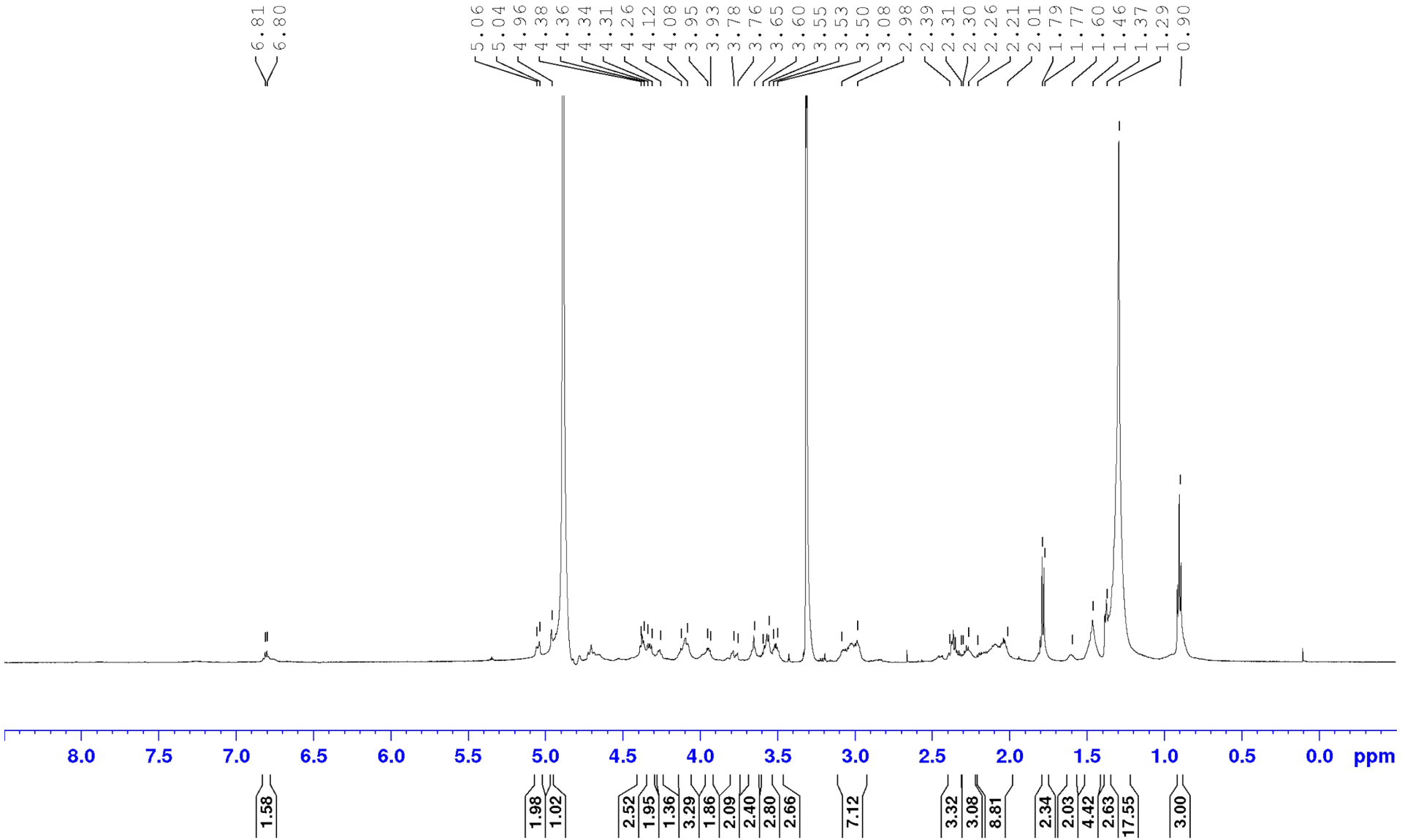

Figure S55 ^{1}H NMR spectrum of keanumycin D (**1**, 600 MHz, CD_3OD).

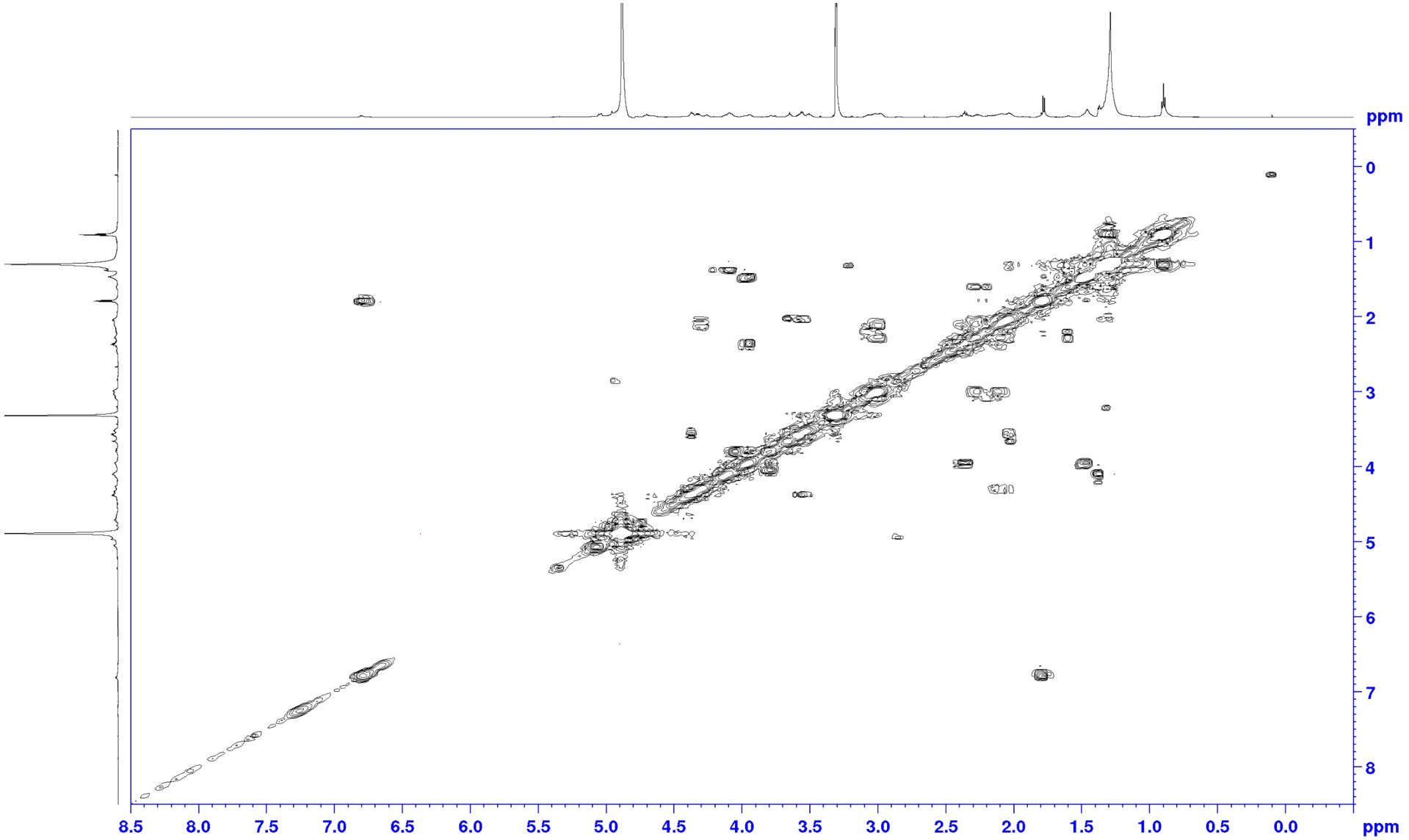

Figure S56 ^{1}H-^{1}H-COSY spectrum of keanumycin D (**1**, 600 MHz, CD_3OD).

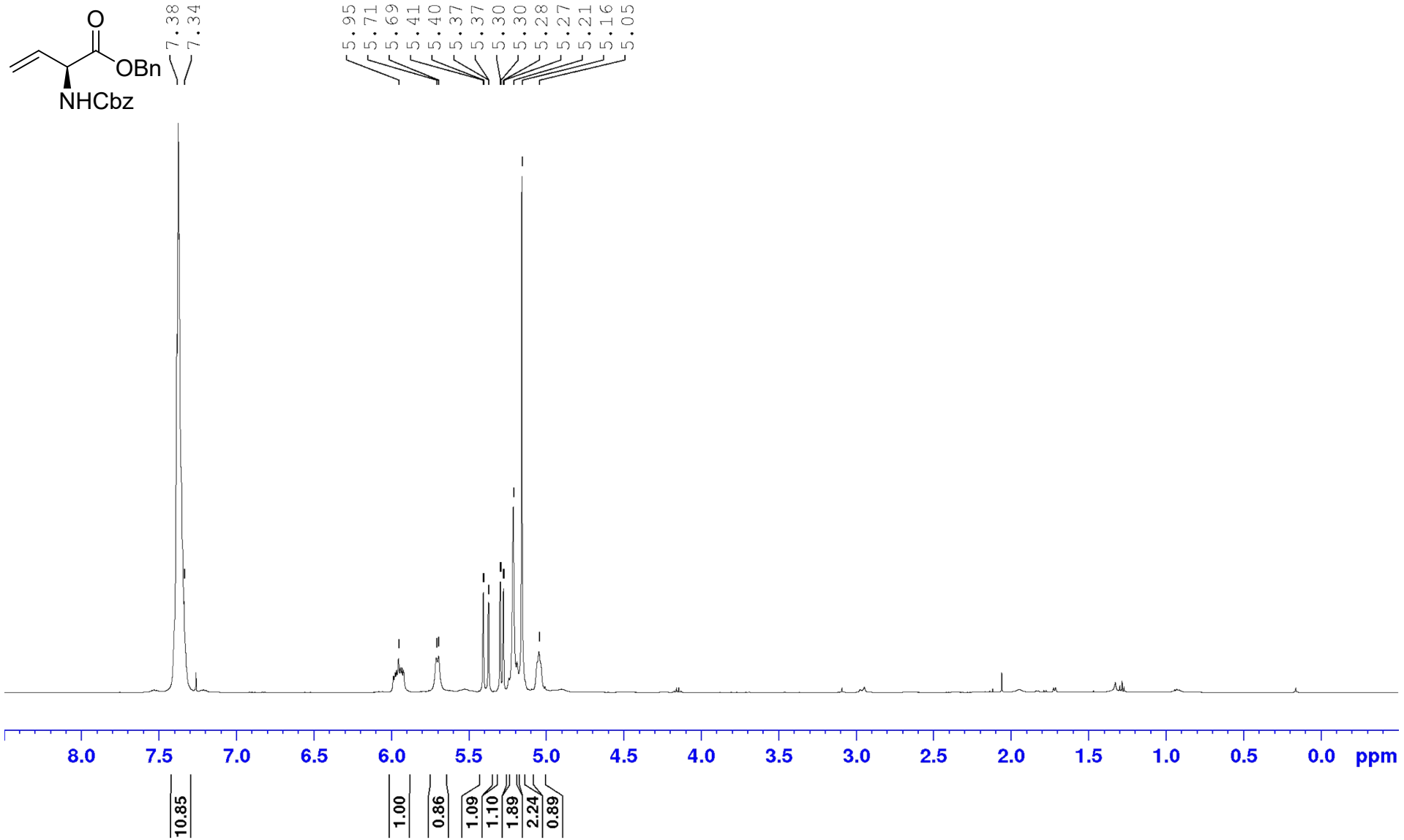

Figure S57 ^{1}H NMR spectrum of protected vinylglycine (**11**, 500 MHz, $CDCl_3$).

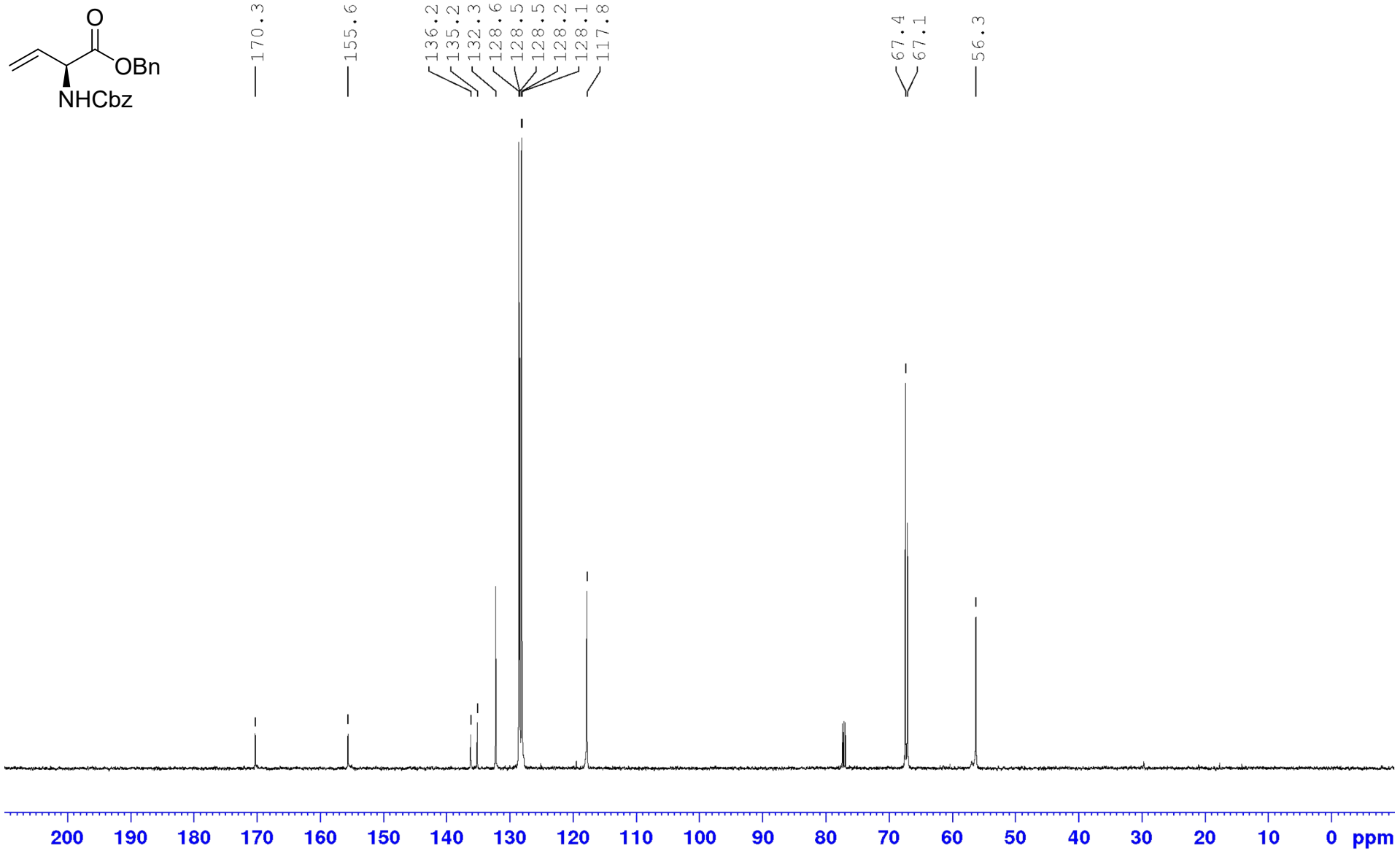

Figure S58 ^{13}C NMR spectrum of protected vinylglycine (**11**, 125 MHz, $CDCl_3$).

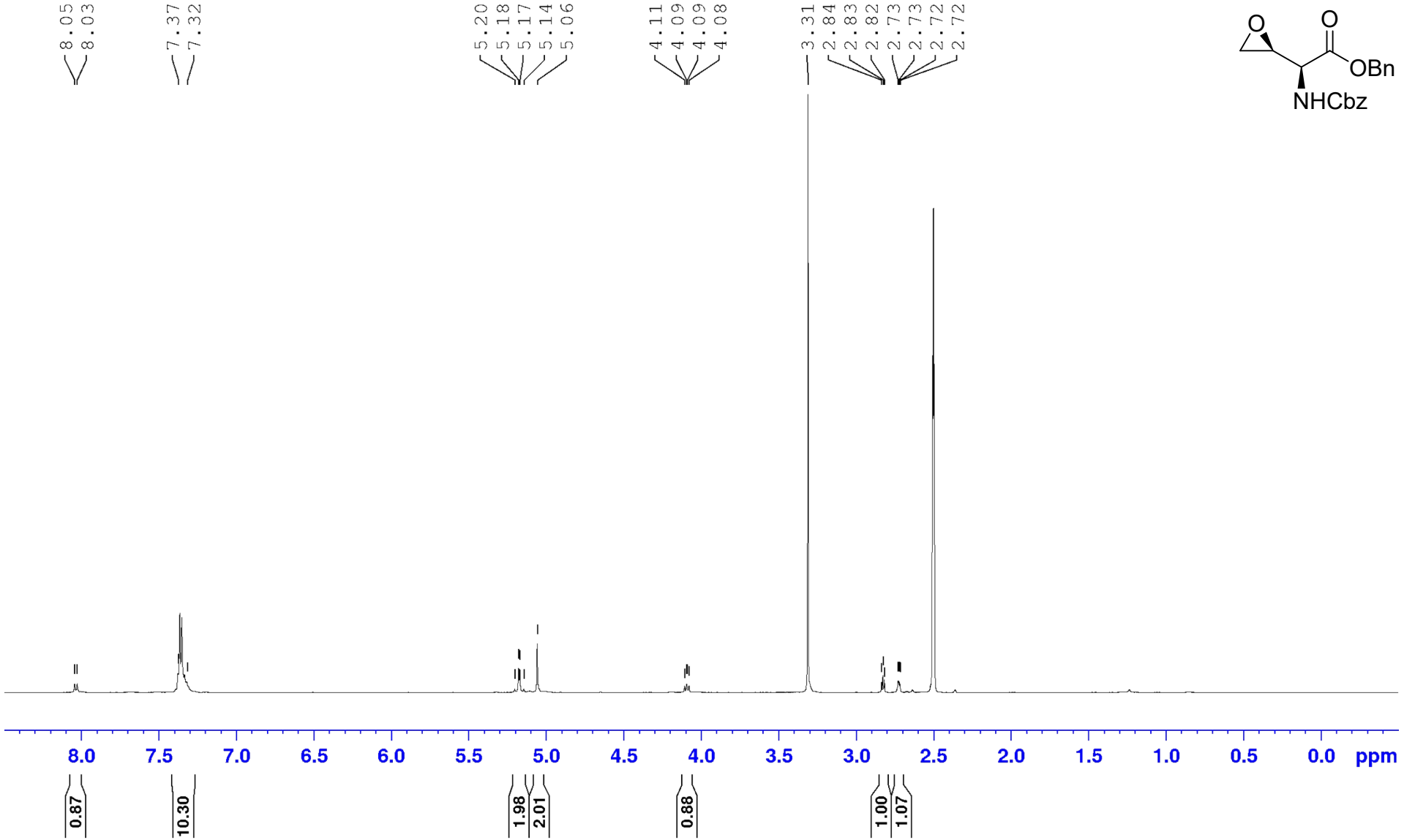

Figure S59 ^{1}H NMR spectrum of protected epoxide (**12**, 500 MHz, DMSO-d_6).

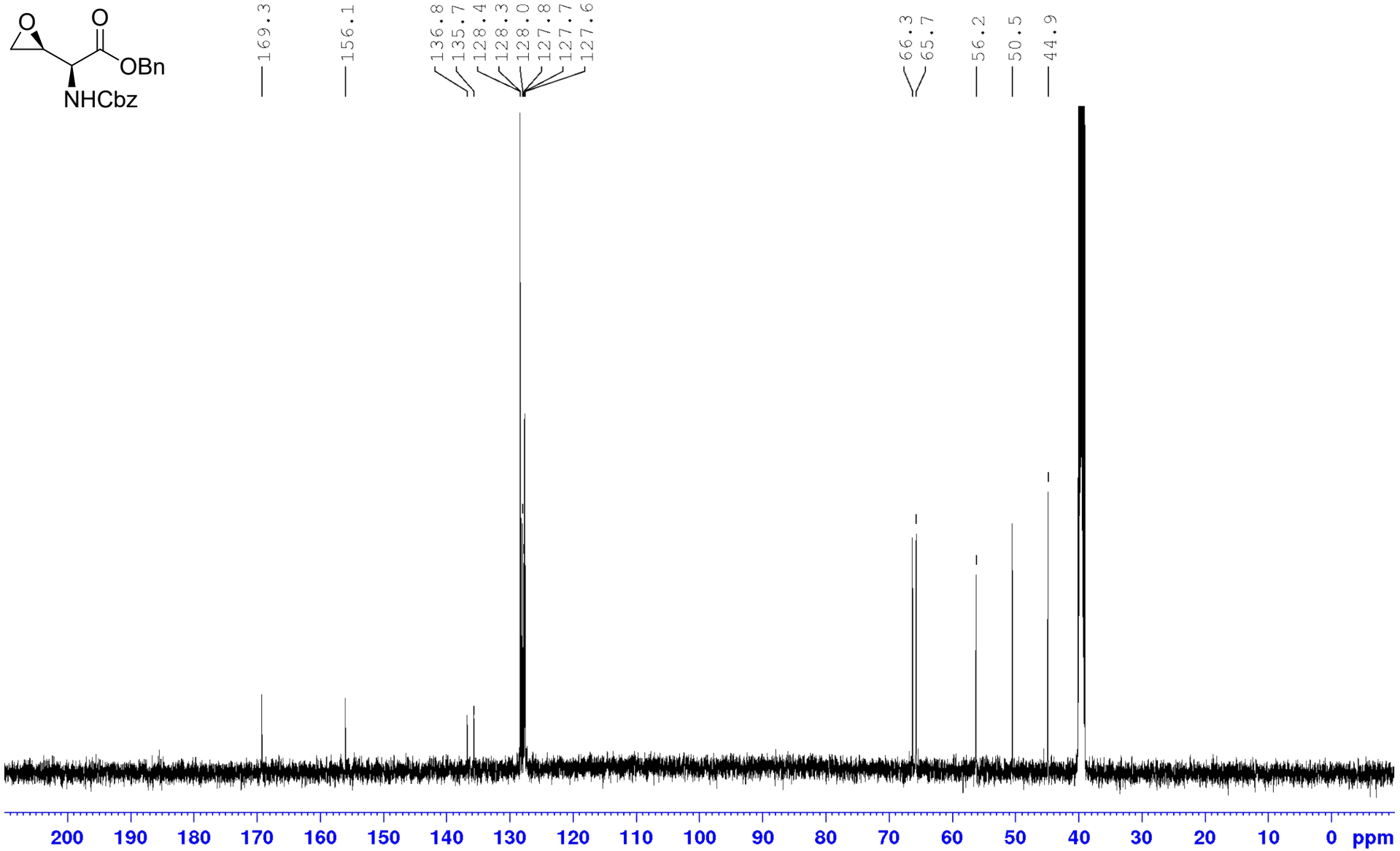

Figure S60 ^{13}C NMR spectrum of protected epoxide (**12**, 125 MHz, DMSO-d_6).

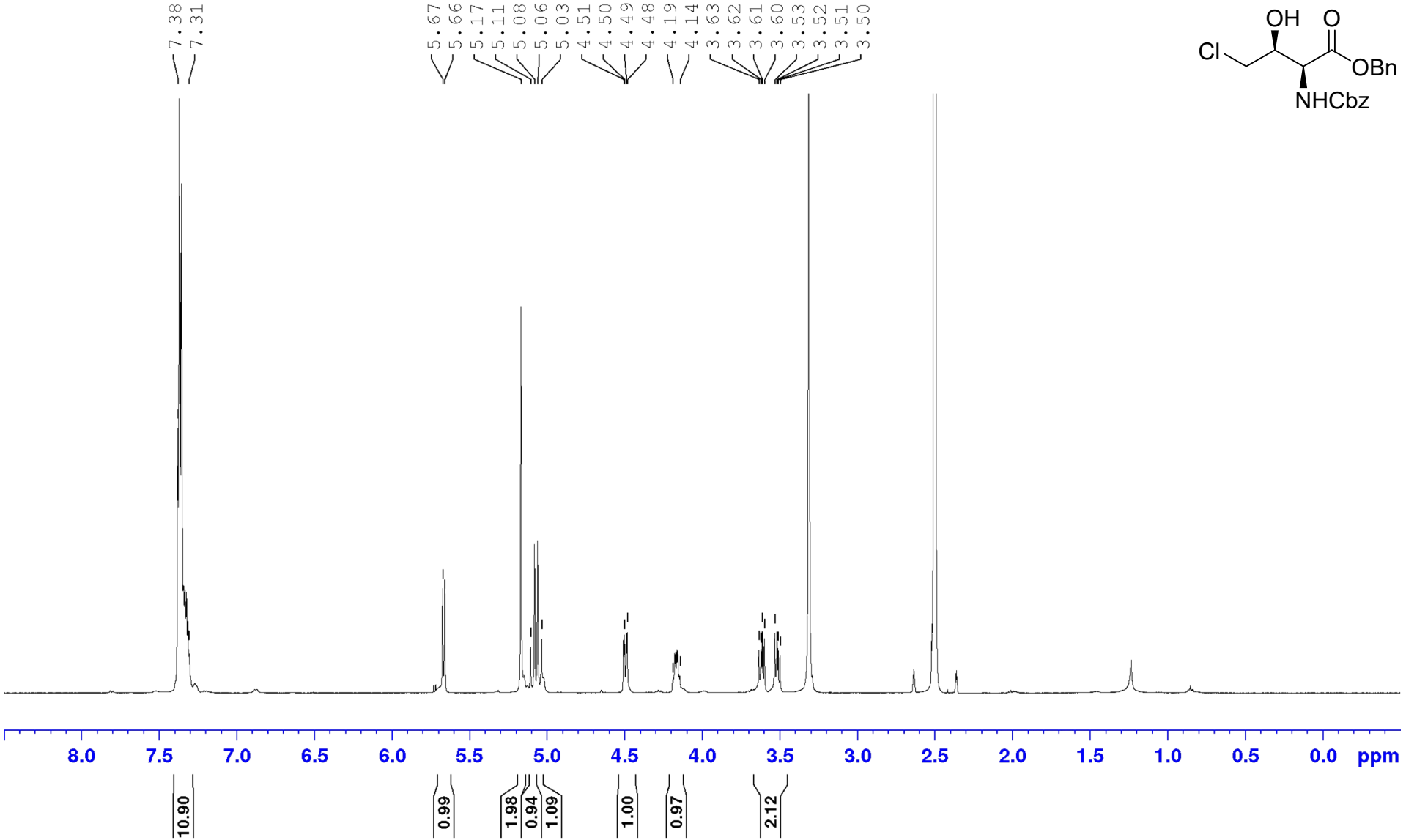

Figure S61 ^{1}H NMR spectrum of protected 4-chloro-L-threonine (**13**, 500 MHz, DMSO-d_6).

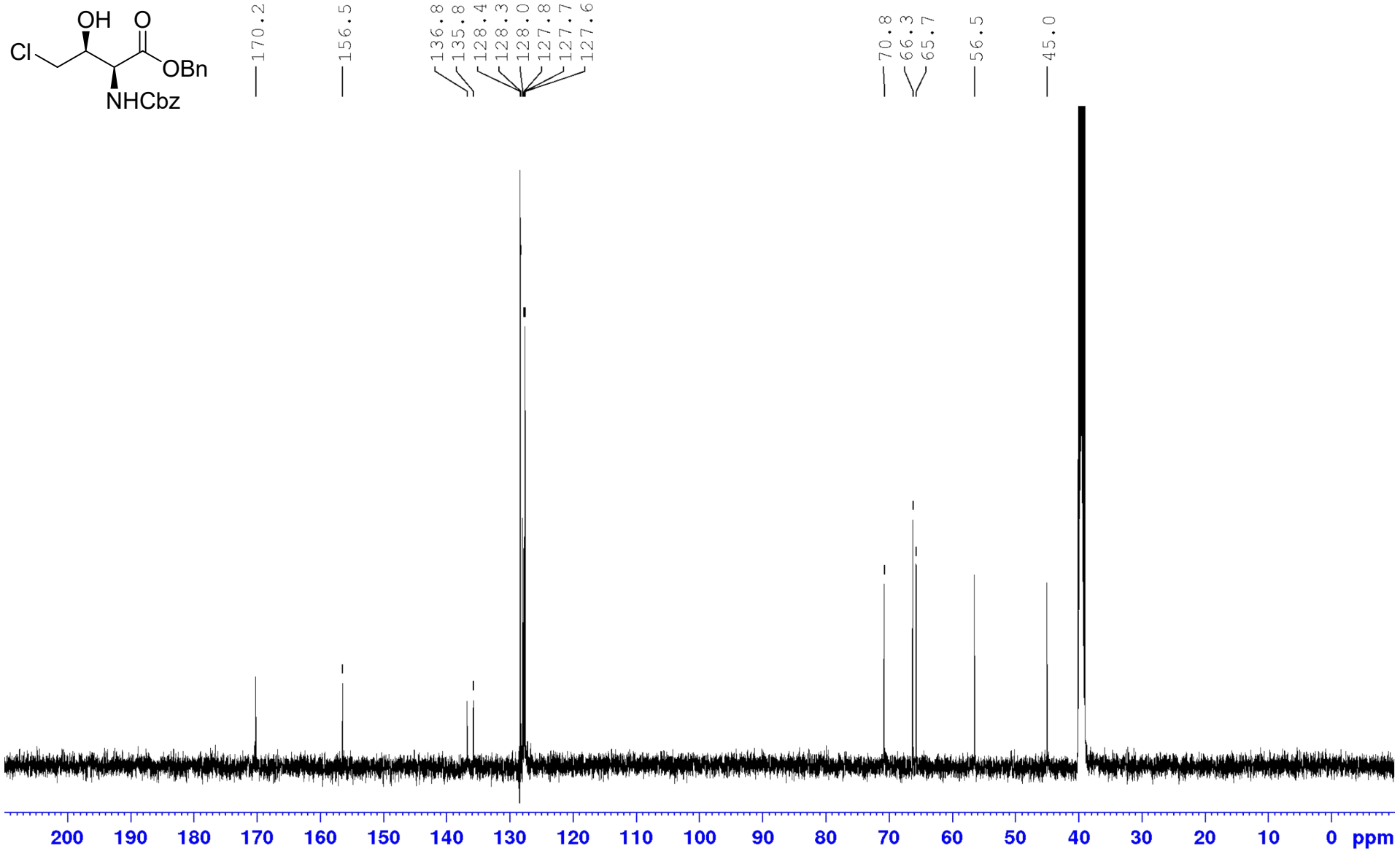

Figure S62 ^{13}C NMR spectrum of protected 4-chloro-L-threonine (**13**, 125 MHz, DMSO-d_6).

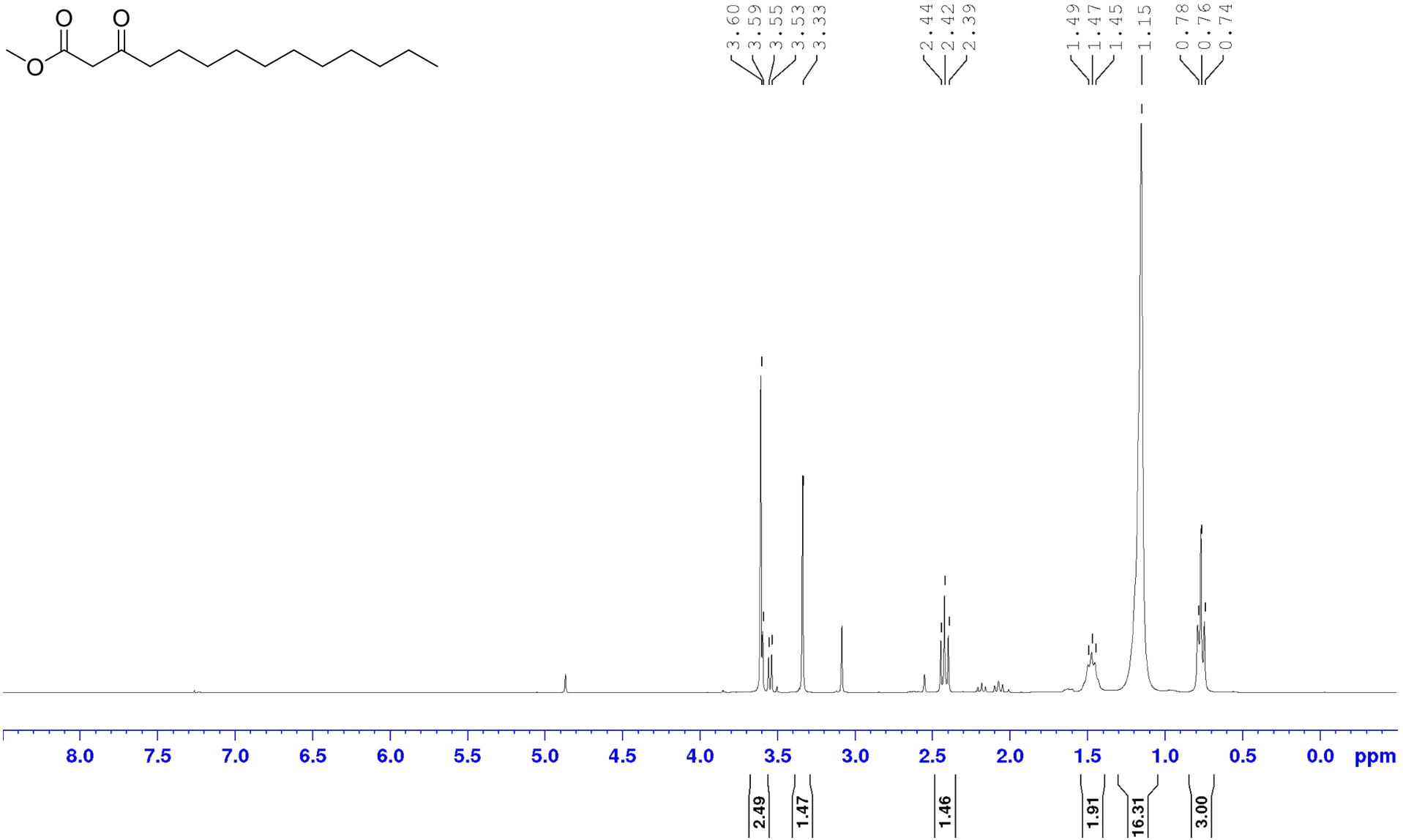

Figure S63 ^{1}H NMR spectrum of methyl 3-oxotetradecanoate (**8**, 300 MHz, $CDCl_3$).

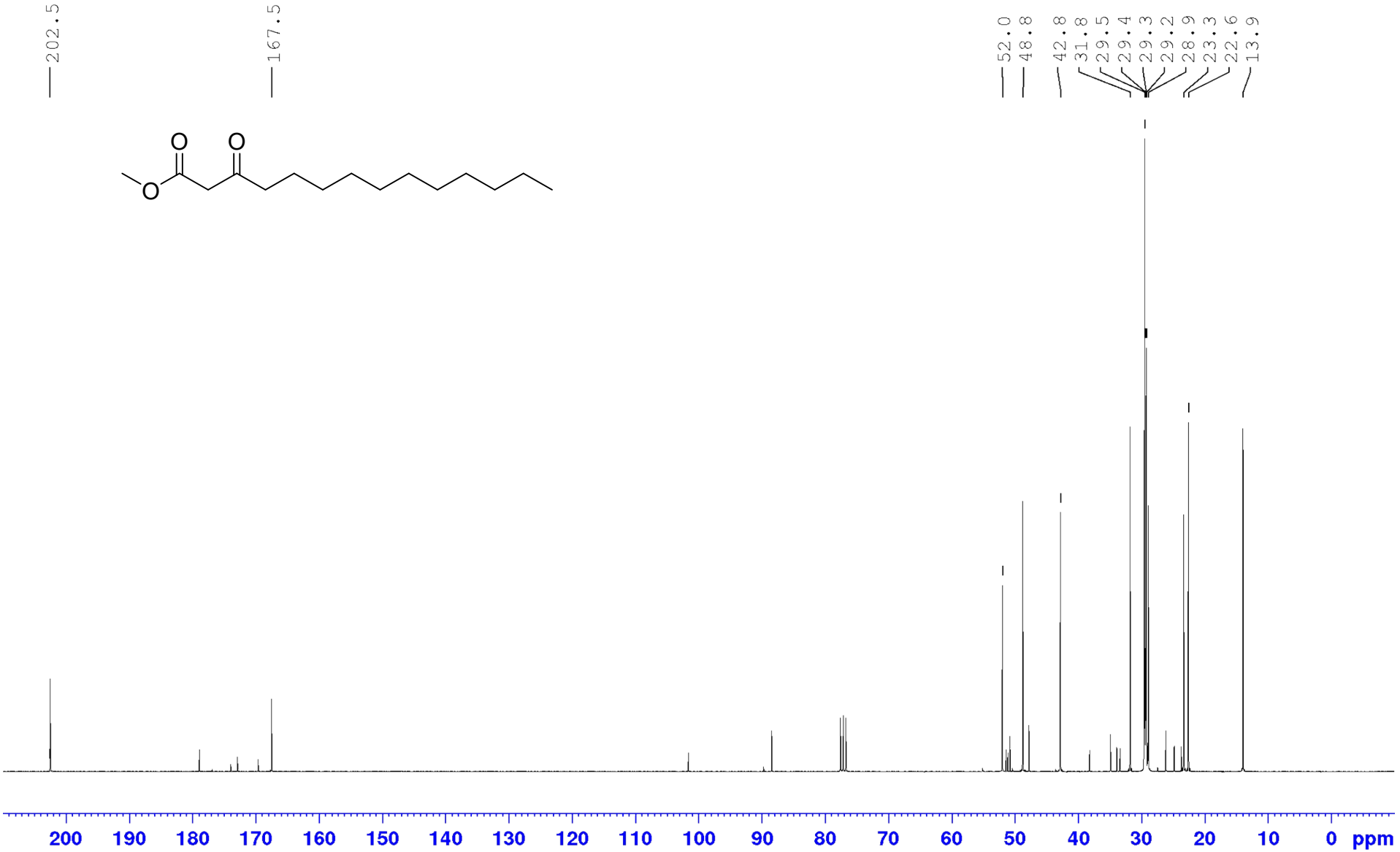

Figure S64 ^{13}C NMR spectrum of methyl 3-oxotetradecanoate (**8**, 75 MHz, $CDCl_3$).

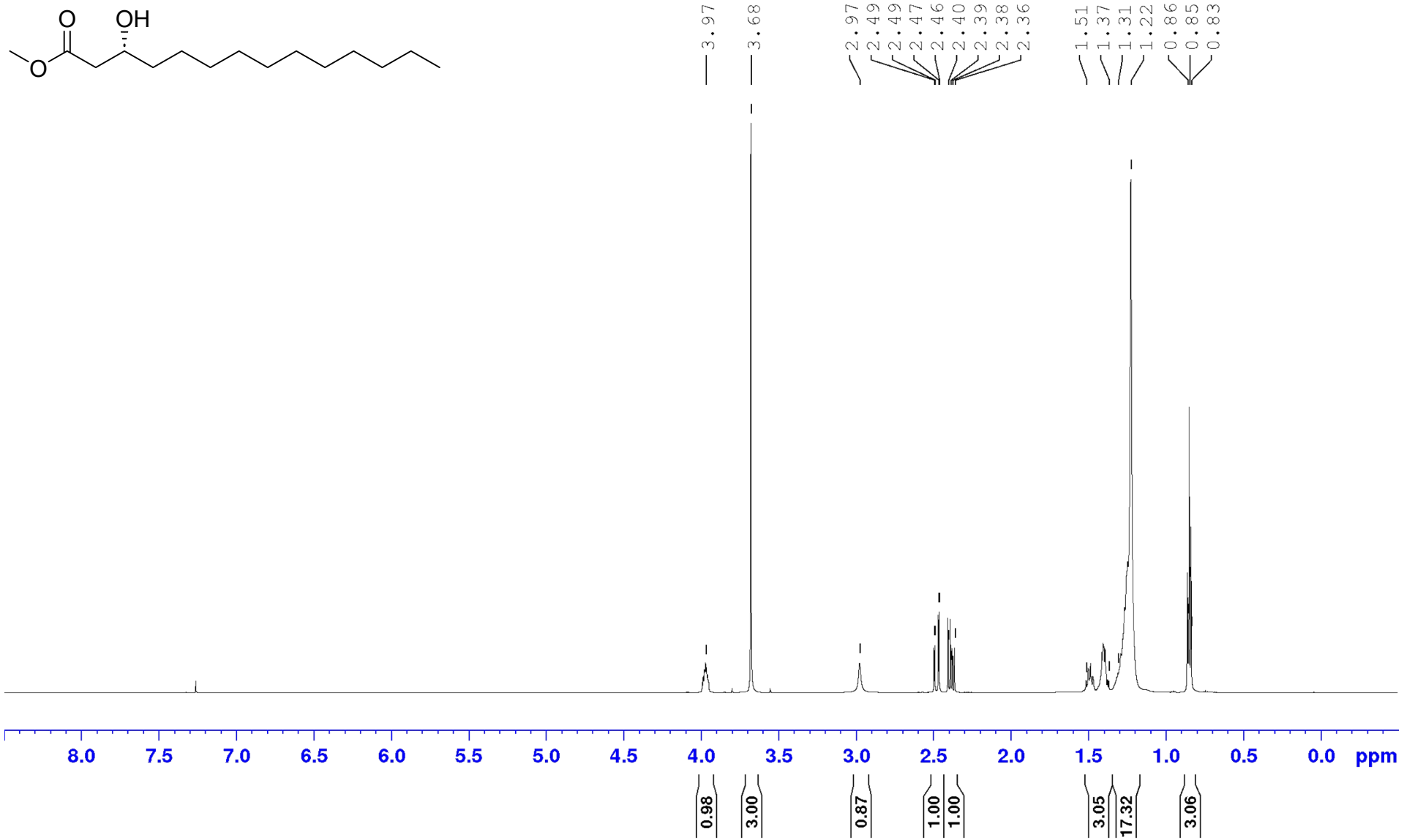

Figure S65 ^{1}H NMR spectrum of methyl (*R*)-3-hydroxytetradecanoate (**9**, 600 MHz, $CDCl_3$).

Figure S66 ^{13}C NMR spectrum of methyl (*R*)-3-hydroxytetradecanoate (**9**, 150 MHz, $CDCl_3$).

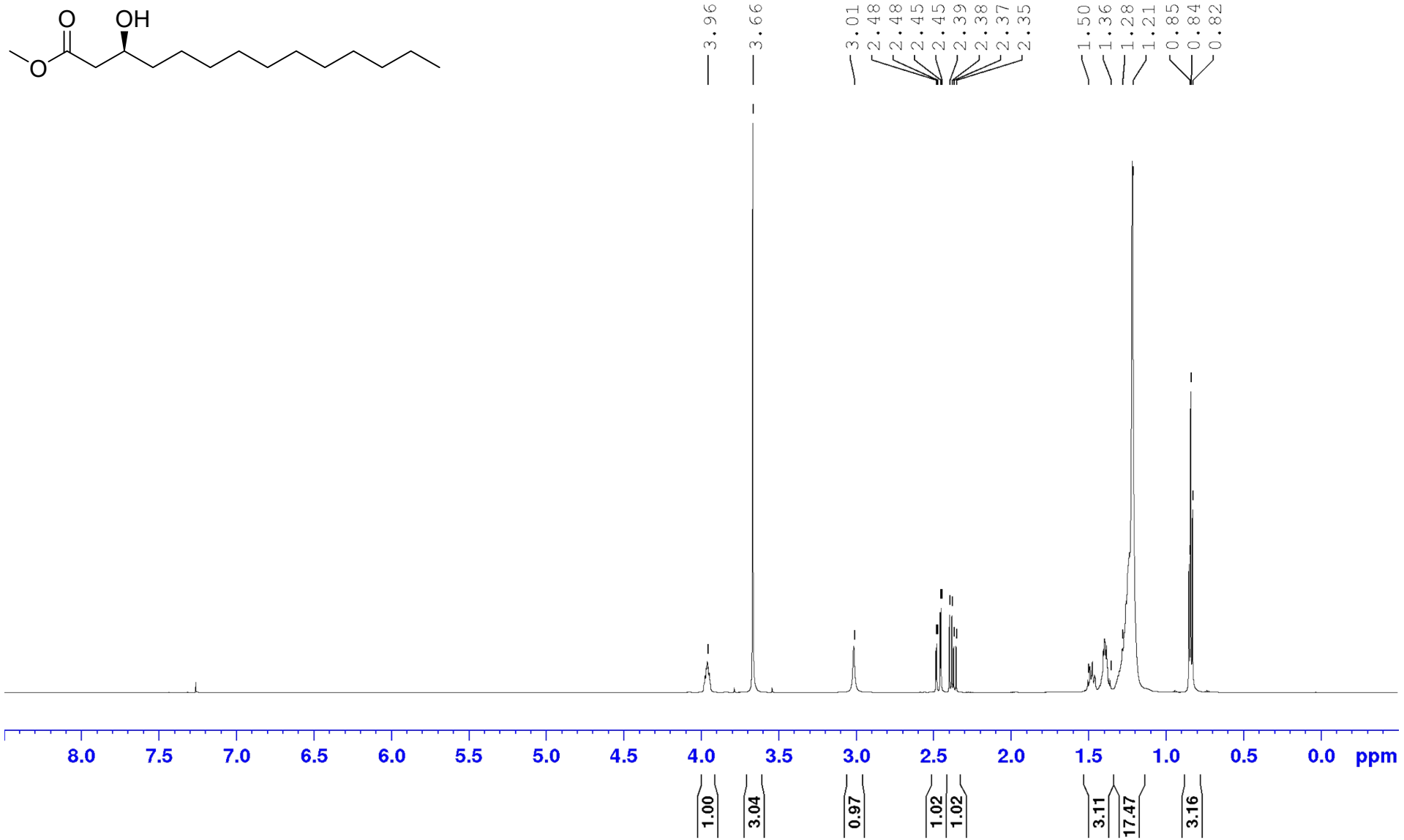

Figure S67 ^{1}H NMR spectrum of methyl (*S*)-3-hydroxytetradecanoate (**10**, 600 MHz, $CDCl_3$).

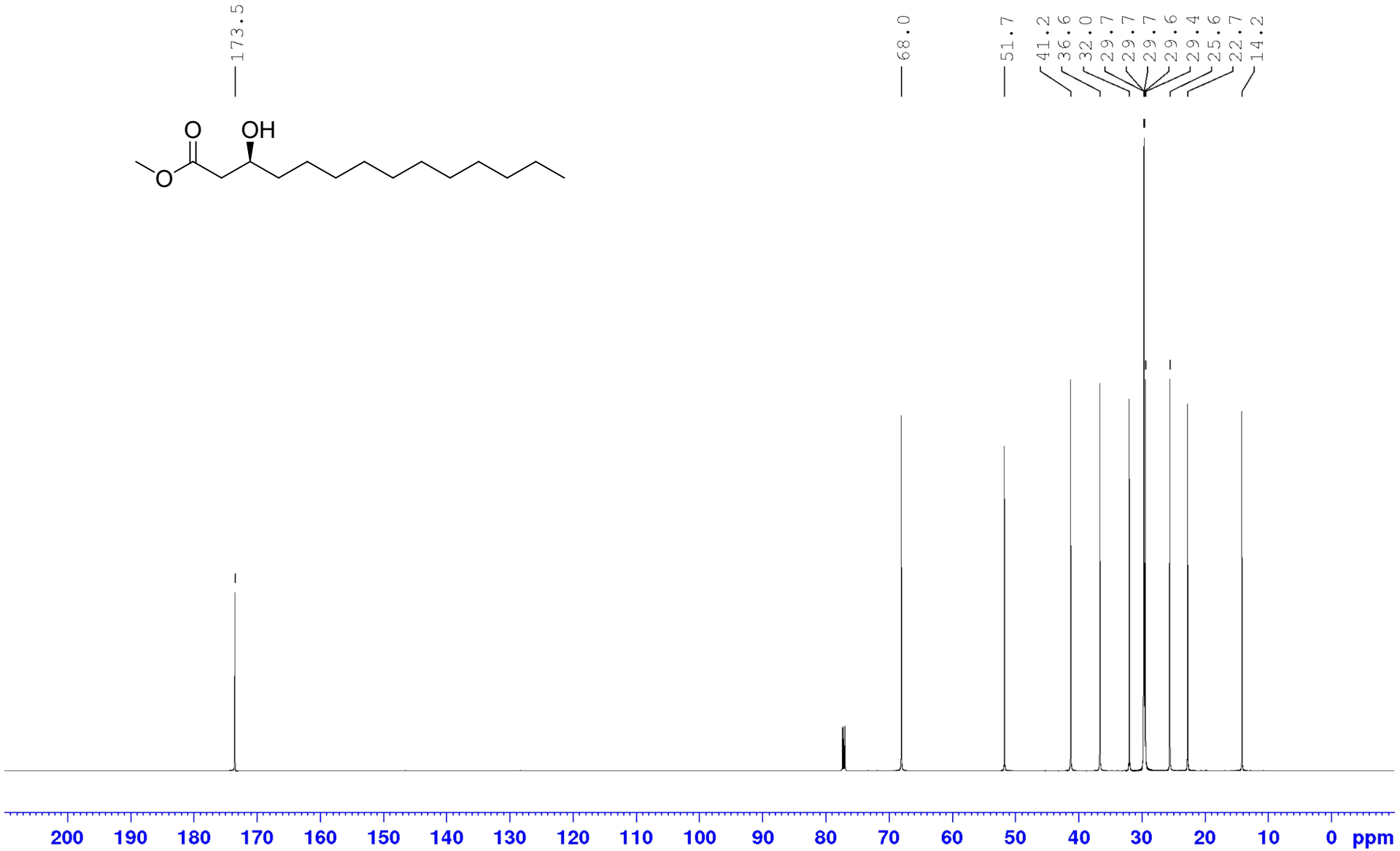

Figure S68 ^{13}C NMR spectrum of methyl (*S*)-3-hydroxytetradecanoate (**10**, 150 MHz, $CDCl_3$).

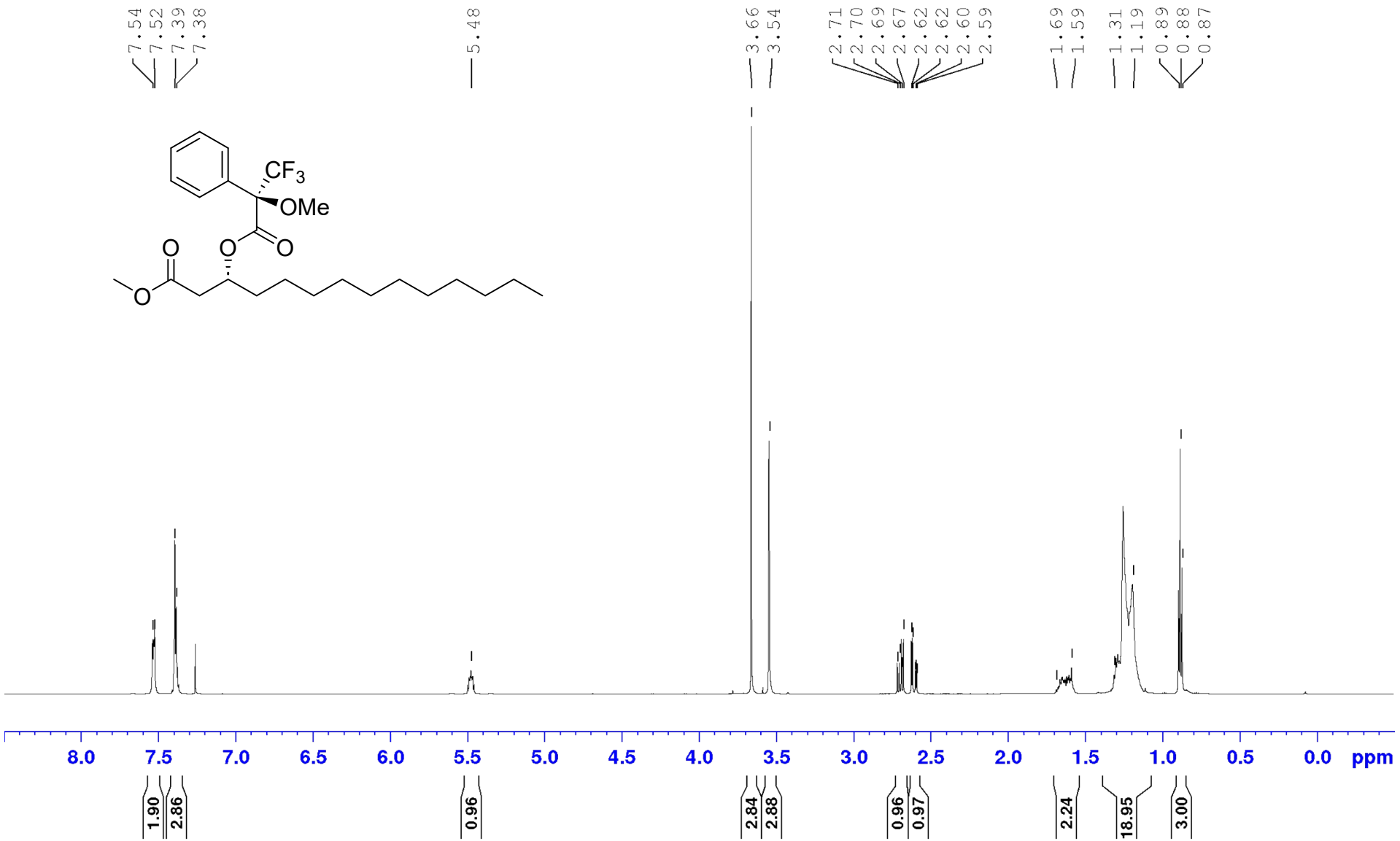

Figure S69 ^{1}H NMR spectrum of Mosher ester (*R*)-3 (**7**, 600 MHz, $CDCl_3$).

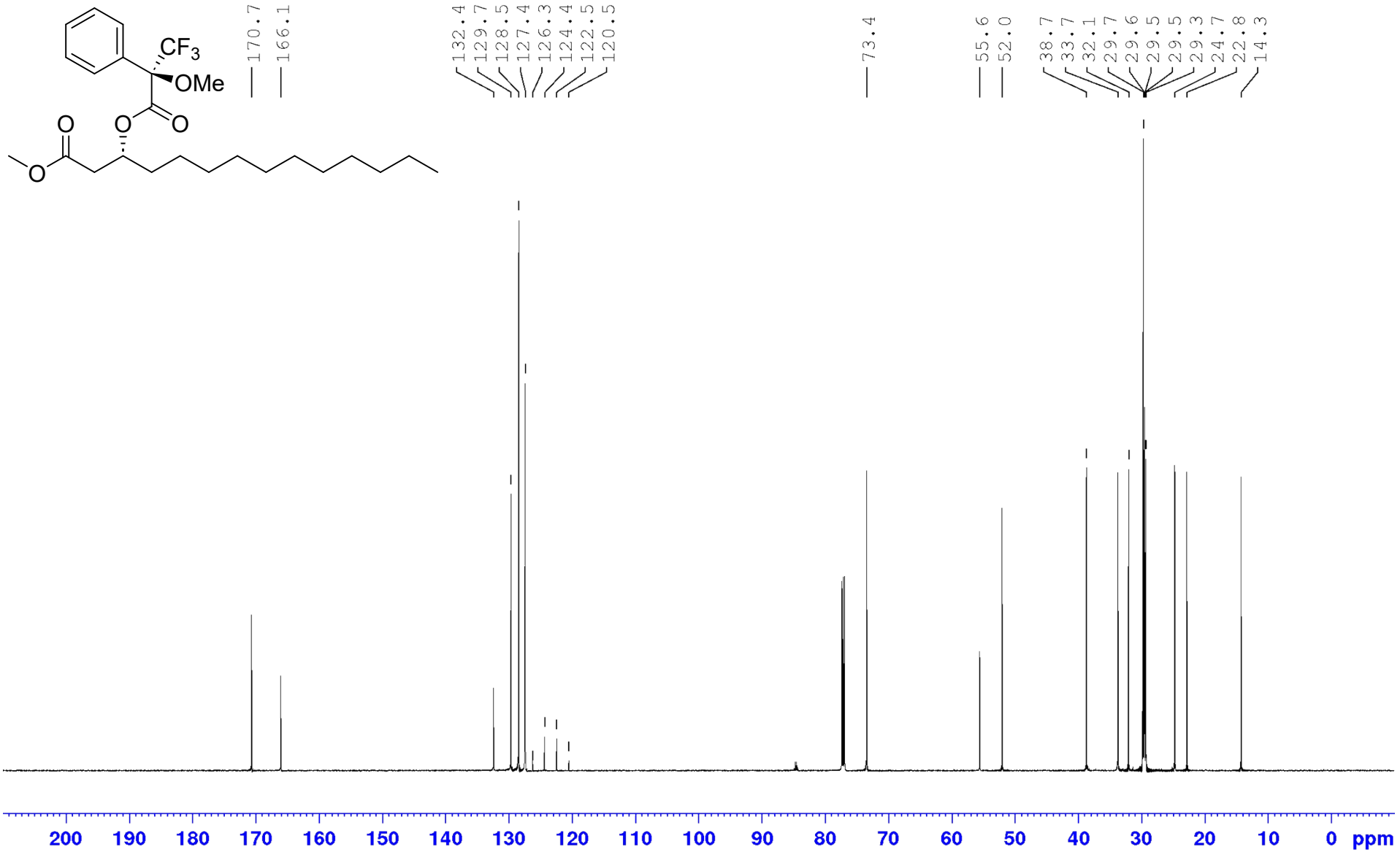

Figure S70 ^{13}C NMR spectrum of Mosher ester (*R*)-3 (**7**, 150 MHz, $CDCl_3$).

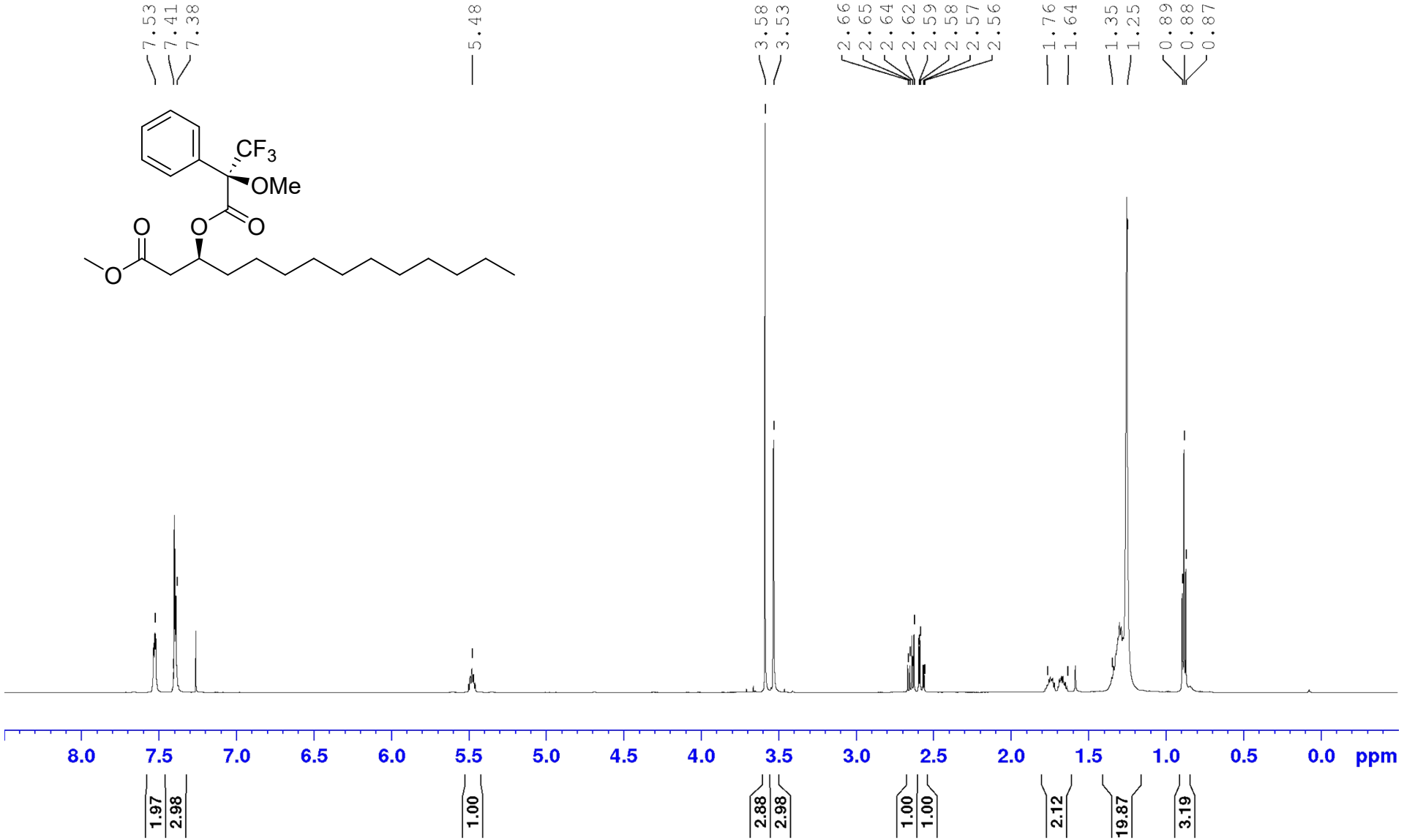

Figure S71 ^{1}H NMR spectrum of Mosher ester (*S*)-3 (**6**, 600 MHz, $CDCl_3$).

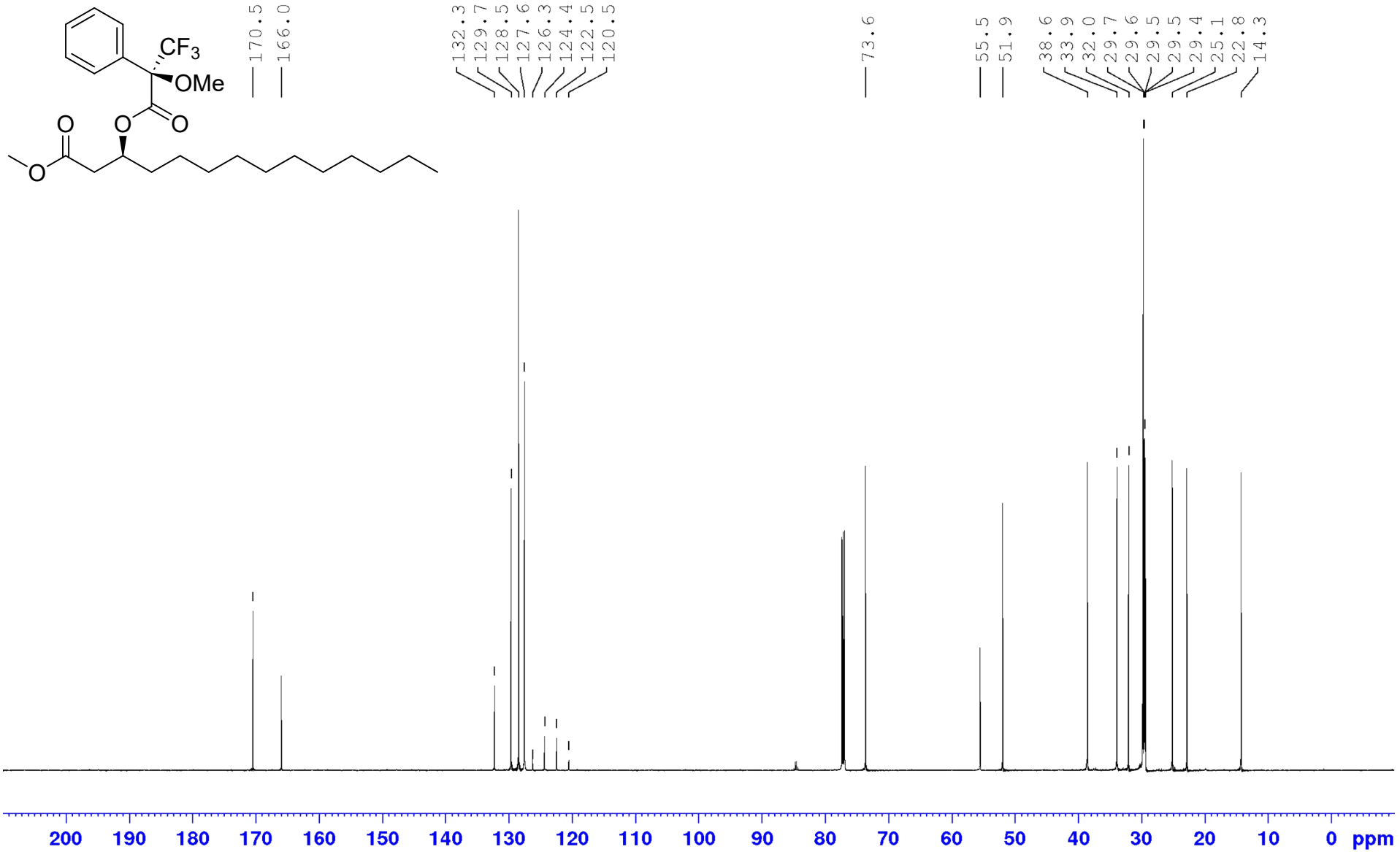

Figure S72 ^{13}C NMR spectrum of Mosher ester (*S*)-3 (**6**, 150 MHz, $CDCl_3$).